

EXAMINING THE POSSIBILITY OF ESTIMATING ACTIVITY
TIME DISTRIBUTIONS FROM RECORDED DOWNTIMES IN TBM TUNNELLING
OPERATIONS USING DISCRETE EVENT SIMULATION (DES) MODELS

by
Hazar Kumas

© Copyright by Hazar Kumas, 2022

All Rights Reserved.

A thesis submitted to the Faculty and the Board of Trustees of the Colorado School of Mines in partial fulfillment of the requirements for the degree of Master of Science (Underground Construction and Tunnel Engineering).

Golden, Colorado

Date _____

Signed: _____
Hazar Kumas

Signed: _____
Dr. Jamal Rostami
Thesis Advisor

Golden, Colorado

Date _____

Signed: _____
Dr. Michael A. Mooney
Program Director of Underground
Construction and Tunnel Engineering

ABSTRACT

While the tunnel boring machines (TBMs) have been broadly accepted by tunneling industry, the calculation of TBM advance rates has always been a challenge in setting project budgets and schedules. TBM advance rate is a function of penetration rate and machine utilization, which is simply the ratio of boring time to total project time. Utilization is an essential factor that must be taken into consideration in performance predictions since it is the part of the advance rate calculation that defines the efficiency of tunneling operations.

Previous researchers have tried to estimate TBM utilization using various models. Some of these models were empirical, some were statistical, and some were numerical. The CSM2020 is a recently proposed model that uses discrete event simulation (DES) to incorporate stochastic nature of tunneling activities in modeling tunneling operation by TBM to estimate machine utilization. The model is based on using recorded downtime data from previous projects as the input to estimate TBM utilization rate as the output.

Given that various activity times have not been commonly recorded or studied in many of the tunneling operations, this thesis aims to evaluate the possibility of estimating these tunneling activity durations from the recorded machine downtimes and utilization rate. This allows for expansion of the databases of activity time distributions that can be used for use of DES modeling for estimation of machine utilization in the future TBM tunneling projects. To that end, recorded downtimes from a selected project site were used to create representative time distributions for completion of a section of the selected tunnel where a slurry shield TBM was employed. These distributions were used to simulate the tunneling operations using DES modeling, or CSM 2020 model, and the results compared with the recorded downtimes in the

project. A new set of time distributions was subsequently created by varying the mean value for the activity times in the original datasets, and the new distributions were used in sensitivity analyses to verify the relationship between the activity times and the resulting downtimes and overall machine utilizations. The sensitivity analyses facilitated observation of the impact of various activity time distributions on utilization and overall downtime contribution, hence making it possible to evaluate the possibility of estimating the activity times from recorded downtime data in the field. Because the CSM2020 uses a combination of activity time and delay times as the input for modeling, it was concluded that estimation of activity times is not possible with the current version of the model. The except is the activities that are directly linked or listed as downtime, such as segment installation.

TABLE OF CONTENTS

ABSTRACT.....	iii
LIST OF FIGURES	vii
LIST OF TABLES.....	xi
ACKNOWLEDGEMENTS.....	xii
CHAPTER 1 INTRODUCTION.....	1
1.1 Background	1
1.2 Research Objectives.....	4
1.3 General Workflow	4
1.4 Thesis Structure.....	6
CHAPTER 2 LITERATURE REVIEW	7
CHAPTER 3 CSM2020 TBM PERFORMANCE PREDICTION MODEL.....	17
CHAPTER 4 PROJECT DETAILS AND OBSERVED TUNNELING ACTIVITIES.....	54
4.1 Geological and Hydrogeological Information	54
4.2 Rock Characterization.....	56
4.3 Tunneling Activities.....	58
4.3.1 Safety Meeting.....	58
4.3.2 Boring.....	59
4.3.3 Segment Installation.....	59
4.3.4 Utility Extension	59
4.3.5 Maintenance	60
4.3.6 Repairs	60
4.3.7 Surveying	60
4.3.8 Intervention.....	61

4.3.9 Transportation of Supplies and Crew.....	61
4.4 Data Collection	62
4.5 Processing of Raw Data.....	62
CHAPTER 5 VALIDATION OF CSM2020 MODEL.....	69
CHAPTER 6 SENSITIVITY ANALYSIS.....	75
6.1 Segment Installation.....	78
6.2 Unscheduled Maintenance	80
6.3 Electrical Systems Repair	81
6.4 Backfill Grout System.....	83
6.5 Loading & Unloading of Supplies	84
6.6 Backup Utilities Repair	86
6.7 Unforeseen Delays	87
6.8 Slurry Line Extension	89
6.9 Slurry Lines Repair	90
6.10 Discussion	92
CHAPTER 7 CONCLUSIONS AND RECOMMENDATIONS FOR FUTURE STUDIES.....	94
7.1 Conclusions	94
7.2 Recommendations.....	96
REFERENCES	100
APPENDIX A PERMISSION TO PUBLISH.....	103
APPENDIX B HISTOGRAMS AND STATISTICAL PARAMETERS OF PROBABILITY DISTRIBUTIONS	104

LIST OF FIGURES

Figure 1.1: Illustration of the general workflow followed in this study.....	5
Figure 3.1: CSM2020 model tunneling activities as modules and their activation process with boring (Khetwal, 2020) (Reprinted with permission).....	23
Figure 3.2: Some of the time distributions used in CSM2020 and their applicability (Khetwal, 2020).	24
Figure 3.3: More time distributions used in CSM2020 (Khetwal, 2020).....	25
Figure 3.4: Summarized flow chart for CSM2020 model (Khetwal 2020) (Reprinted with permission).	30
Figure 3.5: Modules through shift start to segment installation and ground-related delays.	32
Figure 3.6: Sub-sections and modules for probe drilling and utility extension.	33
Figure 3.7: Modules for TBM face and backup system delays.	35
Figure 3.8: The model interfaces for muck transportation, surveying, and unforeseen delays.	36
Figure 3.9: Shift start module.	37
Figure 3.10: Tunnel length module.....	38
Figure 3.11: Meeting module.....	38
Figure 3.12: Crew assign module.	39
Figure 3.13: Crew delay module.....	39
Figure 3.14: Inspection module.	40
Figure 3.15: Probe drilling module interface.....	41
Figure 3.16: Water pipe extension module.....	42
Figure 3.17: TBM type deciding module.....	42
Figure 3.18: Double shield deciding module.....	43
Figure 3.19: Tunnel boring module.	43

Figure 3.20: Module evaluates if the segment installation is required or not.....	44
Figure 3.21: Module decides the frequency of the segment installation.	44
Figure 3.22: Segment installation module.	45
Figure 3.23: Ground issues frequency module. Percentages correspond to ground issues in the same order as their representative modules in Figure 3.5.	46
Figure 3.24: TBM face cutter change module.	47
Figure 3.25: Survey module and delay type.	48
Figure 3.26: Scheduled maintenance module.	49
Figure 3.27: Unforeseen delays module.	49
Figure 3.28: Module that simulates conveyor belt delays.	50
Figure 3.29: Muck dumping module.	51
Figure 4.1: Total time contribution according to field data, after removal of the anomalies.	67
Figure 4.2: Downtime contribution according to field data.....	68
Figure 6.1: Variation in downtime contribution and utilization by changing mean values of segment installation.	78
Figure 6.2: Variation in downtime contribution by variation of the mean value of segment installation.	79
Figure 6.3: Change in TBM Utilization as a function of the mean value of segment installation.	79
Figure 6.4: Variation in downtime contribution and utilization by changing mean values of unscheduled maintenance.	80
Figure 6.5: Variation in downtime contribution by variation of the mean value of unscheduled maintenance.	80
Figure 6.6: Change in TBM Utilization as a function of the mean value of unscheduled maintenance.	81
Figure 6.7: Variation in downtime contribution and utilization by changing mean values of electrical systems repair.	81

Figure 6.8: Variation in downtime contribution by variation of the mean value of electrical systems repair.....	82
Figure 6.9: Change in TBM Utilization as a function of the mean value of electrical systems repair.....	82
Figure 6.10: Variation in downtime contribution and utilization by changing mean values of backfill grout system.....	83
Figure 6.11: Variation in downtime contribution by variation of the mean value of backfill grout system.....	83
Figure 6.12: Change in TBM Utilization as a function of the mean value of backfill grout system.....	84
Figure 6.13: Variation in downtime contribution and utilization by changing mean values of loading & unloading of supplies.....	84
Figure 6.14: Variation in downtime contribution by variation of the mean value of loading & unloading of supplies.....	85
Figure 6.15: Change in TBM Utilization as a function of the mean value of loading & unloading of supplies.....	85
Figure 6.16: Variation in downtime contribution and utilization by changing mean values of backup utilities repair.....	86
Figure 6.17: Variation in downtime contribution by variation of the mean value of backup utilities repair.....	86
Figure 6.18: Change in TBM Utilization as a function of mean value of backup utilities repair.....	87
Figure 6.19: Variation in downtime contribution and utilization by changing mean values of unforeseen delays.....	87
Figure 6.20: Variation in downtime contribution by variation of the mean value of unforeseen delays.....	88
Figure 6.21: Change in TBM Utilization as a function of the mean value of unforeseen delays.....	88
Figure 6.22: Variation in downtime contribution by variation of the mean value of slurry line extension.....	89

Figure 6.23: Variation in downtime contribution by variation of the mean value of slurry line extension.....	89
Figure 6.24: Change in TBM Utilization as a function of the mean value of slurry line extension.	90
Figure 6.25: Variation in downtime contribution and utilization by changing mean values of slurry lines repair.	90
Figure 6.26: Variation in downtime contribution by variation of mean value of slurry lines repair.	91
Figure 6.27: Change in TBM Utilization as a function of the mean value of slurry lines repair.	91

LIST OF TABLES

Table 2.1: Summary of TBM performance prediction models in the literature.	8
Table 3.1: Example Case A and B showing how instantaneous and scheduled utilization is calculated per Arena®.....	20
Table 3.2: Time distributions used by Khetwal (2020) in CSM2020 model.....	27
Table 3.3: Ground issues and their corresponding troubleshoot modules in the CSM2020 model.	47
Table 4.1: Information on geological units within the project area.	55
Table 4.2: Rockmass properties of Units 1, 2, and 3.....	58
Table 4.3: Machine specifications for the tunneling project studied in this research.	62
Table 4.4: Tunneling activities and delay causes on the data recording sheet.	63
Table 4.5: Tunneling activities and their corresponding modeling modules.	64
Table 5.1: Best fitting probability distributions for each activity with their squared error values per the Input Analyzer extension.	71
Table 5.2: VA Time results for the validation test runs (All units are in minutes per activity).	73
Table 5.3: Tunneling activities and their statistical values.	74

ACKNOWLEDGEMENTS

I would like to thank my academic advisor Dr. Jamal Rostami, and my committee members, Dr. Priscilla Nelson, and Dr. Gabriel Walton, for their guidance during my studies. Their suggestions pushed me to expand my knowledge further and contributed to my success. I also want to thank Ryan O’Connell, Tala Tahernia, and Dr. Anuradha Khetwal for their valuable comments on my work during our research meetings.

I also want to thank my one-and-only brother Duyal Kumas, my mother Sukriye Kumas, and my father Ozcan Kumas for their continued support and faith in me.

Above all, my deepest gratitude to my friends Muthu Vinayak Thyagarajan, Muhammad Ishaq, and Prasoon Garg for their unprecedented support during the most challenging of times. Without them, this work wouldn’t be possible.

A special thanks to Dr. Jennifer Briggs for her understanding, guidance, and sincerity when things look despondent.

Lastly, I want to thank all the people who shared their knowledge and positivity with me, including Esad Kaya, Animesh Mishra, Deep Joshi, Nancy Zupick, and many others.

I dedicate this thesis to my grandfather, who lived by the truth, the whole truth, and nothing but the truth.

CHAPTER 1

INTRODUCTION

1.1 Background

Underground construction has always been a challenge for the involved parties. For the owner, designer, and contractor, it is associated with the uncertainty that positions each party for exposure to several risks depending on the terms of project contracts. The number and magnitude of uncertainties is directly related to the project's geological conditions and complexity. For tunneling projects, these two factors have significant importance for determining the overall schedule and cost of the project. To determine the overall schedule and the cost of a project, additional parameters related to the machinery that is planned to be used must be considered. The advance rate (AR) is one of these parameters.

AR is the bored and supported tunnel length per unit, typically represented in meters or feet per day. Accurate and reliable prediction of the AR is critical in determining the feasibility of the selected machinery in a given project. However, AR alone cannot consider all the factors affecting machine performance. Other than the machinery, there are issues such as delays caused by the geological setting of the tunnel or backup tunneling operations. These issues are stochastic and hard to predict. In that sense, using a probabilistic approach to determine the span or statistical distribution of the possible completion time can offer a better understanding of the risks caused by various parameters compared to previous studies.

Certain parameters impact TBM performance but cannot be easily quantified in the calculation of AR, especially the human factors, which include the skill set of the crew, work culture, experience, labor contracts, and performance incentives. To overcome some of these limitations, randomization of events needs to be considered to estimate AR.

Many studies on TBM performance have resulted in prediction models mainly focused on estimating the rate of penetration (ROP). The Norwegian University of Science and Technology (NTNU) model by Bruland (1998), QTBM by Barton (2000), and other models by Nelson et al. (1983), Hassanpour et al. (2011), Yagiz et al. (2008), Yagiz and Karahan (2011), Salimi and Esmaeili (2013), and Armaghani et al. (2017) are examples of empirical models that estimate ROP. On the other hand, prediction models such as the Colorado School of Mines (CSM) by Rostami (1997) are based on theoretical approaches to TBM modeling by estimating ROP and U. These models can predict the ROP with reasonable accuracy (Rostami, 2016).

Prediction of AR requires reasonable estimates of both ROP and machine utilization. Prediction of utilization is problematic because it can be affected by controllable and uncontrollable parameters (Amid et al., 2014). Controllable parameters include TBM specifications, tunnel dimension (diameter, length), and operational parameters. Uncontrollable parameters are associated with geological conditions and unforeseen delays during excavation. Additionally, the experience of the TBM crew, the effectiveness of the management, and communication/coordination between the surface and subsurface teams influence the utilization rate achieved for a given project.

AR is calculated by the following formula below, according to Rostami (2016).

$$AR = ROP \times U \times N_s \times Sh \quad (1.1)$$

AR: Advance Rate (m/day, foot/day)

ROP: Rate of Penetration or Penetration Rate (meter per hour)

U: Utilization (%)

Ns: Number of shifts per day

Sh: Number of hours per shift

Utilization is directly proportional to the boring time of the TBM and inversely proportional to the total time, which is the sum of the boring time and downtime.

$$U (\%) = \frac{\textit{Boring Time}}{\textit{Boring Time} + \textit{Downtime}} \times 100 \quad (1.2)$$

Downtime includes every activity that causes the TBM to stop excavating, such as cutterhead interventions, repairs, maintenances, probe drillings, ground support installations, utility installations, rail extensions, and so on. Because of the nature of downtimes, it is difficult to predict their durations accurately. Moreover, since U is one of the parameters required to calculate AR, its accuracy directly affects the accuracy of predicted AR. For this reason, contractors tend to use an overall number to represent U that is based on their past experiences on similar jobs. To develop a method that can help contractors compare individual aspects of a variety of previous projects with an upcoming one, it would be better to calculate machine utilization based on the stochastic nature of the process and the expected performance of specific subsystems and activities. This objective can be achieved using discrete event simulation (Frough et al., 2019).

Additionally, Farrokh's (2012) comparison between predicted and actual TBM parameters showed that existing models could not offer accurate estimates of TBM performance for new projects. Related to that, Farrokh (2012) stated that creating more complex models by increasing the number of parameters does not always guarantee improved results due to the lack of inherent limits of these initial models. Khetwal et al. (2020) compared utilization estimations of various empirical-based performance prediction models using forward analysis with the utilization estimation of discrete event simulation (DES) approach. An average of 6% difference between these utilization estimations was observed, favoring the DES approach. It was found to

be the DES approach was most reliable among other prediction models in terms of forward analysis.

Khetwal (2020) introduced a discrete event simulation model called the Colorado School of Mines 2020 (CSM 2020) model to estimate utilization for hard rock TBM projects using Arena® software. Due to its reliability, the CSM 2020 was considered for examination of selected tunneling activities to estimate the tunneling activity times, affecting machine utilization.

1.2 Research Objectives

This thesis explores the possibility of estimating tunneling activity times from recorded downtime data using the CSM 2020 DES model. Since tunneling activity times are rarely recorded in the field, estimation of these activity times can provide a better understanding of bottlenecks that can be encountered on a tunneling project.

Additionally, tunneling activities are highly dependent on the occurrence of another tunneling activity either in series or in parallel. Estimation of the activity times can pave the road for further investigation of these dependencies in detail.

Furthermore, since CSM 2020 is a recently developed TBM performance prediction tool using DES modeling, this thesis aims to provide recommendations for future studies on this model and to explore its capabilities and limitations based on the experience gained throughout the analyses conducted in this study.

1.3 General Workflow

To achieve the stated objectives of this study, the CSM 2020 model was used to simulate the tunneling activities of a hard rock slurry TBM operation to observe the ability to recreate the workflow in the tunnel and to examine various components of downtime between the simulation

and field observations. Actual utilization and downtime contributions for the project site were generated from field data collected by the author. This was followed by estimating the downtime distributions as predicted by the CSM2020 model using various activity time distributions as input. The results were then compared to the available field data to verify and validate the modeling approach. This required creation of new probabilistic time distributions for activities that were measured in the field. These distributions were used in the CSM2020 model to simulate a limited section of the tunnel that was monitored. The validation of the model involved matching the actual TBM utilization calculated from the field data.

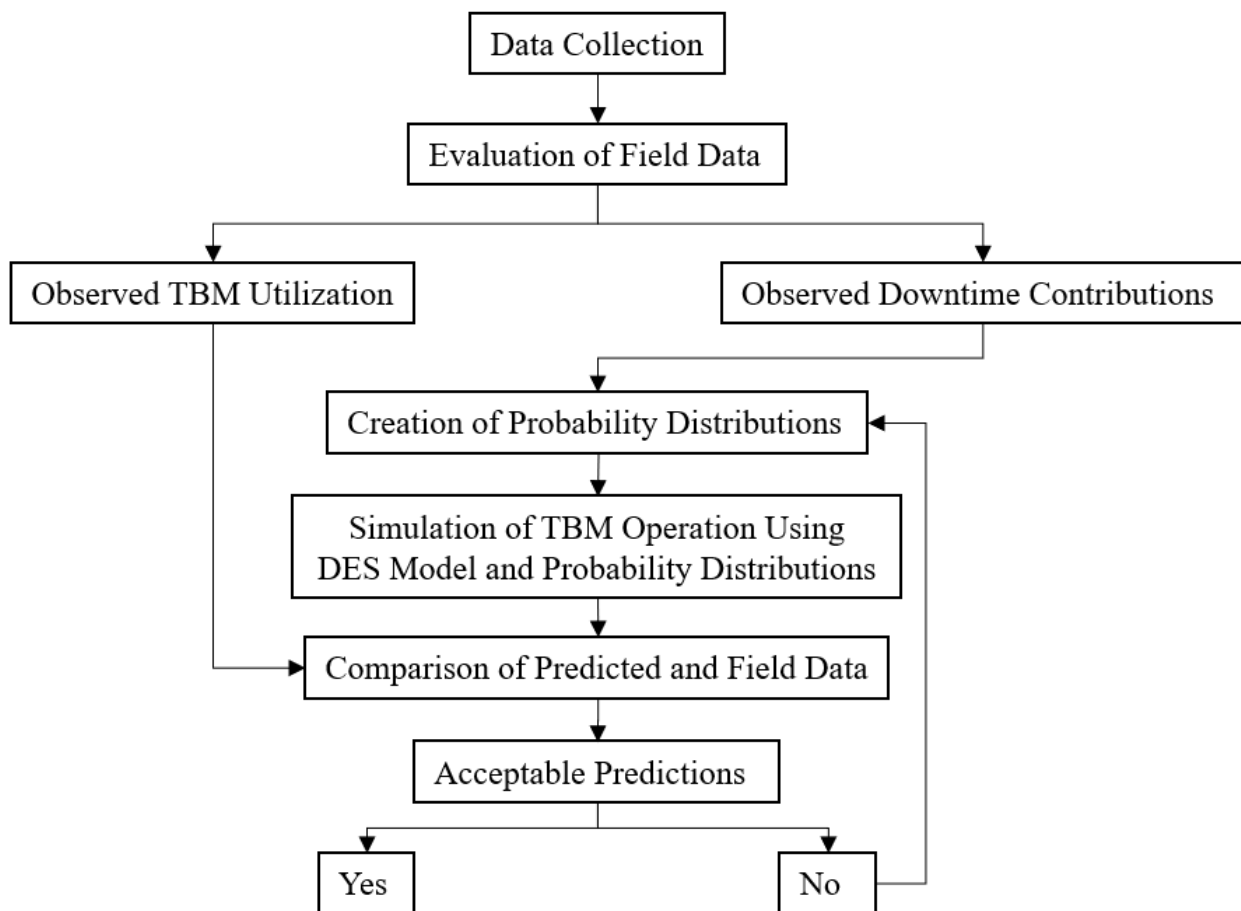


Figure 1.1: Illustration of the general workflow followed in this study.

The follow-up steps included a comprehensive sensitivity analysis by varying different tunneling activities to observe their impact on machine utilization and composition of downtimes. Observed correlations between the actual utilization and downtimes and an increase or decrease in estimated activity time durations by the model were used to indicate the cause-and-effect relationship between these parameters and, hence, confirm the possibility of estimating relevant activity times. This was simply done by monitoring the changes in estimated delay times as a function of each tunneling activity time distribution. Figure 1.1 illustrates the general workflow that is described in this section.

1.4 Thesis Structure

This thesis is organized into seven chapters. Chapter 1 is the introduction to the topic and the objectives and methodology of this study. Chapter 2 discusses previous studies on TBM performance prediction in the literature. In Chapter 3, the operating logic and activity modules of the CSM2020 model are explained in detail. Chapter 4 discusses the tunneling activities that were observed during the data collection process at a TBM tunneling operation. The data collection process and geological information about the project site are also provided in the same chapter. Chapter 5 explains the modification process of CSM2020 to simulate the slurry TBM operation. This chapter discusses the creation of new time distributions and their statistical parameters in detail. After the validation process, the sensitivity analyses that were conducted on individual model modules are presented in Chapter 6. This chapter also provides the utilization of the model for different time distributions, changes in downtime contributions, and their evaluation for this study. Chapter 7 presents an overall discussion of the results, the conclusions of the study, and recommendations for follow-up studies.

CHAPTER 2

LITERATURE REVIEW

The first concepts of tunnel boring machines were developed as early as the 1840s to excavate the Thames Tunnel. Since then, the industry has grown rapidly along with the industrial revolution, and new technologies have been developed, including more advanced tools for tunneling. The underground work environment has become safer and more efficient, leading to faster tunneling. However, one thing that has not changed through time is the significance of the excavation or daily advance rate. Research and development on the fundamental parts of tunnel boring machines, such as new cutterhead designs and drive engines, provided increased penetration rates, thrust force, and advance rates. AR, however, can also be affected by other parameters, such as geological and geotechnical properties of the excavated ground, groundwater conditions, and crew experience.

AR is typically used to indicate daily advance rate. Using the AR, project duration and cost can be calculated (Alber, 2000). As a result, a target date for project completion can be developed, and schedules for project milestones can be made. AR has the highest priority among the parameters that must be determined after exploration studies and before the bidding process since it directly determines the completion time of a given tunnel and its related cost.

Numerous studies of TBM performance have been completed, and performance prediction models have been developed. Some of these models are more accurate in predicting the TBM performance and, as a result, are more accepted by the industry. Table 2.1 summarizes the performance prediction models presented in the literature.

Table 2.1: Summary of TBM performance prediction models in the literature.

Model References	Approach	Output
Roxborough and Philips (1975)	Theoretical	Cutter force
Ozdemir (1977)	Empirical	Cutter force
Nelson et al. (1983)	Statistical	ROP
Rostami and Ozdemir (1993)	Theoretical	ROP, U, and AR
Al-Jalil (1998)	Simulation	Project completion time and cost
Laughton (1998)	Statistical	AR, and U
Bruland (1998)	Empirical	ROP, U, and AR
Barton (2000)	Empirical	ROP, U, and AR
Yagiz (2002)	Empirical	ROP
Bernados and Kaliampakos (2004)	Simulation	AR
Kim (2004)	Simulation	U
Bieniawski (2007)	Empirical	AR
Yagiz (2008)	Empirical	ROP
Hassanpour et al. (2009, 2011)	Empirical	FPI based ROP
Khademi et al. (2010)	Empirical	RMR based FPI
Farrokh (2012)	Statistical	U
Frough et al. (2013)	Statistical	Downtime prediction
Rostami et al. (2014)	Simulation	AR
Frough and Torabi (2016)	Empirical	U
Rostami (2016)	Simulation	U
Mikaeil et al. (2018)	Simulation	ROP

The original Colorado School of Mines (CSM) model (Ozdemir, 1977) was developed by using an extensive database of laboratory testing results from the Earth Mechanics Institute (EMI), which represented an empirical solution to the problem. The CSM model focused on predicting the rate of penetration by using machine specifications, such as torque and thrust, and intact rock properties, such as rock strength and rockmass structure. The CSM model was mainly developed for hard rock conditions and is limited in predicting penetration rate for fractured rockmasses. In the 1980s, the CSM model database was broadened by gathering data from specific hard rock TBM sites. Eventually, this model was improved with further studies (Rostami & Ozdemir, 1993, Rostami, 1997, Yagiz, 2002, Yagiz, 2003) and has become capable of providing a reasonably accurate estimate of machine performance in a broader range of hard rock

conditions. However, with the technological advancements in tunneling and the emergence of new applications, the CSM model requires updates like any other model. The original and extended databases are based on cases utilizing old tunneling technology and therefore do not necessarily reflect the nature of current tunneling projects using TBMs.

Furthermore, the CSM model does not account for rock mass conditions, crew experience, unexpected delays due to geological conditions, or major breakdowns at the TBM. An advantage of using the CSM model rather than other utilization prediction tools is that the CSM model can evaluate conditions such as curves and slope of the alignment. The rate of penetration changes in curves along the alignment, which directly affects the advance rate. Muck transportation time changes with the slope steepness, which impacts the overall utilization due to possible delays, especially for projects using muck cars.

The Nelson model (Nelson, Al-Jalil, Laughton, 1994) was developed using an extensive database from 630 projects. The model uses this database to find and match similar properties of the new project and calculates penetration rate, cutter life, and project cost by using statistical methods. Depending on the available details of each project, the model divided projects into four levels, from Level 1 with less detailed data to Level 4 with the most detailed data. The main limitation of the Nelson model is directly related to the available information in the database it was based on.

The Laughton model uses a limited database of penetration rates and boring times. Regression analysis showed the relationship between two parameters: Unit Boring Time (UBT) and Unit Advance Time (UAT). Laughton (1998) showed that decreases in penetration rate result from an increase in boring time.

$$UAT = 0.286 + 1.2 \times UBT \quad (2.1)$$

A third parameter, Unit Down Time (UDT), is also used to calculate the machine utilization by dividing UBT into total time. To get these parameters, Laughton used recorded delays and their durations. These delays are associated with ground conditions, tunnel diameter (excavation of larger periphery takes more time), and properties of the excavated rock mass (such as frequency of discontinuities). Overall, the Laughton model can be considered as a pioneer for the probabilistic performance prediction approach since it used delay times and time distributions as an input parameter into the prediction model. However, the model's applicability is limited by the small database used in its development. Also, this model does not consider factors like machine specifications and crew efficiency.

The Norwegian University of Science and Technology (NTNU) model was first developed in 1976 for hydropower development projects in Scandinavian hard rock conditions. The 1998 version of the model was improved by Bruland (1998) using data from tunnels that are more than 200 kilometers in total length (Macias, Jakobsen, Bruland, Log, Grøvd, 2014). Further development of the model was carried out by Bruland (2000) and Macias (2016). Since the NTNU model is frequently updated (and has been more recently updated than most other models), it has an advantage in evaluating recent tunneling projects. This advantage has made the model widely accepted by the tunneling industry. It indirectly accounts for rockmass properties such as Q, RMR, RQD, joint orientation (fracturing factor, k_s), and intact rock properties such as UCS through Drilling Rate Index (DRI) and porosity. The model uses cutter thrust, cutter diameter, and average cutter spacing for machine parameters. Output parameters of the NTNU model are machine utilization, cutter life, advance rate, and excavation cost.

Furthermore, the NTNU model considers crew efficiency based on the tunnel length. However, it must be noted that the intact rock properties used in this model are not frequently

available in many projects. When available, they are used by incorporating them indirectly through some empirical charts. Also, the model does not account for groundwater inflow, which can dramatically change the utilization.

The QTBM model developed by Barton (2000) is an enhancement of the Q system, which is a widely accepted rock mass classification model developed especially for the Sequential Excavation Method (SEM) or the New Austrian Tunneling Method (NATM). The QTBM model is based on the data from 145 TBM tunnels (Barton, 2000). Just like the Q system, QTBM uses rock mass discontinuity properties and rock quality index (RQD), with the addition of new parameters such as joint inclination, quartz content, porosity, cutter life index (CLI), and biaxial stress on tunnel face to develop an AR prediction:

$$AR = PR \times T^m \quad (2.2)$$

AR: Advance Rate

PR: Penetration Rate

T^m: Utilization (m variable represents the negative gradient for the decelerating average advance rate by the tunneling performance of 145 TBM tunnels totaling more than 1000 km. T is the total time for excavation in hours.)

The QTBM method requires more than twenty parameters as inputs. A large number of input parameters complicates the calculation process. Moreover, the model does not consider machine specifications, and possible delays can be caused by the crew, logistics, machine backup systems, or the TBM itself.

Yagiz (2008) developed a formulation to calculate the rate of penetration primarily for jointed and fractured hard rock conditions. The equation uses UCS, rock brittleness (estimated via punch penetration test), the distance between discontinuities, and discontinuity set

orientations. Each parameter has a weighted constant representing its effect on the result, which was determined using regression analysis.

$$ROP \left(\frac{m}{h} \right) = 1.093 + 0.029PSI - 0.003UCS + 0.437Log(\alpha) - 0.219DPW \quad (2.3)$$

ROP: Rate of Penetration

PSI: Peak Slope Index (ratio of the maximum load (kN) to corresponding displacement (mm) of the indenter from the punch penetration test apparatus)

UCS: Uniaxial Compressive Strength

DPW: Distance Between Plane of Weakness

α : Angle Between Tunnel Axis and Planes of Weakness

However, this equation was developed using data from only one project, and there are no machine properties involved in the calculation, meaning that this model can be considered site-specific.

Hassanpour et al. (2011) developed a prediction model using data from various hard rock TBM operations, including tunnels in sedimentary, igneous, and metamorphic rocks. The model uses both single and multivariable regression techniques for field penetration index and rate of penetration and can be applied to a wide range of ground conditions. However, a user should exercise caution when applying the model to highly fractured rock masses and water-sensitive rock conditions (Hassanpour et al., 2011).

Khademi et al. (2010) used regression analyses to create a multivariate model based on the widely accepted RMR system input parameters to calculate FPI. However, this approach uses data from only one project, thus making it site-specific.

Farrokh (2012) presented two methods for calculating machine utilization. The first method uses a direct formula to calculate the advance rate. From there, utilization can be calculated by using the penetration rate:

$$AR = e^{3.67 - 0.0589UCS - 0.851D + 0.0285Dc + 0.0988M} \quad (2.4)$$

UCS: Uniaxial compressive strength (MPa)

D: Tunnel diameter (m)

Dc: Disc cutter diameter (in)

M: 1 for conveyor belt, 0 for muck cars

The second method presented by Farrokh focused on downtime analysis. It uses boring time and downtimes, such as TBM breakdowns, backup systems breakdowns, cutter changes, support installations, regripping, muck transportation, maintenance, ground-related issues, probe drilling, utility extensions, surveys, and other unclassified delays to calculate the utilization. The data for these activities come from more than 300 TBM projects. For the FPI, an indirect formula can be used if the required parameters are known:

$$FPI = EXP(1.97 + 0.0063RQD + 0.103CAI + 0.00685UCS) \quad (2.5)$$

$$ROP = \frac{0.06RPM \times Fn}{FPI} \quad (2.6)$$

RQD: Rock Quality Designation

CAI: Cerchar Abrasion Index

UCS: Uniaxial Compressive Strength (MPa)

RPM: Cutterhead Revolutions Per Minute

Fn: Normal Force Per Cutter (kN)

FPI: Field Penetration Index (kN/cutter) (mm/rev)

The Rock Mass Excavatability (RME) indicator was introduced by Bieniawski et al (2006) and further developed by Bieniawski et al (2007a), Bieniawski et al (2007b), Bieniawski et al. (2008). Just like the QTBM, RME is also an extension of another rock mass classification system called rock mass rating (RMR). RME evaluates similar tunnel sections based on their geotechnical properties. UCS, DRI, discontinuity frequency and orientation according to tunnel alignment, arching time, and water inflow are the main parameters for the RME rating calculations for each section. These ratings are used for the calculation of the average rate of advance (ARA) by the following formula:

$$ARA = 60 \times \left(\frac{RME}{100} \right) \times Cd \times Ce \times Cl + (0.23 \times RME) - 14.5 \quad (2.7)$$

Cd: Coefficient of excavation diameter (m)

$$C_D = 1.2058 - 0.0588D \quad (2.8)$$

Ce: Coefficient of crew efficiency

$$C_E = 0.5 + C_c + C_m + C_a \quad (2.9)$$

Where Cc is the experience of the contractor undertaking the job and changes between 0 to 0.2. Cm is the quality of the crew and changes between 0 to 0.15. Ca is the logistic conditions of the project site and changes between 0 to 0.15.

Cl is the coefficient of the crew learning period. It depends on the length of the tunnel to be bored and varies between 0.85 and 1.

RME is based on a limited database, which limits the application of this method to a narrow range of similar tunneling projects. Also, RME assumes that individual tunnel sections along the alignment cannot have machine utilization of less than 30%. Furthermore, RME does not consider the impact of TBM breakdowns, interventions, and ground-related delays.

Frough and Torabi (2016) developed a model that allows for geology and rock mass related downtimes (GRRD) and machine utilization to be estimated using the rock engineering systems (RES) approach with interaction matrix methodology (Hudson, 1992). The model considers parameters such as instability potential, discontinuity spacing, the orientation of discontinuities, UCS, groundwater, presence of clay and sticky materials, rock abrasion, squeezing, mixed face conditions, and poisonous gases as the factors that have the most impact on downtimes and utilization. Among these factors, instability potential represents any type of face instability, raveling, or collapse. Clay and sticky materials drive the risk of clogging and issues with muck transportation. Rock abrasion accounts for disc wear and tear due to abrasive minerals or high quartz content. Frough and Torabi (2016) calculated geology and rockmass related downtimes index (GRDI) values for each rockmass unit along the tunnel alignment considering these factors. Once the GRDI values are estimated, it is possible to calculate the GRRD based on a regression analysis, allowing the calculation of utilization with other delays such as machine-related.

Recently, simulation tools and numerical models are gaining more popularity due to their flexibility and capability of evaluating the combining effects of numerous factors that are crucial to consider during the calculation of utilization and advance rate. Al-Jalil (1998) was the first to implement a simulation approach. Al-Jalil used three programs for discrete event simulation that were initially developed by Einstein et al. (1989) and combined them with the database assembled by Nelson et al. (1994) for the creation of an integrated set of tools for the identification of TBM-based excavation systems. The final outputs of the Al-Jalil model are probability density functions for the time to complete tunneling and the total cost. These outputs also allow engineers to determine an overall project completion time and cost.

Bernardos and Kaliampakos (2004) used an artificial neural network (ANN) to model AR concerning geological and geotechnical conditions. The ANN allows the identification and understanding of both the way and extent to which the involved parameters affect the tunneling process. However, the model was developed using data from only one tunnel. Kim (2004) used the fuzzy logic method to generate a utilization prediction model. This model was changed into a new model by Mikaeil et al. (2018) to calculate the penetration rate. Gong et al. (2005, 2006) implemented numerical modeling to evaluate the effects of joint spacing on rock fragmentation by TBM cutters, which eventually developed a rock mass characteristics model for ROP prediction (Gong et al., 2009). Rostami et al. (2014) and Rostami (2016) used discrete event simulation to evaluate AR, U, and tunneling activity time distributions of hard rock TBMs. Models using artificial intelligence were developed recently by some researchers, including Grima et al. (2000), Okubo et al. (2003), and Gholamnejad et al. (2010). The complex structure of artificial intelligence, which mimics the human brain, can learn and adapt to new situations after learning from past project data. These studies pointed out that process simulation software has a promising potential in evaluating TBM performance.

Finally, Khetwal et al. (2019) conducted sensitivity analyses on tunneling activities regarding the utilization factor with discrete event simulation (DES). This study was the first step towards the creation of the CSM2020 model. Khetwal et al. (2019) also evaluated the impact of geology on muck transportation by simulating TBM operations. Furthermore, Khetwal et al. (2020) investigated the effects of TBM downtimes on utilization based on sensitivity analyses. Also, Khetwal et al. (2020a) compared the DES approach with some of the existing empirical models. As the final product of these studies, the CSM2020 model was presented by Khetwal (2020). In the next chapter, the CSM2020 model is explained in detail.

CHAPTER 3

CSM2020 TBM PERFORMANCE PREDICTION MODEL

The need to evaluate the impacts of combined effects of various parameters such as machine type and backup system, geology, and specific tunneling activities on TBM performance led to the development of the CSM2020 model. Khetwal (2020) introduced the CSM2020 discrete event simulation model using the Monte Carlo modeling to evaluate the stochastic nature of tunneling activities in Arena® software. Arena® is a process simulation software used in a wide range of industries and modeling industrial processes. The flexibility of the software enables the simulation of tunneling activities as modules, which are interconnected with each other. These connections can be arranged as series or parallel activities, considering that most mechanized tunneling activities depend on another tunneling activity. For example, segment installation cannot happen on a single shield machine before boring for a given ring finishes. On the other hand, some activities can coincide, which means they can be considered parallel activities. Arena® is capable of simulating activities both in series and in parallel with respect to each other, which is an essential factor to consider for modeling TBM tunneling operations.

However, deciding which activities will be parallel and which ones will be in series can be complicated for a tunneling process. Especially from the downtime allocation perspective, breakdowns, malfunctions, or other delays can coincide. Creating a model with the proper interdependencies can be challenging due to the uncertainty of the nature of downtimes. Since the user must create individual modules to represent each activity, the relationships between modules will be a complex web of interconnections.

Arena® is based on a series of fundamental building blocks, such as Entities, Attributes, Variables, Resources, Statistical Accumulators, and Events (Kelton et al., 2015). Each of these is described in the following paragraphs.

Entities are dynamic objects that travel within the models during runs. They visit modules that can represent different kinds of activities. CSM2020 uses one entity to carry out operations during the model run and another one named “Shift” to represent shifts.

Attributes characterize the entities by attaching to them, such as defining a color, priority, or even due date. Attributes can have values depending on the entities since the definition of every entity may require different characteristics. The CSM2020 uses attributes to define delays, TBM types, crews, and transportation options, such as conveyors or muck cars.

Variables provide information about the system that is simulated. They are usually global and don't change according to entities. All entities can access them. The CSM2020 doesn't describe any specific variables, but it uses some built-in variables, such as the simulation clock. In CSM2020, the simulation clock keeps track of the total time spent according to a defined total number of shifts before running the model.

Resources represent elements to be used by the entities during the operations, such as crew, equipment, and storage area. The CSM2020 uses resources to define processes, such as boring, segment installation, utility extension, shotcrete, etc., that are placed in modules. These processes use the resource with the same name to simulate the tunneling activities and delays. Some of them use more than one resource. For example, the “water inflow troubleshoot process” module uses resources such as shotcrete, waterproofing membrane, bolt drill, bolt strap channel, and grout.

Statistical Accumulators record various information based on how they are defined. The CSM2020 uses these accumulators to record cumulative time spent by each activity (value-added time), how long the modules are kept busy (number busy), and so on.

Events simulate operations, activities, and their occurrence. Events are shown to happen instantaneously within the model; however, their durations are recorded. When an entity enters a module, it starts the event. The entity spends time within the module before its departure, and this time is added to the simulation clock. However, the entity only spends a second within the module in real-time. The time spent between an entity's entrance into the module (not its arrival, because it might spend time in the queue recorded as waiting time) and departure from it corresponds to the duration.

Furthermore, additional concepts, such as Number Scheduled, Number Busy, Value Added (VA) Time, Instantaneous Utilization, Scheduled Utilization, and Number In/Out, need to be explained to understand the operation of the CSM2020. These concepts define how the CSM2020 provides its output and are essential to understand.

“Number Scheduled” can be described as the total amount of available resources at a given time to carry out an operation, such as a tunneling activity. “Number Busy” refers to how many resources are being used throughout this operation. “VA Time” is a record of how much time was spent to complete the operation. “Instantaneous Utilization” corresponds to the utilization at each instant (operation), and “Scheduled Utilization” is the overall utilization through the combination of operations. Lastly, Number In & Out are the entity arrival and departure records to/from each module.

$$\text{Instantaneous Utilization} = \frac{\text{Number Busy}}{\text{Number Scheduled}} \quad (3.1)$$

$$\text{Scheduled Utilization} = \frac{\text{Average Number Busy}}{\text{Average Number Scheduled}} \quad (3.2)$$

To illustrate, two simple cases that describe the operation of a factory are used to explain these concepts with an example. In both cases, each shift takes 4 hours.

Table 3.1 presents data on each parameter with further calculations.

Table 3.1: Example Case A and B showing how instantaneous and scheduled utilization is calculated per Arena®

	Case A		Case B	
	Shifts (4 hours each)		Shifts (4 hours each)	
	1	2	1	2
Number Busy	50	50	50	50
Number Scheduled	150	150	200	100
Total Hours Busy	50 * 8 = 400		50*8 = 400	
Total Hours Scheduled	150 * 8 = 1200		(200*4) + (100*4) = 1200	
Avg. Number Busy	(50 * 8) / 8 = 50		(50*8)/8 = 50	
Avg. Number Scheduled	(150 * 8) / 8 = 150		((200*4) + (100*4))/8 = 150	
Scheduled Utilization	50 / 150 = 33.3%		50 / 150 = 33.3%	
Instantaneous Utilization	(33.3 * 8) / 8 = 33.3%		(((50/200) *4) + ((50/100) *4))/8 = 37.5%	

The CSM2020 uses the same “Number Scheduled” for all activities, which is 1. Also, “Number Busy” is not defined before the model runs; instead, it is calculated as an output. Because of these reasons, “Instantaneous Utilization”, “Scheduled Utilization”, and “Number Busy” parameters are the same in every model run.

Moreover, the CSM2020 uses the total number of shifts as an input. Users must define the number of shifts required to finish the desired tunnel length. This input is directly related to the calculation of utilization by the model because Arena® uses the simulation clock to determine the total time spent to complete the simulation. As mentioned earlier, the simulation clock equals the whole duration of the number of shifts defined before running the model. The model divides the time spent for tunnel boring activity into simulation clock to calculate TBM utilization. This approach creates high likelihood to make mistakes, because the user must input the total number of shifts before running the model to get a reasonable machine utilization. This situation means that the model does not concern about the time spent on the other activities because the simulation clock is equal to the duration of the total number of shifts. The model does not consider any activity duration (except boring), given under “VA Time” records. Unless the duration of all the shifts is equal to the cumulative “VA Time” of all the activities and delays, it is impossible to expect correct utilization rates from the model. According to this model setup, the number of shifts should be changed every time the model is run. This is especially important for sensitivity analyses where the variables are changed and run the model. The user is expected to predict the model outcome (“VA Time” values) and adjust the number of shifts to match and get the correct utilization rate.

Instead of adjusting the number of shifts at each model run, one can simply calculate the utilization rate manually. For the manual calculation, the total sum of “VA Time” records of each activity should be considered. The user can get the utilization rate by dividing the “VA Time” for tunnel boring by total “VA Time”.

Having described the basics of Arena® and their use in the CSM2020, other model settings can be discussed. Importantly, in CSM2020, modules are the main components of the

model and represent various tunneling events. These modules use two individual variables to define their relative activities, such as frequency and a probability distribution.

The frequency of occurrence must be defined for each module by dividing the total number of data points for the relevant activity into the total number of strokes required to complete the simulated tunnel. Unfortunately, the CSM2020 model cannot simultaneously evaluate individual modules with various frequencies of occurrences. This limitation is significant to note regarding downtime analysis. Depending on the frequencies of the modules, the model selects one of them and applies the predefined time delay per the probability distributions. Figure 3.1 shows tunneling activity modules and their interdependencies regarding their sequencing in the model.

Modules that represent tunneling activities in the model are individually given a probability density function. Each function provides a range of values for the duration of the relevant tunneling activity. These durations are considered as delays in the tunneling process if they prevent boring activity. Modules let a user select the type of delay distribution. The delay distribution type can be either Constant, Normal, Triangular, Uniform, or an Expression, such as Exponential, Gamma, Lognormal, and Poisson. Also, the unit for the duration can be selected as either seconds, minutes, hours, or days. These distributions are classified based on their shape, scale, threshold, or location. Figures 3.2 and 3.3 provide graphical examples for the time distributions and their applicability.

For the Constant delay time, the user can only define one value. This value is used by the model for that module and applied in every cycle. If that module's desired duration of the simulated delay is always the same, then this delay type can be used.

Parameters	Activities	Series / parallel with boring process
Excavation	Boring	-
Ground troubleshooting	Rock bolts installation	Series / parallel
	Wire mesh installation	Series / parallel
	Grouting	Series
	Rockfall clear at invert	Series / parallel
	Clean cutterhead	Series
	Cutter inspection	Series
	Cutter change	Series
	Segment installation	Series / parallel
	Water proofing membrane installation	Series / parallel
	Regrip	Series
	Probe drilling	Series
	Shotcrete	Series
	Other ground troubleshooting	Series / parallel
	Maintenance	Routine maintenance
Regular Clean TBM		Series
Utilities	Mechanical	Series
	Electrical	Series
	Hydraulic	Series
	Water pipe	Series
	Ventilation cassette installation	Series
	Power cable stacking	Series
Transportation	Waiting for train	Series
	Derailment delays	Series
	Train pass delays	Series
	Track placement and repair	Series
	Muck dumping	Series
	Supplies delay	Series
Survey	Surveying delay	Series
Miscellaneous	Shift change	Series
	Safety meeting / daily progress meeting	Series
	Lunch break	Series
Unexpected breakdown	Other Unexpected delays	Series
	Failure of equipment	Series
Crew	Effect of crew	-

Figure 3.1: CSM2020 model tunneling activities as modules and their activation process with boring (Khetwal, 2020) (Reprinted with permission).


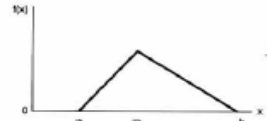
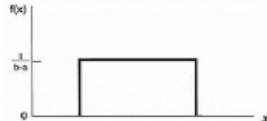
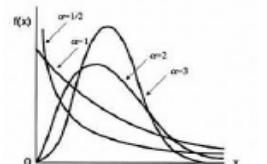
Distribution types	Expression	Range	Applicability
 <p>Poisson</p>	POIS (Mean(λ))	{0, 1,}	Used to represent events that occur in fixed time interval. Is not appropriate for time allocation of tunneling activities.
 <p>Triangular</p>	TRIA (Min(a), Mode(m), Max(b))	[a,b]	Limited data available, only minimum, maximum and mode can be interpreted
 <p>Uniform</p>	UNIF (Min(a), Max(b))	[a, b]	Used when no information other than range is available
 <p>Weibull</p>	WEIB (β, α) β = Scale parameter α = Shape parameter	[0, $+\infty$)	It is versatile and used to represent positive task times for systems with large parts that fail independently.

Figure 3.2: Some of the time distributions used in CSM2020 and their applicability (Khetwal, 2020).

For the Normal delay time, the model considers a normal distribution for the predefined data using the mean value and standard deviation. Before selecting this delay type, the user must verify that the dataset for the relevant tunneling activity conforms to the desired distribution. In other words, the actual delay times associated with the module have a normal distribution.

For the Triangular delay distribution, the user defines the minimum, maximum, and most likely value (mode). This delay type should be used when no other distribution adequately represents an individual dataset. The triangular distribution typically represents the lack of detailed information for the associated dataset but known limits and the most expected outcome.

For the Uniform delay time, the user defines the minimum and the maximum value for the distribution. The uniform distribution is appropriate when the probability of occurrence of each outcome within the data range is the same.

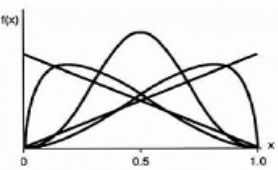
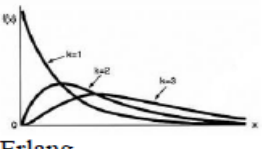
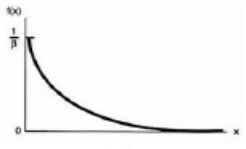
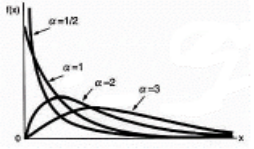
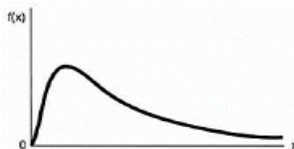
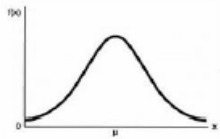
Distribution types	Expression	Range	Applicability
 <p>Beta</p>	$B(\beta, \alpha)$ $\beta, \alpha =$ Shape parameters	[0,1]	Range limits its applicability for tunneling activities as the time allocation can be more than 1 hour
 <p>Erlang</p>	ERLA (ExpMean (β), k) k = Exponential random variables	[0,+ ∞)	In case the activity time is integer, it is used to represent task completion time. Since the time allocation is given in hours, integer values are not fully representative
 <p>Exponential</p>	EXPO(Mean (β))	[0,+ ∞)	Inappropriate for modeling process delay times
 <p>Gamma</p>	GMM(β , α) $\beta =$ Scale parameter $\alpha =$ Shape parameter	[0,+ ∞)	Used in representing task completing time
 <p>Lognormal</p>	LOGN(LogMean (μ), LogStd (σ))	[0,+ ∞)	Used to represent positive quantities like task times that are skewed to right. Can give very large processing time and can cause misrepresentation
 <p>Normal</p>	NORM (Mean (μ), StdDev(σ))	(- ∞ , + ∞)	It is not used for positive values like processing times.

Figure 3.3: More time distributions used in CSM2020 (Khetwal, 2020).

For the Expression type of distribution for delays, the user can select one of the following probability distributions: Exponential (EXPO), Erlang (ERLA), Beta (BETA), Gamma (GAMM), Johnson (JOHN), Lognormal (LOGN), Poisson (POIS), and Weibull (WEIB).

Exponential distributions represent events that occur continuously and independently at a constant rate. For this reason, this distribution type is not suitable to use as a tunneling activity duration type in the models. The Erlang distribution is a sum of k , a positive integer described as the shape of the distribution, independent exponential variables with mean $1/\lambda$, which λ is a positive real number as a scale. This type of distribution considers waiting times in queueing systems, thus can also be used to calculate the delay time for the stochastically natured tunneling activities. The Beta distribution can consider only two possible outcomes: success or failure. It may not be the best distribution for the delay times since it is mainly concerned about the values at the extreme ends of the dataset. The Gamma distribution is suitable for evaluating continuous variables that are always positive. The Johnson distribution is a transformation of actual field data by normalization. It normalizes the dataset to follow a normal distribution and is unsuitable for use as a distribution type. The Lognormal distribution occurs when the mean of the dataset is low, but the variance is high (i.e., for bounded data sets; also, for data sets where values vary over multiple orders of magnitude). The Poisson distribution can be used to show how many times an event occurs within a specific period. It is not suitable to be used as a delay type due to the stochastic nature of tunneling activities. Finally, due to its flexibility and capability to evaluate various applications, Weibull distribution is a suitable option to use as a delay distribution expression. It is a continuous probability distribution that can fit a variety of datasets observed in the field. It is similar to the normal distribution in this sense; however, it can model skewed data, unlike the normal distribution.

Table 3.2 shows CSM2020 modules, corresponding original time distributions, and the units. Khetwal (2020) used data from eight different projects to create these distributions.

Table 3.2: Time distributions used by Khetwal (2020) in CSM2020 model.

Module	Time Delay Type	Distribution	Unit
Safety Meeting	Expression	LOGN (1.4,0.07)	Hours
Crew A delay	Triangular	(0, 10, 20)	Minutes
Crew B delay	Triangular	(0, 20, 30)	Minutes
Crew C delay	Triangular	(10, 20, 30)	Minutes
Crew D delay	Triangular	(15, 30, 45)	Minutes
Face backup cutter inspection	Triangular	(0.25, 0.5, 1)	Hours
Tunnel Boring	Triangular	(10, 15, 30)	Minutes
Segment Installation	Expression	GAMM (2.805,2.547)	Hours
Shotcrete	Expression	GAMM (1.085,2.781)	Minutes
Grouting	Expression	GAMM (3.041,0.7055)	Minutes
Wiremesh	Expression	GAMM (1.335,3.517)	Minutes
Bolt drill	Expression	GAMM (1.132,1.086)	Hours
Bolt strap channel	Expression	3 + WEIB (10.5, 1.4)	Hours
Ribs lagging	Expression	LOGN (3.4,0.067)	Hours
Gripper rock reaction	Expression	GAMM (1.132,1.086)	Hours
Scaling muck jam	Expression	LOGN (1.144,0.2709)	Hours
Clearance	Expression	3 + LOGN (1.22, 0.519)	Hours
Water inflow	Expression	GAMM (4.732,1.023)	Hours
Cutter change	Expression	GAMM (2.950,0.8533)	Hours
TBM maintenance	Expression	LOGN (1.94,0.11)	Hours
TBM electric systems	Expression	LOGN (2.54,0.09)	Hours
TBM hydraulics	Expression	LOGN (2.54,0.09)	Hours
Cutterhead motors	Expression	GAMM (2.726,0.8780)	Hours
Track placement and repair	Expression	LOGN (1.49,0.03)	Hours
Loading and unloading	Expression	GAMM (2.297,1.020)	Hours
TBM backup derail	Expression	LOGN (1.4,0.002)	Hours
TBM backup utilities	Expression	3 + GAMM (22.7, 0.762)	Hours
TBM backup car pass	Expression	GAMM (2.213,1.361)	Hours
Shaft operations	Expression	3 + ERLA (10.7, 2)	Hours
Trailing conveyor	Expression	LOGN (4.13,0.21)	Hours
Probe Drill (30 m)	Triangular	(5, 5.5, 6)	Hours
Probe Drill (25 m)	Triangular	(5, 6, 7)	Hours
Probe Drill (10 m)	Expression	GAMM (3.336,1.445)	Hours
Ventilation extension	Expression	LOGN (2.27,0.05)	Hours
Power cable extension	Expression	LOGN (2.27,0.05)	Hours
Water pipe extension	Expression	LOGN (2.27,0.05)	Hours

Table 3.2: Continued.

TBM conveyors	Expression	LOGN (4.13,0.21)	Hours
California switches 1, 2, 3	Constant	3	Minutes
Survey	Expression	LOGN (1.93,0.12)	Hours
Maintenance	Expression	GAMM (0.7531,7.213)	Hours
Unforeseen delays	Triangular	(0.5, 1, 1.5)	Hours
Transfer through portal	Uniform	(0, 2)	Minutes
Dump muck	Triangular	(10, 15, 25)	Minutes
Back to portal	Uniform	(0, 2)	Minutes

The CSM2020 model is developed based on delay data of hard rock TBM tunneling (Khetwal, 2020) and is applicable for open, double shield, and single shield machines working in open mode (not pressurized face). The model uses tunneling delay times as input data and provides machine utilization as the output. As was mentioned earlier, these durations must be introduced to the model as time distributions. For that purpose, raw data can be used to create distribution fitting plots. The creation of time distributions will be explained in more detail related to the model validation process described in Chapter 5.

Each cycle of the CSM2020 model represents one stroke or push. As the simulation covers the desired tunnel distance, the model evaluates each module during every machine stroke. If any of these modules cause any delays by preventing the boring, such as ring build, breakdowns, etc., the model applies the delay per the defined time distribution. After each stroke, the model calculates the utilization value. Therefore, the time distributions are essential and must be created with caution before using the model. In addition, this model also accounts for the distance of the face from the portal with each stroke. Distance increases per the defined stroke length after each cycle. When the model completes enough cycles to cover the desired tunnel length, it will also check the number of shifts defined and stop the cyclic process of a stroke; this entire process constitutes a single “replication”. Each replication is an individual simulation of

the whole tunnel length defined by the user. Khetwal (2020) suggests 50 replications per model run for optimum results. Using different iterations (5, 10, 25, 50, 100, 250, 500, 1000) for the same model and observing the results, Khetwal (2020) determined that the model output was not sensitive to the changes in the number of iterations above 50.

For calculation purposes of machine utilization, the model uses the following equation for each push (Khetwal, 2020):

$$Utilization (U \%) = \frac{Tb}{Tb + Tg + Tm + Tu + Tt + Ts + Tub + To + \dots} \times 100 \quad (3.3)$$

Tb: Boring time (excavation time)

Tg: Ground related delays

Tm: Maintenance delays

Tu: Utility extensions

Tt: Transportation-related delays

Ts: Survey

Tub: Unforeseen delays

To: Other activities

Figure 3.4 provides the model's flowchart during the tunneling simulation process. Following the flow of the steps, the model checks each module for predefined settings, which the user arranged before running the model and processes the relative actions accordingly. For example, suppose the user enabled the probe drilling activity. In that case, the model will perform this activity (which also means applying the relative delay by the predefined time distribution) and will continue to check if utility extension is required or not.

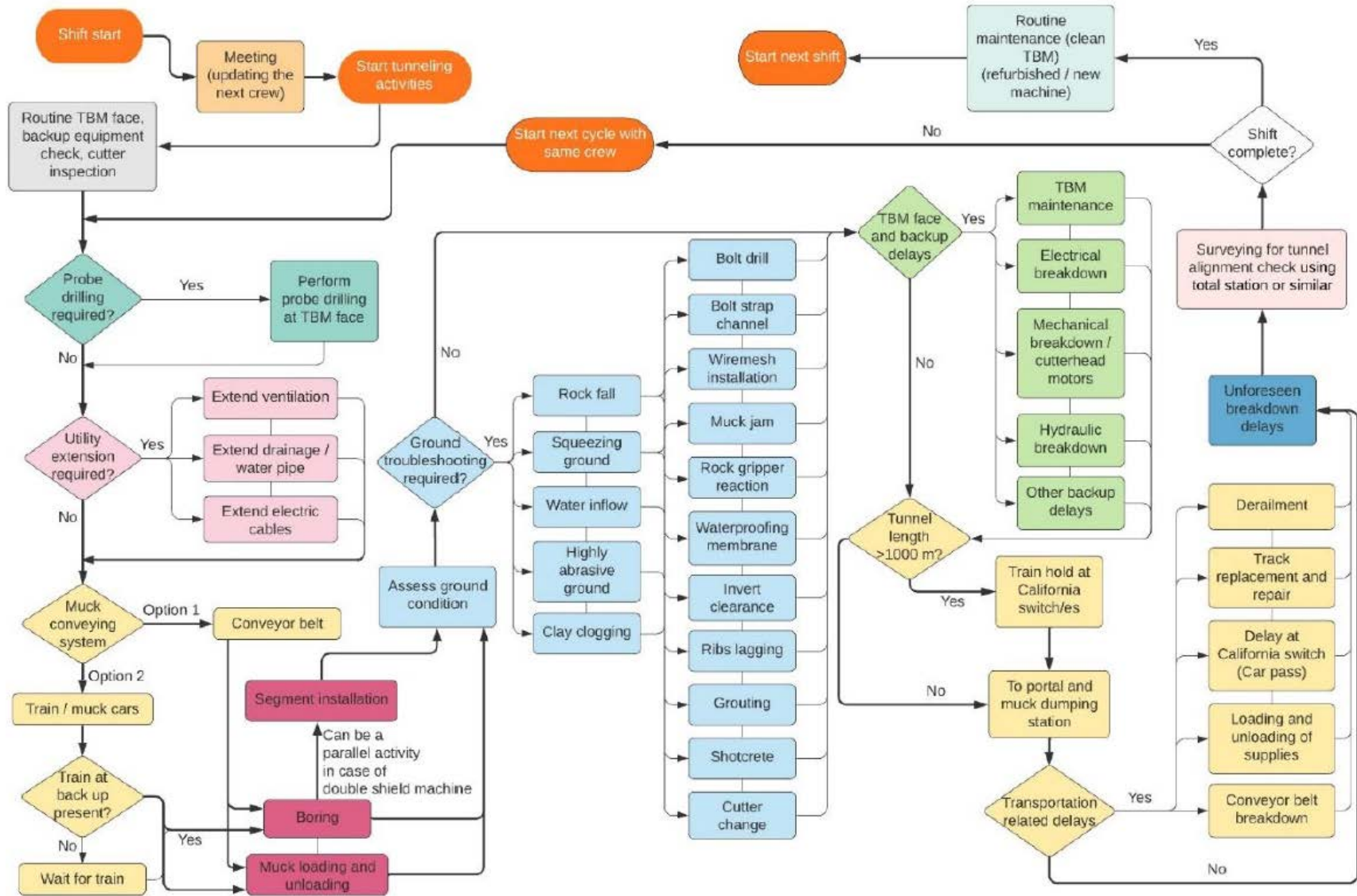


Figure 3.4: Summarized flow chart for CSM2020 model (Khetwal 2020) (Reprinted with permission).

It is important to note that the flow of the model tries to mimic a regular hard rock TBM operation. Tunneling activities that can occur in a hard rock TBM operation, such as probe drilling, utility extension, tunnel excavation, muck transportation (via conveyor belt or muck cars), support installation (precast segments, rock bolts, wiremesh, shotcrete, and steel arches), surveying, maintenance, logistic activities (train passes at California switches, loading and unloading of supplies, and rail extensions), and repairs are represented by interconnected modules.

These modules represent the actions that need to be taken to solve the related problems. For example, suppose the user enables the rock fall module. In that case, the model will activate the wiremesh installation, bolt drilling, bolt installation, and shotcreting activities to apply proper delays introduced via pre-defined time distributions to the current push. These activity modules were divided into two groups by the developer. The first group of activities represent ground-related problems, such as rockfall, ground squeezing, water inflow, and clay clogging. The second group represents TBM-related problems, such as electrical, hydraulic, and cutterhead motor issues.

Figure 3.5 shows the model interface for shift start, TBM type selection (single shield, double shield, open), tunnel boring, segment installation, and ground-related delays.

The model starts with a shift meeting module. After applying the delay for this module, it evaluates the crew efficiency if the user enables it. The user can define different crews and corresponding efficiency modifiers as time distributions to apply a desired amount of delay. After evaluating the crew efficiency, the model checks if the probe drilling module is active or not. If active, the model goes through a sub-section of the model shown in Figure 3.6, applies the necessary delay, and continues to look for utility extensions.

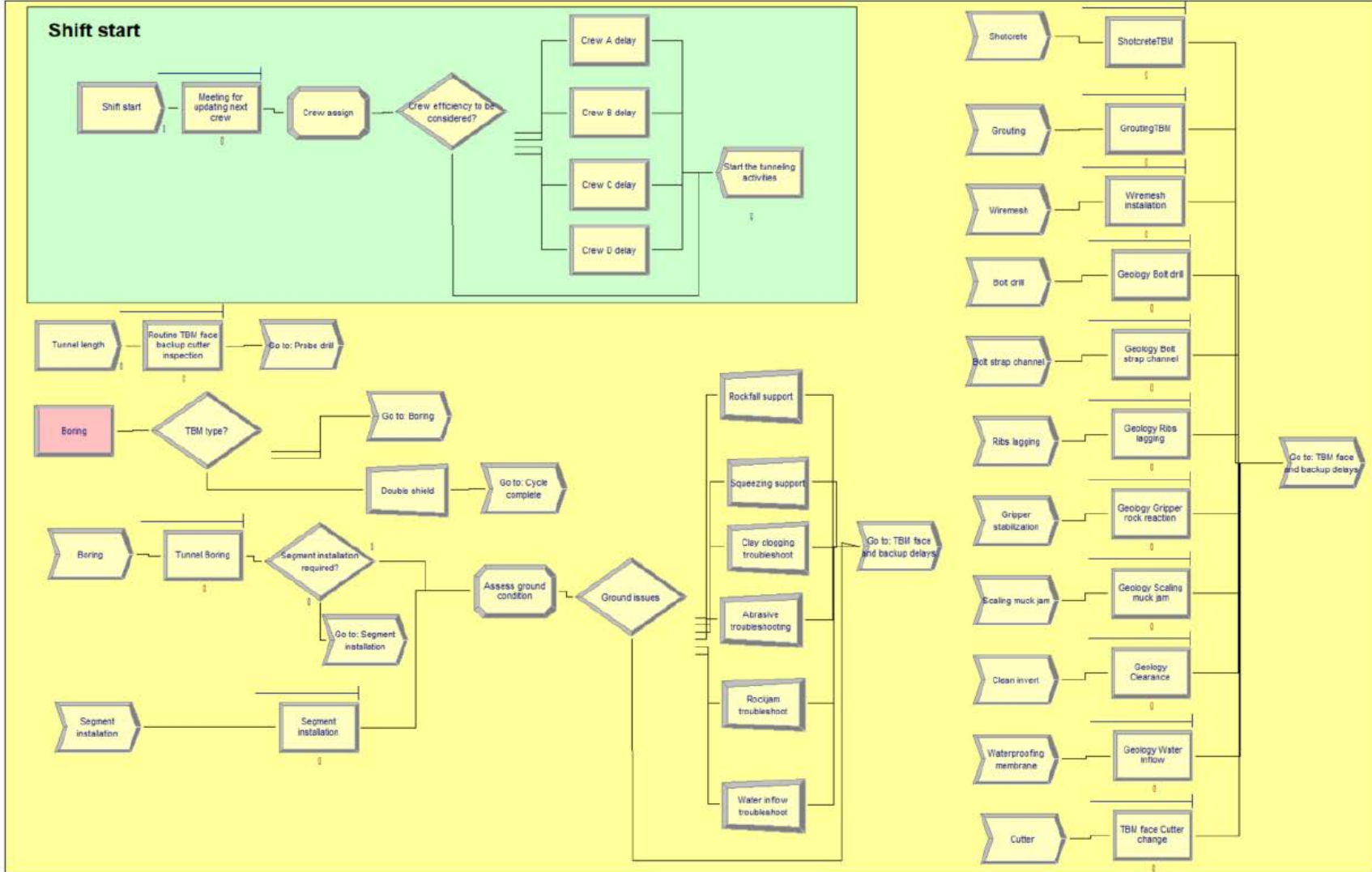


Figure 3.5: Modules through shift start to segment installation and ground-related delays.

There are three utility types in this sub-section of the model: Ventilation, power cable, and water pipe. Utility extensions are applied at the predefined excavated tunnel length intervals. If the excavated length of the tunnel matches with any of those numbers, the model applies delay(s) per the relative time distributions.

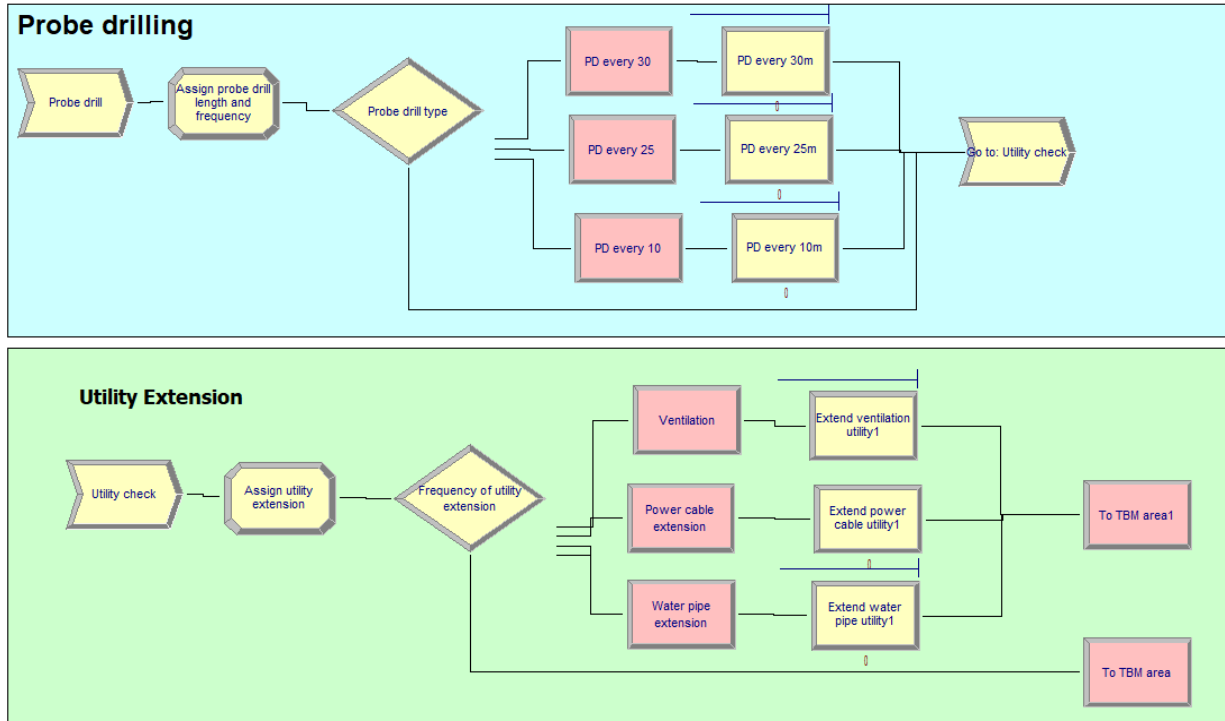


Figure 3.6: Sub-sections and modules for probe drilling and utility extension.

After the utility extension check, the model starts the tunneling process by selecting the machine type. The user can choose between a single shield, a double shield, or an open-type TBM. If the double shield is selected, the model simultaneously activates the tunnel boring and the segment installation modules. If the single shield is selected, the model activates the tunnel boring module first. After that, the segment installation module gets activated. If the open-type is selected, the model goes through the tunnel boring module and activates the segment installation module depending on a user-defined frequency for installation of the precast segments.

Following the boring and segment installation processes, the model looks for ground-related issues. If there are any active ground-related issues, the model goes through the relevant delay modules to apply delays, such as installing wiremesh and drilling for rock bolts. As the next step, the model checks for any breakdowns caused by the TBM itself, such as hydraulic and electrical problems. After that, the model continues looking for any backup-related delays, such as backup utility issues, train derailment, shaft, surface operations, etc. The model interface for these modules is illustrated in Figure 3.7.

At the last part of the cycle, the model checks for the requirement of California switches if muck cars are used instead of a conveyor belt. The model puts an extension at the desired tunnel length interval if the conveyor belt is used. Finally, the model applies delays caused by the surveying and any unforeseen problems, and the next cycle starts. The interfaces of the sub-sections for muck transportation, surveying, and unforeseen delays are illustrated in Figure 3.8.

As can be seen, some modules run in parallel with the boring activity, which means that the corresponding activities are happening simultaneously as excavation. However, most of the modules are connected in series. These modules refer to the tunneling activities bound to another tunneling activity. Thus, they happen sequentially. The CSM2020 model uses this logic to simulate the tunneling cycle and related activities in the correct order. The model uses “entities” as dynamic objects and describes their “arrival” to the modules for each shift cycle. Arrivals in different modules also represent the relative tunneling activity occurrences. The CSM2020 model is a combination of individual modules. Each module has its contribution and importance. Therefore, the working principles of the modules are described in the following paragraphs.

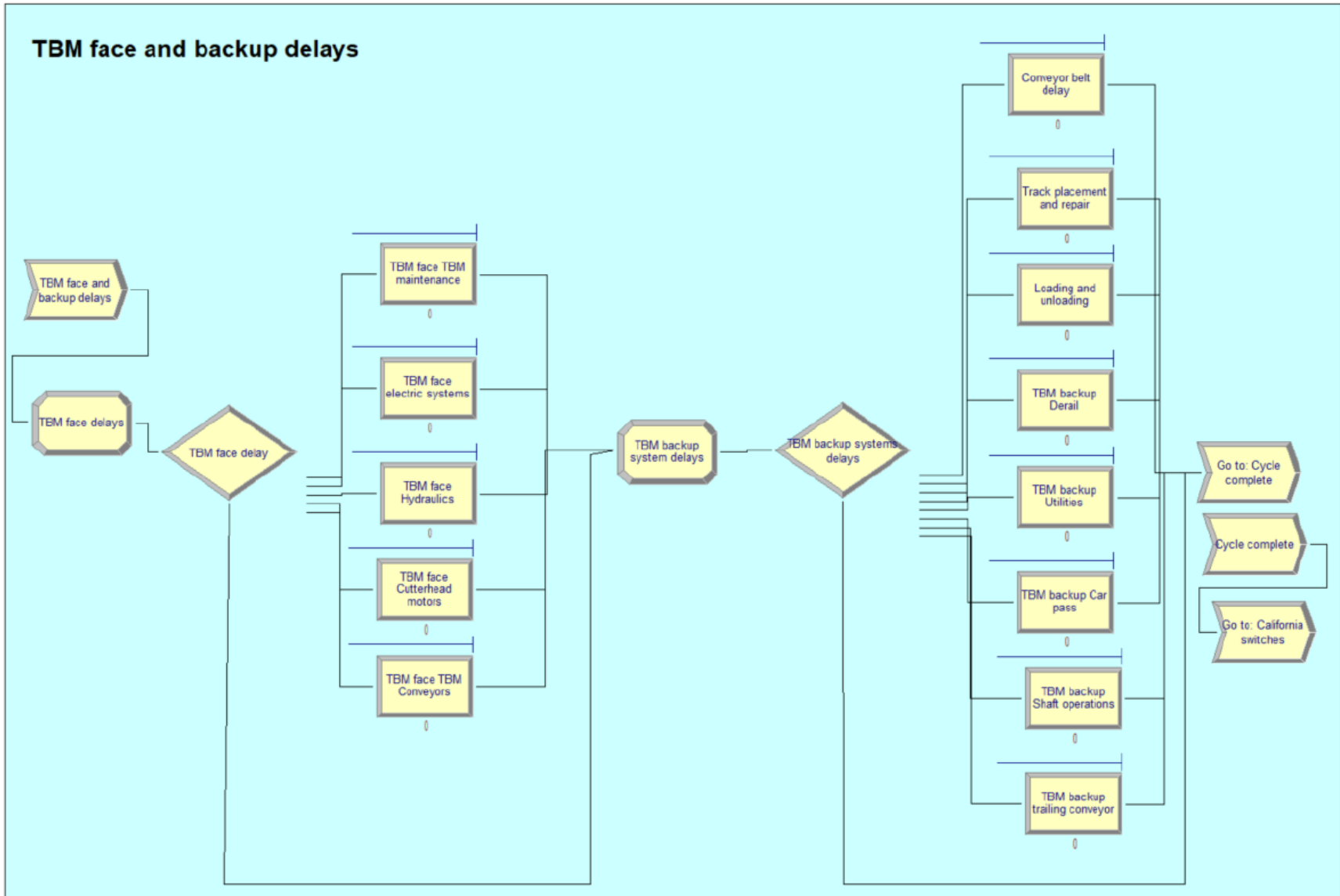


Figure 3.7: Modules for TBM face and backup system delays.

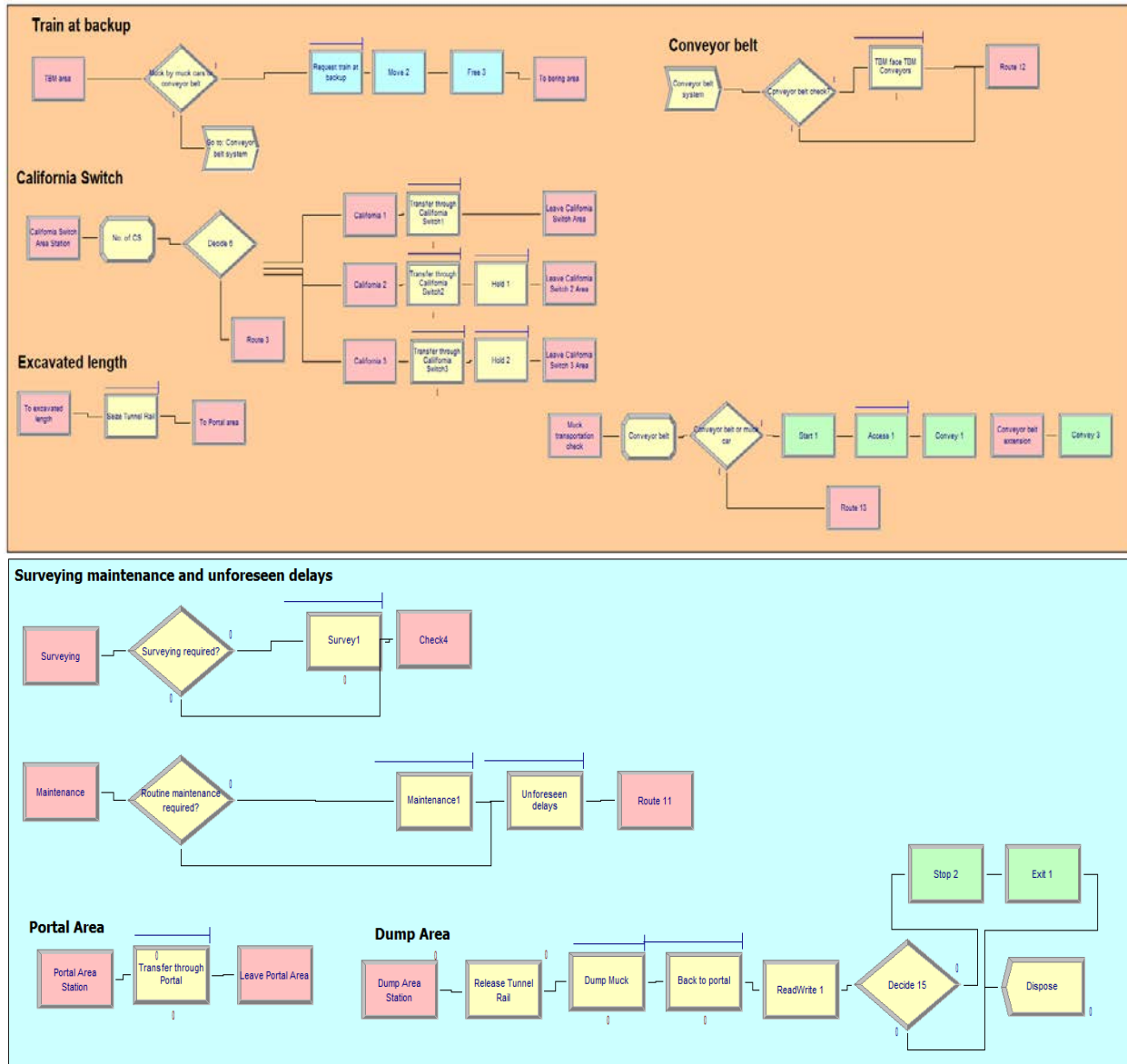


Figure 3.8: The model interfaces for muck transportation, surveying, and unforeseen delays.

The first module is “Shift Start”, and it describes the shift hours and how many shifts are required to finish the desired tunnel length. This module is verified by another module called “Tunnel Length”. First, the user must decide on the tunnel length to be modeled. The tunnel length used in this study was 348 m (1142 ft). Next, the tunnel length needs to be divided by the

length of one complete stroke, which in the project that is studied is the same length as the segmental liner (1 ring), or 1.524 m (5 ft) long.

$$\frac{348}{1.5} = 232$$

According to the calculation, 232 rings must be built to complete a 348-meter-long tunnel. The average push duration must be defined within the “Tunnel Length” module, which was 47 mins for this study. This duration determines how many pushes can be made during a shift, with 100% utilization. That’s why the user must evaluate this number and determine the number of shifts required to finish the simulated tunnel length. As mentioned earlier in this chapter, this is counterintuitive with using the model as a prediction tool. One can simply provide an extreme number for the shifts and use manual utilization calculation. Figures 3.9 and 3.10 show module interfaces of Shift Start and Tunnel Length.

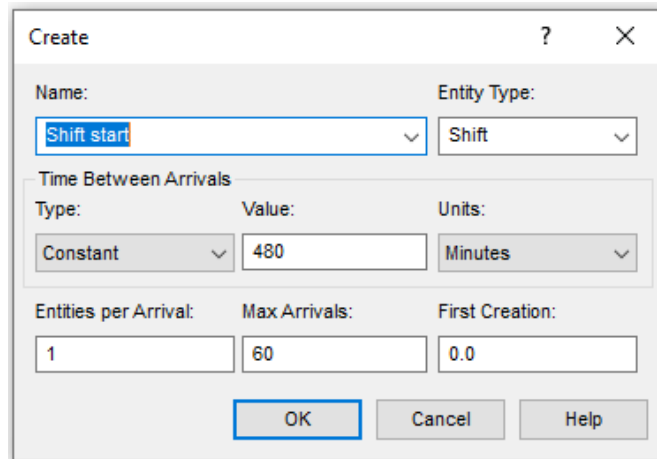


Figure 3.9: Shift start module.

After the shift start, the model activates the “Meeting for Updating Next Crew” module. This module represents the safety meetings and updating the next crew regarding the current

tunneling processes. The interface for this module and the time distribution expression are shown in Figure 3.11.

The 'Create' dialog box is titled 'Create' and contains the following fields and controls:

- Name:** A dropdown menu with 'Tunnel length' selected.
- Entity Type:** A dropdown menu with 'Entity 1' selected.
- Time Between Arrivals:**
 - Type:** A dropdown menu with 'Constant' selected.
 - Value:** A text input field containing '47'.
 - Units:** A dropdown menu with 'Minutes' selected.
- Entities per Arrival:** A text input field containing '1'.
- Max Arrivals:** A text input field containing '232'.
- First Creation:** A text input field containing '0.0'.

At the bottom of the dialog are three buttons: 'OK', 'Cancel', and 'Help'.

Figure 3.10: Tunnel length module.

The 'Process' dialog box is titled 'Process' and contains the following fields and controls:

- Name:** A dropdown menu with 'Meeting for updating next crew' selected.
- Type:** A dropdown menu with 'Standard' selected.
- Logic:**
 - Action:** A dropdown menu with 'Seize Delay Release' selected.
 - Priority:** A dropdown menu with 'Medium(2)' selected.
- Resources:** A list box containing 'Resource, Shiftmeeting, 1' and '<End of list>'. To the right of the list are three buttons: 'Add...', 'Edit...', and 'Delete'.
- Delay Type:** A dropdown menu with 'Expression' selected.
- Units:** A dropdown menu with 'Hours' selected.
- Allocation:** A dropdown menu with 'Value Added' selected.
- Expression:** A dropdown menu with 'LOGN(1,4,0.07)' selected.
- Report Statistics:** A checked checkbox.

At the bottom of the dialog are three buttons: 'OK', 'Cancel', and 'Help'.

Figure 3.11: Meeting module.

The following module is “Tunnel Length”, which is already covered above. After this, the model activates the “TBM face backup cutter inspection” module. This module represents the inspections of the face and cutters at the start of the shift, checking for supplies and verifying the needs for current and future tunneling activities. Figure 3.14 shows the relevant module interface with the assigned time delay distribution.

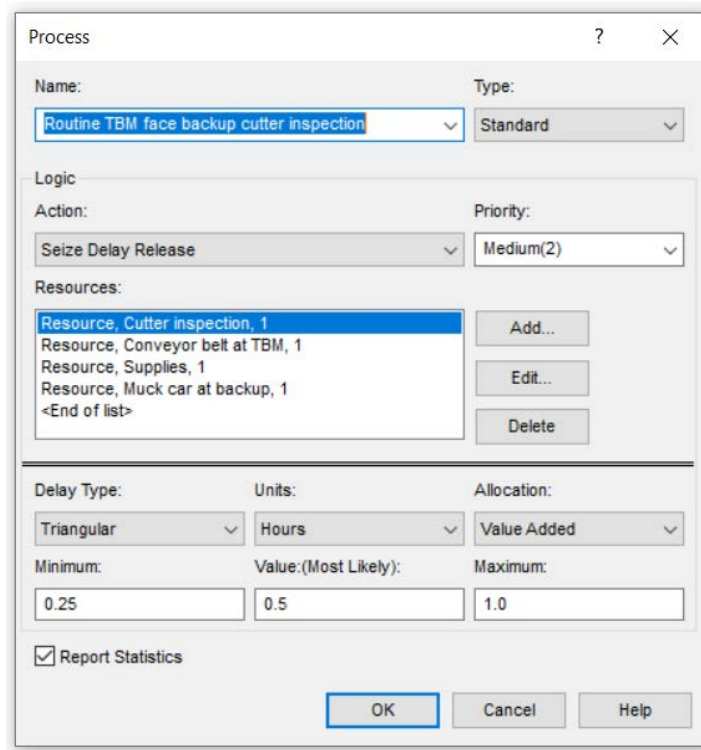


Figure 3.14: Inspection module.

After the inspection, the model activates the “Probe Drilling” module. This module becomes activated, if enabled, to simulate probe drilling activity at predefined intervals with a triangular time-delay type. Figure 3.15 shows the module interface.

The following module is “Utility Check”, which decides which kind of utility extension is required at the current interval. After selecting the utility type, the model activates the relevant

utility extension module, either ventilation, power cable, or water pipe, and applies delay per the assigned time distribution. Figure 3.16 shows the water pipe extension module as an example.

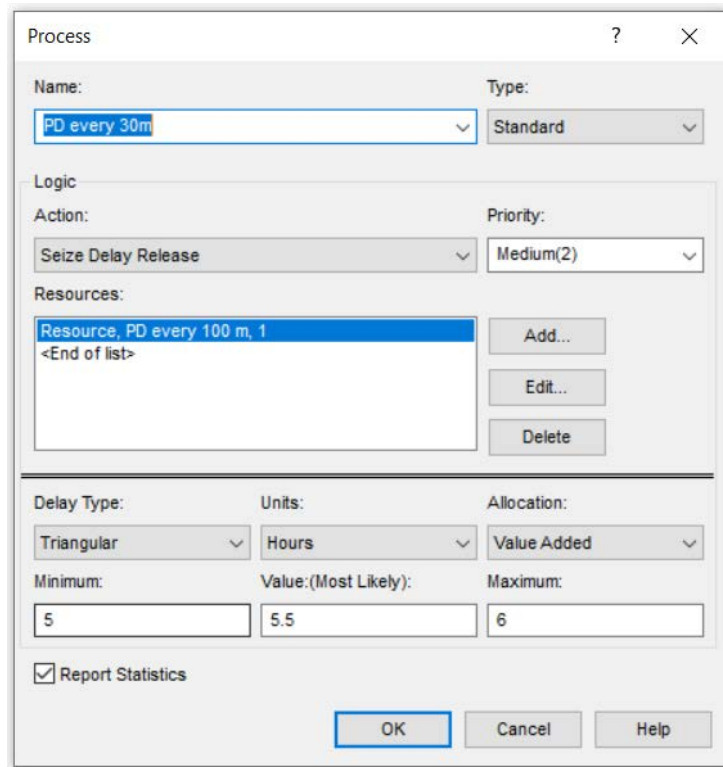


Figure 3.15: Probe drilling module interface.

After utility extensions, the model checks on the TBM type at the first cycle. The user can select open or single shield TBM type at this step. If the single shield is set, the user can define the TBM as a double shield by assigning the same number to clone branches (boring and segment installation) under the double shield clone module. Clone modules enable Arena® to run simultaneous actions. Figures 3.17 and 3.18 show the TBM type selection process with relevant model modules.

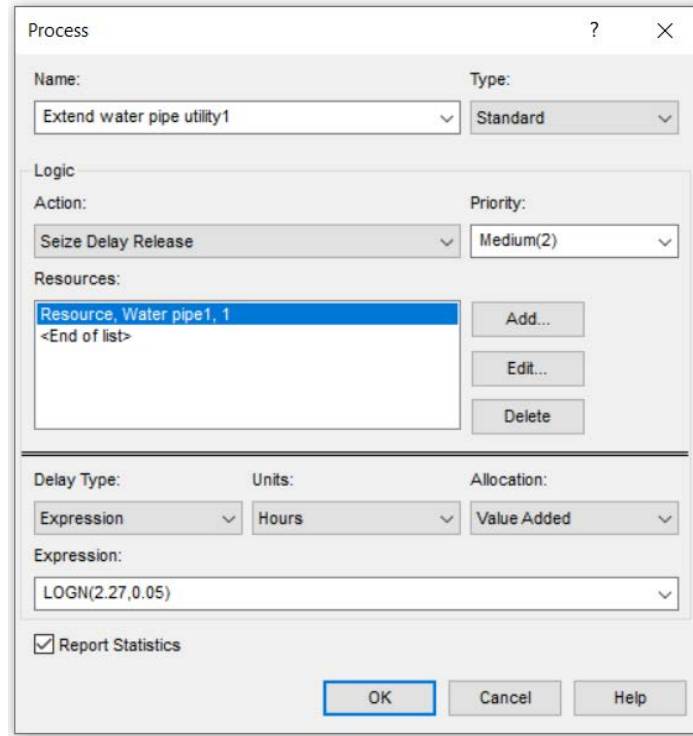


Figure 3.16: Water pipe extension module.

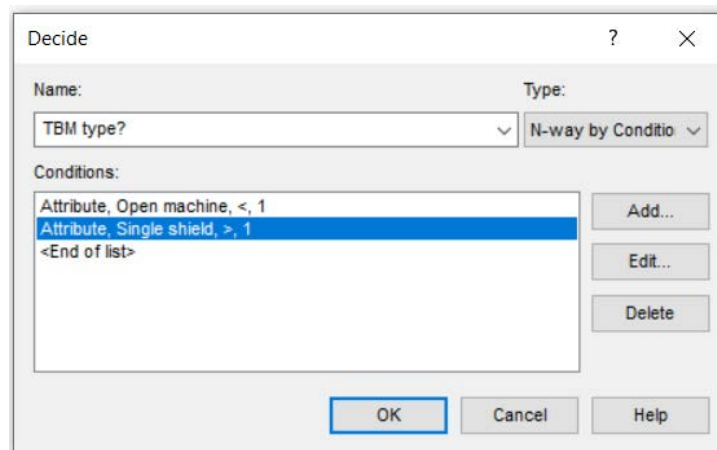


Figure 3.17: TBM type deciding module.

The model continues by activating the “Tunnel Boring” module. This module simulates the tunnel excavation and muck transportation at the face. The user in this module must define

the exact time limits of boring activity. Figure 3.19 shows the module interface and assigned delay type by the developer.

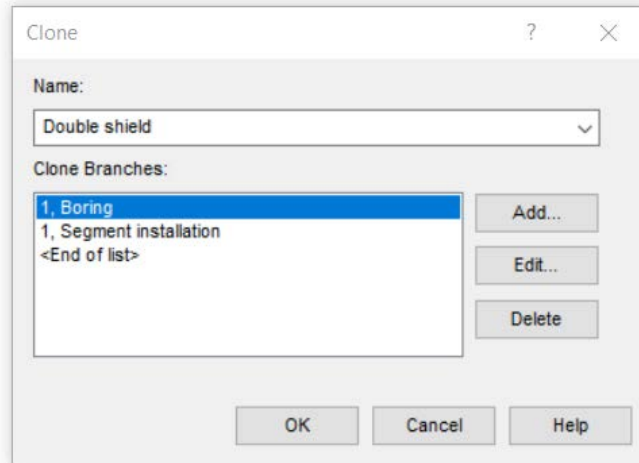


Figure 3.18: Double shield deciding module.

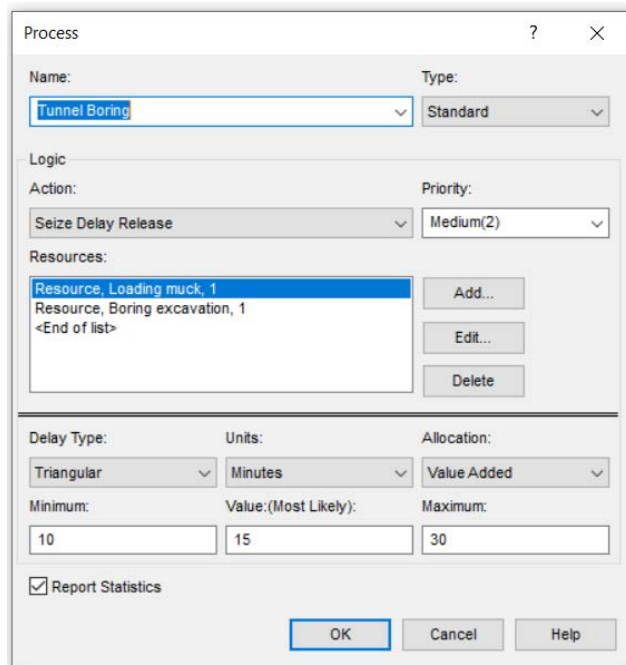
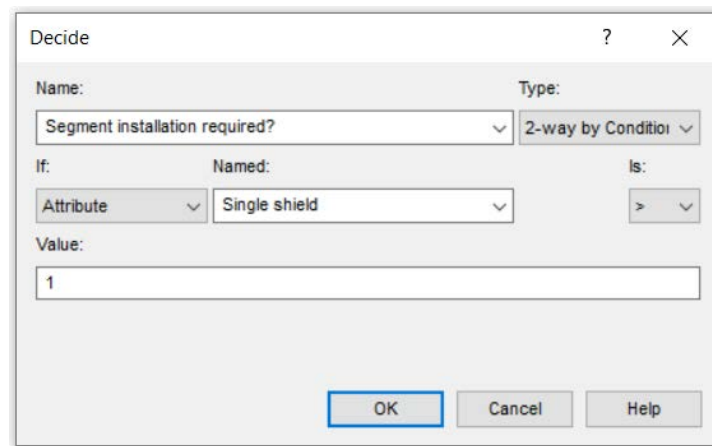


Figure 3.19: Tunnel boring module.

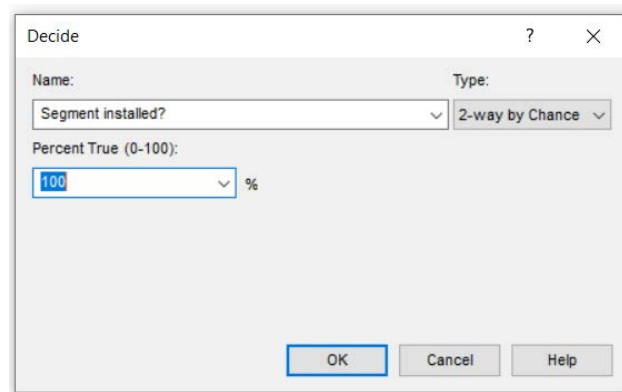
Activation of tunnel boring is followed by check for segment installation. If segment installation is not required/enabled, the model directly goes for the assessment of ground conditions. If it is enabled, the frequency of segment installation can be adjusted. For open-type machines, it can depend on the ground conditions. For single shield machines, frequency should be kept at 100%. Figures 3.20 and 3.21 show module interfaces relative to segment installation and its frequency.



The screenshot shows a dialog box titled "Decide" with a question mark icon and a close button. It contains the following fields and controls:

- Name:** A dropdown menu with "Segment installation required?" selected.
- Type:** A dropdown menu with "2-way by Condition" selected.
- If:** A dropdown menu with "Attribute" selected.
- Named:** A dropdown menu with "Single shield" selected.
- Is:** A dropdown menu with ">" selected.
- Value:** A text input field containing the number "1".
- Buttons: "OK", "Cancel", and "Help" at the bottom.

Figure 3.20: Module evaluates if the segment installation is required or not.



The screenshot shows a dialog box titled "Decide" with a question mark icon and a close button. It contains the following fields and controls:

- Name:** A dropdown menu with "Segment installed?" selected.
- Type:** A dropdown menu with "2-way by Chance" selected.
- Percent True (0-100):** A dropdown menu with "100" selected, followed by a percent sign "%".
- Buttons: "OK", "Cancel", and "Help" at the bottom.

Figure 3.21: Module decides the frequency of the segment installation.

The next activation is the “Segment Installation” module. This module simulates the installation of the precast segmental lining of the tunnel for support purposes. Figure 3.22 shows the module interface and assigned time-delay type.

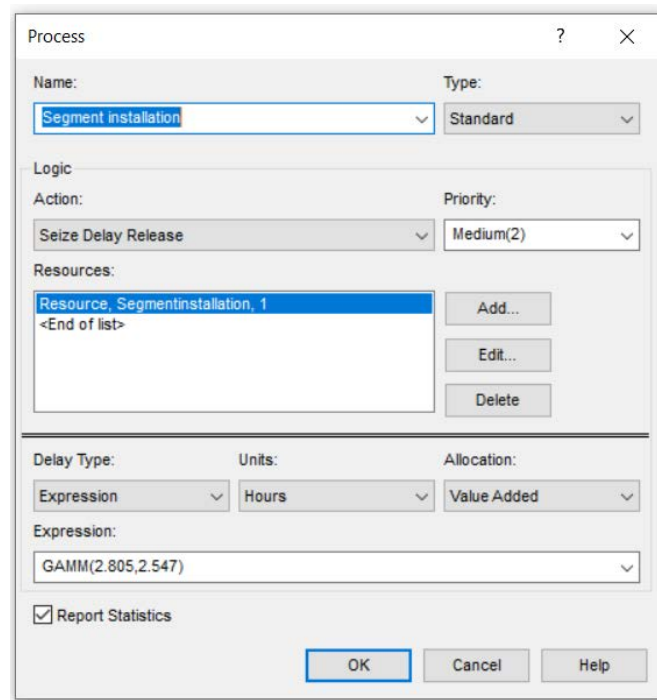


Figure 3.22: Segment installation module.

After segment installation, the model checks for ground conditions and instability issues. The model implements six ground issue types. All these issues are connected to their relevant tunneling activities to calculate the delays caused by them. These tunneling activities are described as activities required to mitigate the defined ground issues. Before activating the mitigation activities, the model checks for the frequency of occurrence of each ground issue in percentages. Figure 3.23 shows the module which controls these activity frequencies. The activities and frequencies are in the same order in the model flow.

Defined ground issues in the CSM2020 model are rockfall, squeezing, clay clogging, abrasiveness, rock jam, and water inflow. Figure 3.24 shows the “TBM Face Cutter Change” troubleshoot module connected to the abrasiveness issue as an example. Table 3.3 provides all troubleshoot modules under their assigned ground issue type.

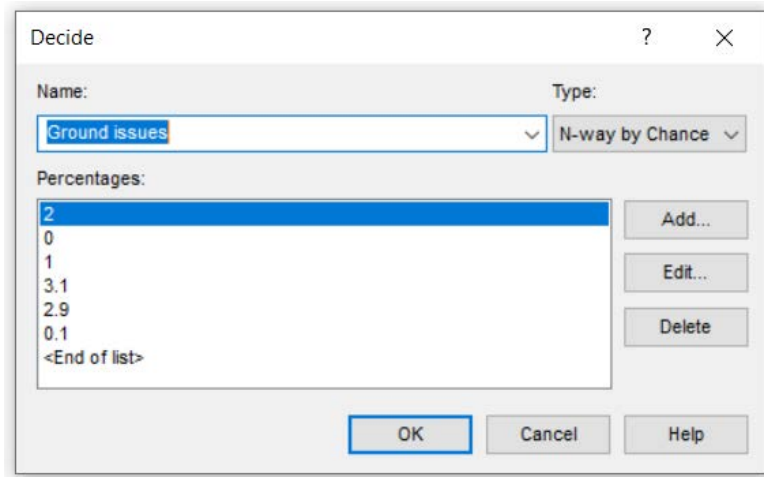


Figure 3.23: Ground issues frequency module. Percentages correspond to ground issues in the same order as their representative modules in Figure 3.5.

Following the activation of ground issues and troubleshooting modules, the model continues to evaluate “TBM face and backup delays”. The model classified heading delays are maintenance, electrical, hydraulic, and cutterhead motors. The model classified backup delays are track placement and repair, loading and unloading, TBM backup derail, TBM backup utilities, TBM backup car pass, TBM backup shaft operations, and TBM backup trailing conveyor. Each is assigned to a module with an adjustable frequency of occurrence and time delay type.

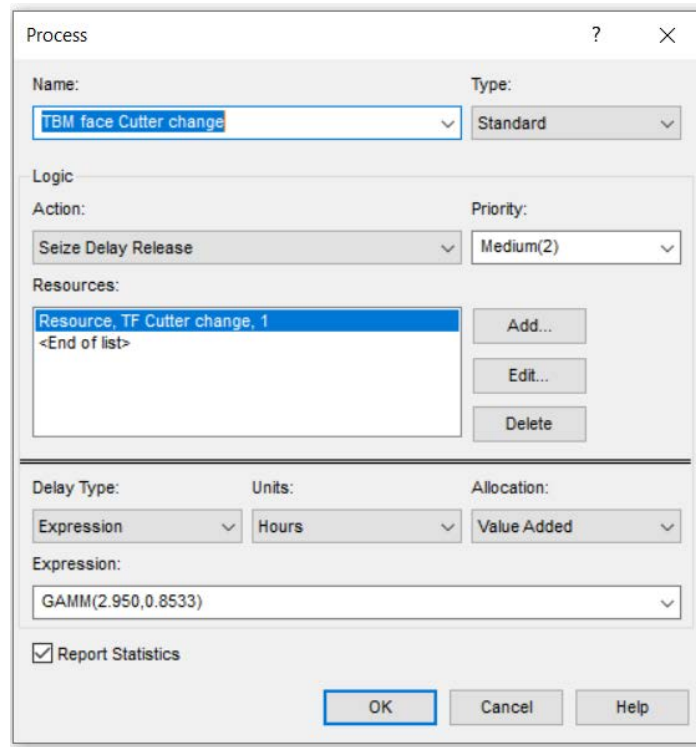


Figure 3.24: TBM face cutter change module.

Table 3.3: Ground issues and their corresponding troubleshoot modules in the CSM2020 model.

Ground Issue	Troubleshoot Modules
Rockfall	Bolt drill, Bolt strap channel, Wiremesh
Squeezing	Shotcrete, Wiremesh, Bolt drill, Ribs lagging
Clay clogging	Scaling muck jam, Clean invert
Abrasive	Scaling muck jam, Cutter change
Rock jam	Scaling muck jam, Bolt drill, Bolt strap channel, Wiremesh
Water inflow	Shotcrete, Waterproofing membrane, Bolt drill, Bolt strap channel, Grouting

After evaluating the face and the backup delays, the CSM2020 activates the “Survey” module, which simulates the surveying activity crucial to excavate on the project alignment. Surveying is carried out automatically by the total stations and surveying software installed on the TBM. When required, engineers move the total station and re-set or relocate it to function

automatically again. The model checks for the surveying activity's frequency of occurrence and then applies the necessary delay per the module time distribution. Figure 3.25 shows the Survey module interface.

The model continues by activating the “Scheduled Maintenance” module. This module simulates the scheduled maintenance activity for the TBM, such as going through a checklist provided by the manufacturer. After completion of maintenance, the “Unforeseen Delays” module is activated by the model, and delays are applied per the assigned module time distribution. Figures 3.26 and 3.27 show maintenance and unforeseen delay modules with their assigned time delay types by the developer, respectively.

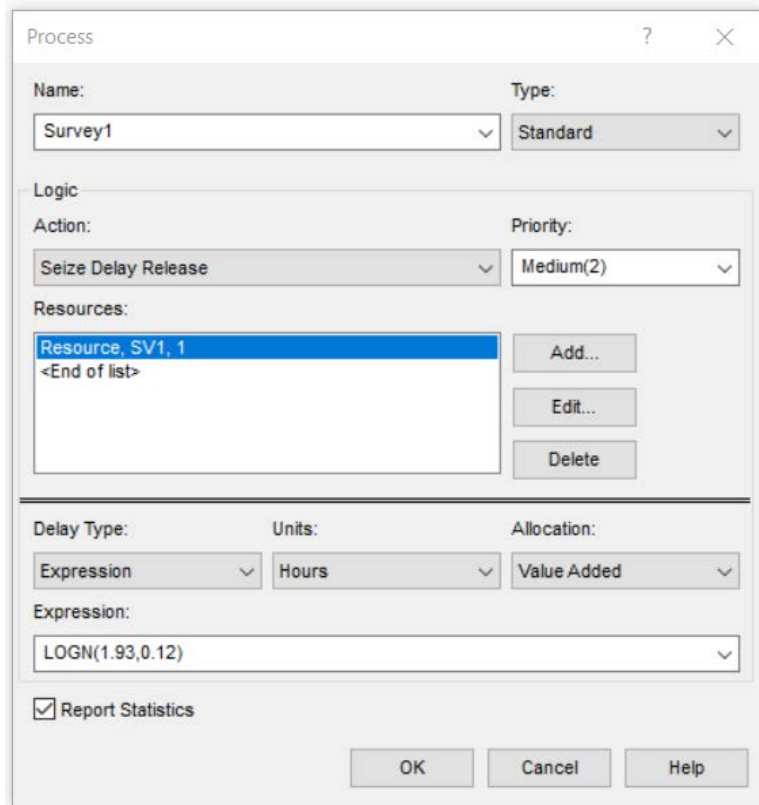


Figure 3.25: Survey module and delay type.

Process ? X

Name: Type:

Logic

Action: Priority:

Resources:

Resource, MT1, 1	<input type="button" value="Add..."/>
<End of list>	<input type="button" value="Edit..."/>
	<input type="button" value="Delete"/>

Delay Type: Units: Allocation:

Expression:

Report Statistics

Figure 3.26: Scheduled maintenance module.

Process ? X

Name: Type:

Logic

Action: Priority:

Resources:

Resource, Unforeseen delays1, 1	<input type="button" value="Add..."/>
<End of list>	<input type="button" value="Edit..."/>
	<input type="button" value="Delete"/>

Delay Type: Units: Allocation:

Minimum: <input type="text" value=".5"/>	Value:(Most Likely): <input type="text" value="1"/>	Maximum: <input type="text" value="1.5"/>
--	---	---

Report Statistics

Figure 3.27: Unforeseen delays module.

As the next step, the model goes through the muck transportation check. First, it checks if the muck is transported via conveyor belt or muck cars. The model starts the muck transportation if the conveyor belt is used. At every predefined tunnel length interval, the model applies the extension of the conveyor belt and continues the muck transportation. Any delays caused by the conveyor belt, such as belt damage, are evaluated under the “TBM Face TBM Conveyors” module. Figure 3.28 shows the interface of this module.

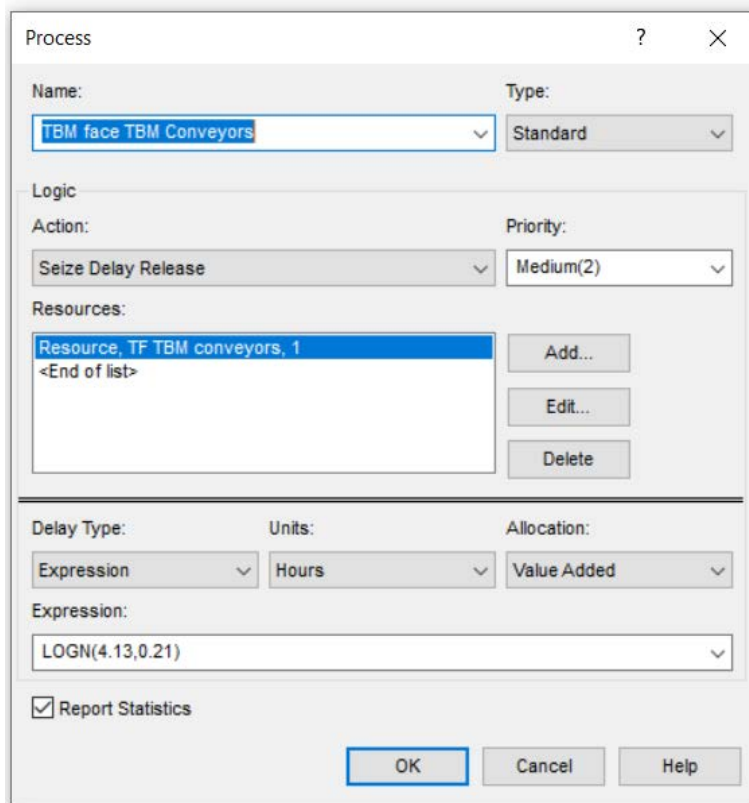


Figure 3.28: Module that simulates conveyor belt delays.

If muck is transported by muck cars, then the model checks for the availability of the rail and the number and location of California switches. The user must define each California switch at desired tunnel length intervals. The model applies a constant three-minute delay on each

California switch. The model extends rail on each push to enable trains to reach the TBM face area and load the muck.

As the final step, the muck train exits through the portal, dumps the muck, and returns to the portal. The model applies appropriate delays for these activities and completes the cycle by generating the utilization factor. Figure 3.29 shows the interface of the “Dump Muck” module.

It must be noted that the CSM2020 was developed using data from hard rock TBM projects. The application of the model is limited to hard rock conditions. Any TBM tunnel excavated through hard rock can be simulated by processing the data accordingly to fit under the relevant modules of CSM2020.

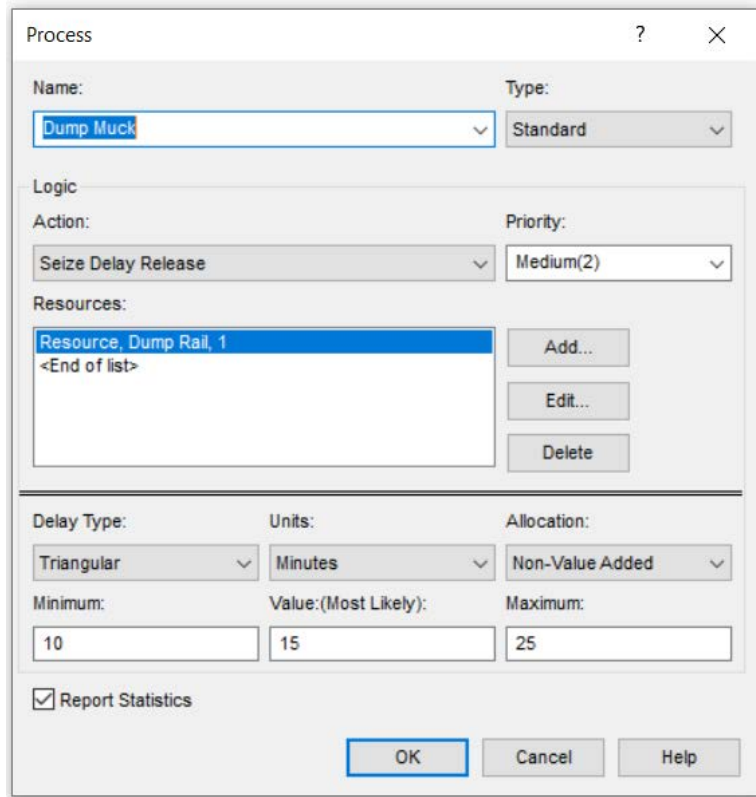


Figure 3.29: Muck dumping module.

The CSM2020 calculates utilization on each stroke, and with the increased length of the tunnel, the utilization rate decreases cumulatively. The model applies delays on a per-stroke basis. Tunnel boring and segment installation are always happening during a complete stroke. However, other modules represent delays are bound to their frequencies, and the model entity may not visit them during the first stroke.

The Input Analyzer extension of Arena® was used in the original development of the model to create the time distributions for relative tunneling activities to define the delays of each module. The extension compares and identifies the best fitting distribution to the presented data and provides the expressions.

Khetwal (2020) conducted sensitivity analyses for some modules to determine their accuracy and effect on the final utilization output. It must be noted that Khetwal (2020) varied the mean of each dataset that represented the relative tunneling activities only by plus or minus 50%. Using only 50% intervals for the sensitivity analysis is explained to be due to an effect called overshadowing. According to Khetwal (2020), overshadowing happens when the change in the mean of a selected dataset is less than the mean of the dominant downtime contributor in the dataset. The utilization output of the model may remain insensitive to the changes in the mean of the relevant dataset. According to these analyses, maintenance-related delays have the most impact on utilization (6%). Other delays impacted the utilization by only 3%, except in some cases where the ground-related delays had high frequencies. Khetwal (2020) also pointed out the relation between ground conditions and downtime natures. When a TBM performs at high capacity due to fair ground conditions (maximum penetration rate due to frequency of discontinuities), utilization is most impacted by maintenance delays because ground-related delays are at a minimum.

Khetwal (2020) showed that the model is responsive to changing ground conditions and their impact on the nature of the dominant downtime type. Ground-related delays gain importance where geology worsens and creates possible squeezing-like problems. Moreover, transportation-related delays showed a 3% – 4% impact on utilization. Survey and unexpected delays made an impact of around 0.5%. Cutter change delays were about 2%, water inflow-related delays about 3%, and probe drilling activities about 2.5% to 3%.

Khetwal (2020) also discussed the limitations of the model. CSM2020 is not capable of directly considering factors such as excavation diameter, cutterhead parameters, and geological unit parameters, such as UCS, BTS, DRI, and RQD.

CHAPTER 4

PROJECT DETAILS AND OBSERVED TUNNELING ACTIVITIES

This section provides the background information on the project that was used to verify the possibility of estimating the tunneling activity times from delay times using the DES simulation process. The name and location of the project is not disclosed to maintain anonymity of the project since it is an ongoing tunneling project and there are a few construction claims that could be brought up by the parties involved in the project.

4.1 Geological and Hydrogeological Information

The project area consists of the following geological rock unit formations in descending order that is described in Table 4.1. Due to confidentiality reasons, names and locations of the geological units will not be mentioned. All the information under this section was directly collected from the project geological baseline report (GBR).

The GBR mentions open joints and solution features in the bedrock along the tunnel alignment due to ground water activity on the bedrock surface. It also notes that various geological units have horizontal to near horizontal bedding planes; however, actual bedding plane orientation varies along the tunnel alignment with natural undulating deposition of the rock and the influence of an arch geologic structure and a basin. The GBR also mentions no major faults or shear zones along the project alignment, but it notes that minor faults and shear zones are likely to be encountered in the bedrock.

The tunnel follows three different major orientations through the alignment. The tunnel starts in the NW direction. After a wide curve, the tunnel continues in the SW direction, and another wide curve changes the direction into S.

Table 4.1: Information on geological units within the project area.

Age	Rock Type	Thickness (m)	Color	Description
Devonian	Shale	0.6 to 1.3	Brownish black	
	Shale/Limestone		Medium gray	Calcareous
	Dolomitic limestone	6.1 to 18.3	Gray	Massive, argillaceous
	Limestone		Gray to dark gray	Medium grained crinoidal
	Limestone		Gray	Granular to shaly thin-bedded, very fossiliferous, cherty
	Dolomite	9.1 to 15.2	Dark brown	Granular, interbedded with dark shale, cherty
Silurian	Limestone	15.2 to 33.5	Light to medium gray	Fine-grained, vuggy, slightly dolomitic, cherty
	Limestone	15.2 to 33.5	Dark gray to black	Dense to fine-grained, argillaceous
	Limestone		Dark greenish gray	Dolomitic shale interbedded with fine-grained argillaceous
	Limestone	No information	Light to brown	Fine-grained, argillaceous, dolomitic
	Limestone		Dark to mottled	Sublithographic to fine-grained
	Dolomite			Nodular carbonate structure with shale
	Limestone		Whitish	Impure, fine-grained, argillaceous, dolomitic
	Dolomite			Coarse-grained, bioclastic, vuggy

According to the GBR, the predominant joint set trends approximately N60E dipping to the east and is near vertical. A secondary, near-vertical joint set generally trends approximately

N20W dipping towards the north and is nearly perpendicular to the primary set. Both sets are spaced at intervals ranging from 0.9 – 3 m (3 to 10 feet) based on observations of rock that remain standing after blasting a rock bench at a quarry and based on a historical literature review.

According to the GBR, the project area is within an aquifer system containing thick layers of tills with some fine-grained glaciolacustrine deposits. A few thin sand and gravel lenses occur between these sequences, and the underlying material can be bedrock or glacial till. The GBR notes that this system has a low susceptibility to surface contamination. Per project GBR, pumping rates in test wells installed along the alignment varied from 367 lpm to 29411 lpm. Hydraulic conductivity of the rock mass controlled by joints, bedding planes, and discontinuities ranged from 2×10^{-3} cm/s to 3×10^{-2} cm/s. The GBR also mentions that the testing indicated that the wells were essentially connected to near-infinite sources of recharge.

4.2 Rock Characterization

The GBR identified three rock engineering units based on the field and laboratory testing results and expected behavior during excavation. These units will be referred to as Unit 1, Unit 2, and Unit 3.

The GBR describes Unit 1 as thinly to thickly bedded, ranging from 5 to 91 centimeters, with near horizontal bedding and consists of light to medium gray, medium-grained, fossiliferous shaley limestone with chert nodules and chert layers present. The description continues with chert nodules varying from widely spaced and sporadic to tightly spaced within a nearly continuous horizontal zone comprising up to 10 percent of the unit thickness. It is noted that the fractured limestone varies in thickness from 6.1 to 18.2 meters and makes up the bedrock-overburden interface in most of the borings.

The GBR describes Unit 2 as thinly to thickly bedded, ranging from 10 to 91 centimeters with near horizontal bedding, and is blocky. According to the GBR, the upper portion of this unit consists of light to medium gray, fine-to medium-grained, massive, conglomeritic dolomite, and argillaceous layers of varying thickness are present in this upper zone. It is mentioned that the lower portion of this unit consists of dark brown to tan dolomitic limestone or dolomite, banded with white, crystalline calcite and shale beddings with some coarse sandy zones, and vugs are present in both the upper and lower zones. Still, it is less vuggy than Unit 3. The GBR mentions that multiple discrete lenses of chert layers are noted within this unit and vary in thickness from 5 to 20 centimeters. The thickness of Unit 2 ranges from 10.6 to 15.2 meters in the project area, according to the GBR.

The GBR describes Unit 3 as thickly bedded to massive sedimentary rock, free of chert, consisting of medium to dark gray, dense, vuggy, massive argillaceous dolomite with greenish-gray shale partings and near-vertical features. Per the GBR, pressure dissolution features such as stylolites, evidence of bioturbation, and reef facies are prevalent in this unit. The GBR mentions that Unit 3 is vuggy, and reef facies comprise 73% of the rock. Bedding with this unit is not distinct but based on visual observation of the reef facies structure within a quarry nearby the project area. The GBR points out that the observed bedding based on fractures and coloring is inclined between 15 to 25 degrees from horizontal and the remaining 25% is materially identical. Still, bedding is near flat with distinct bedding planes. Per the GBR, the thickness of Unit 3 ranges from 15.2 to 33.5 meters. Rockmass properties, such as UCS, PLI, BTS, and PPI, for Units 1, 2, and 3 are provided in Table 4.2.

Table 4.2: Rockmass properties of Units 1, 2, and 3.

Geological Unit	Unit Weight (kg/m ³)	UCS (MPa)	PLI (MPa)	BTS (MPa)	Cerchar Abrasivity Index	Punch Penetration Index (N/mm)	Drill Rate Index	Cutter Life Index
1	2675	117.2	5.17	7.58	-	-	-	-
2	2450.8	73.7	3.65	4.82	1.1	10.87	High	Extremely High
3	2450.8	73.7	3.65	4.82	2.2	12.32	High	Extremely High

4.3 Tunneling Activities

Every TBM tunneling operation involves a series of common activities, such as boring, support installation, muck transportation, etc. However, project needs and TBM type selection can create subtle differences in tunneling activities. The data used in this study are collected from a slurry-type TBM project. Slurry machines do not need muck transportation, i.e., muck car or conveyor belt, since they transport the muck by the slurry line and send it to a separation plant on the surface.

Tunneling activities mentioned in this section are directly observed and recorded in the field. It must be noted that these activities are specific to the project and machine type.

4.3.1 Safety Meeting

Each day, safety managers inform crew members of issues for each shift on a different safety topic in these meetings. Also, recorded incidents on the job site and examples from other projects are shared to create awareness for such events. The crew members have been thoroughly explained the mitigation options for these risks and hazards. During these meetings, superintendents also gave a brief explanation about the day's work plan. Any other announcement from the management is also delivered to the crew during these meetings. Safety meetings happen at the start of every shift and are a part of scheduled downtime.

4.3.2 Boring

Boring activity describes the excavation cycle and advance of the TBM. Each boring cycle is called one stroke or a push. The cutterhead is pushed against the tunnel face by 16 x 2400 mm thrust cylinders. The thrust system simultaneously pulls the TBM backup compartments installed within gantries along with the machine. Thrust cylinders numbered from 1 to 16, starting from the crown they are pushing against the concrete segments installed inside the shield after each push. Each push is limited by the length of the thrust cylinders, which was 2400 mm. The average advance speed was 36 mm/rev. The average thrust force was 21153 kN. The average cutterhead rotation was 5 rpm.

4.3.3 Segment Installation

After each push, precast concrete segments were installed inside the TBM shield. There were 6 (5+1) segments for each ring. The machine moves forward by pushing on the last built ring with the thrust cylinders. Proper installation of the ring is crucial for single shield TBMs. The gap between the segment extrados and TBM shield intrados must be measured, and the measurements should be communicated with the surveying software. The software provides a ring number, which defines the number of the thrust cylinder where the first segment (counter keystone) will be placed. This process is crucial to prevent tail shield dragging and correct articulation to the TBM. The segments are the final support for the excavated tunnel, and each ring is 1.5 meters wide.

4.3.4 Utility Extension

TBMs need electricity, airflow, water, slurry mix, and grout for a routine tunneling process. Electricity is the only power source that can be used on TBMs to energize the cutterhead motors, machines thrust system, and the entire heading. Thus, power cables extend at each

predetermined interval along the tunnel by adding new sections. Utility pipes carrying water, slurry mix, grout, and air are also extended at various intervals. Utility extensions usually happen during the segment installation to prevent delays. However, utility extension may cause a delay depending on the segment installation duration. This means shorter delay times caused by segment installation. The relationship between these two events can be evaluated through sensitivity analyses.

4.3.5 Maintenance

Maintenance is an important activity that helps to keep the TBM operational. Maintenance of the machine and backup usually involve planned activities aiming to prevent severe and unexpected malfunctions in the future. Depending on the mechanical, hydraulic, and electrical system conditions on the TBM, maintenance can be, and often is done every day. During maintenance, scheduled or unscheduled, mechanics and electricians go through a checklist that the TBM manufacturer had created. The checklist enables them to identify major system errors.

4.3.6 Repairs

Repairs happen when an unexpected problem occurs, including anything from grout lines to cutterhead drive units, backup utilities to surface plants, and so on. The duration of the repairs is mainly related to identifying the problem. Thus, experience and knowledge of the crew and availability of data collection sensors through the TBM are essential for this activity.

4.3.7 Surveying

Surveying is carried out by the communication of VMT® software and the total station at the heading. Predetermined alignment introduced to the software with machine specifications. The survey is done automatically during the strokes. Total station hits the laser target on the first

gantry to get the alignment data. This provides information to the TBM operator, who can adjust alignment via thrust and articulation cylinders. Delays incur when the total station must be moved closer to the first gantry where the target is placed due to the curves and increased distance between the total station and target by time.

4.3.8 Intervention

An intervention disrupts the excavation operation where some repair has to be done on the cutterhead. This happens by entering the excavation chamber after the muck is removed to the desired level to allow divers entry into the chamber, sometimes under elevated pressure by compressed air to support the face. Interventions require the excavation chamber to be depressurized for the slurry-type machines to allow for injection of compressed air. After depressurizing, the crew can go inside the excavation chamber and carry out the necessary operations.

4.3.9 Transportation of Supplies and Crew

Any transportation needs, except muck, were carried out by the trains at the tunnel. Concrete segments, utility pipes, supplies (bolts, lubricants, grease barrels, etc.), power cables, crew members, and any other transportable items were moved from shaft to TBM with train. There were two trains at the site, one always at the launch shaft for loading supplies and one making the trip to TBM to deliver the supplies and transport the crew. There was only one California switch at the launch shaft. Transportation delays were caused due to train breakdowns, weather conditions (risk of a lightning strike to the crane, malfunctions, etc.), and longer than usual loading/unloading times.

4.4 Data Collection

Data used in the current study to create site-specific time distributions were collected from a slurry-type hard rock TBM. Project and machine specifications are presented in Table 4.3. The crew worked on a three 8-hour shifts schedule. During data collection, the total advancement was 348 meters. Earlier data was gathered from company records and used for overall project utilization calculation. The project's specifics are not discussed in detail to keep the project anonymous.

The data collection sheet that is used at the site allowed the recording of the tunneling and TBM activities at five-minute intervals. TBM operators and tunnel engineers used the same sheet, so it was possible to cross-check the recorded data from additional sources.

Table 4.3: Machine specifications for the tunneling project studied in this research.

TBM Type	Single Shield Slurry
Drive Engines	7 x 160 kW
Thrust Cylinders	16 x 2400 mm (94.5 in)
Tunnel Length	7467.6 m (2450 ft)
Number of Curves	10
Overall Curve Radii	396.2 m (1300 ft)
Tunnel Depth	56.3 – 67 m (185-220 ft)
Tunnel Slope	0.15% uphill, 1.16% uphill, 0.11% uphill
Excavation Diameter	5.79 m (19 ft)
Supported Diameter	4.87 m (16 ft)
Support Type	Precast Segmental Lining (5+1)
Segment Erector	Mechanized Grabber
Excavation Chamber Pressure	3.5 – 4.5 bars
Maximum Water Inflow	15141.6 lpm (4000 gpm)
Transportation	2 trains (2 mantrip + 2 flatbed, Max speed: 15 km/h)
California Switches	1 at the shaft (1 train always at the shaft)

4.5 Processing of Raw Data

The CSM2020 model uses predefined modules to simulate individual tunneling activities. The CSM2020 was not originally developed to simulate slurry-type machines. However, it was

deemed possible to modify the program and adjust and use the field data and define related activities under the correct modules. O’Connell (2021) made a study on simulating the slurry TBM process and was able to achieve good agreement with actual utilization values within the 3% margin using the CSM2020 model. The model had to be validated before continuing with sensitivity analyses by matching actual utilization and recorded delay time distributions. For that purpose, raw data was processed for use in the CSM2020. Tunneling activities and delay causes recorded individually on the datasheet and are presented in Table 4.4. Some activities, such as the safety meeting, are not listed in the data recording sheet.

Table 4.4: Tunneling activities and delay causes on the data recording sheet.

Production		
Advance		
Ring Build		
Delays		
STP (Slurry Treatment Plant)	Backfill Grout System	Slurry Lines
TBM Hydraulics	Segment Erector	Grout Lines
TBM Electrical	Segment Crane	Crane Breakdown
TBM Mechanical	Cylinder Adjustment	Waiting for Train
Slurry Pumps	Cooling System	Utilities Extension
Water Supply	Cracks on Segment	Logistics
VMT® Surveying System	Grout Batching Plant	Other
Scheduled		
Maintenance	Invert Cleaning	MV Cable Extension
TBM Ordinary Cleaning	Cutterhead Intervention	Ventilation Extension
Backup Cleaning	Rail Extension	Grout/Water/Slurry Extension

Some tunneling activities and causes of delays were evaluated under the most relevant CSM2020 modules. Table 4.5 shows the tunneling activities and delays under their relevant model modules. Three different activities are not listed in the timesheet but were identified during the data collection process.

Table 4.5: Tunneling activities and their corresponding modeling modules.

CSM2020 Module Name	Activity Name
Shift Meeting	Safety Meeting
Tunnel Boring	Advance
Segment Installation	Ring Building
Shaft Operations	STP (Slurry Treatment Plant)
	Grout Batch Plant
TBM Face TBM Conveyor	Slurry Lines
Track placement and repair	Water Test
TBM Electric Systems	TBM Electrical
TBM Face CH Motors	Backfill Grout Systems
TBM Backup Utilities	Slurry Pumps
	Water Supply
	Backup Cleaning
	Cooling System
Survey	VMT® Surveying System
Unforeseen Delays	TBM Mechanical
	Backfill Grout System
	Segment Erector
	Segment Crane
	Cracks on Segment
	Cutterhead Drive Engines
Crane Breakdown	
Slurry Line Extension (added)	Slurry Line Extension
Water Pipe Extension	Grout/Water/Slurry Extension
Power Cable Extension	MV Cable Extension
Ventilation Extension	Ventilation Extension
Loading and Unloading of Supplies	Logistics
	Waiting for Train
Maintenance	Maintenance
	Cylinder Adjustment
	TBM Ordinary Cleaning
Cutter Change	Cutterhead Intervention

Slurry line extension delays were considered under the “TBM Face TBM Conveyors” module. This activity causes short delays during the boring process. Slurry-type TBMs transport muck in the slurry lines and deliver it to STP at the surface. To prevent muck accumulation and damage inside the slurry lines at the shaft when the boring stops, TBM operators stop excavation for a period depending on the distance between the face and the shaft. During this time, slurry

pumps are active to push the muck and keep the slurry circulating to prevent material settlement in the pipes. This activity keeps slurry lines unclogged and open at the shaft when boring is stopped. Another activity is Water Test. Water Test delays are considered under the “Track placement and repair” module. Water testing is carried out by the tunnel engineer, TBM operator, and STP operator. According to geotechnical and hydraulic data through the tunnel's alignment, water tests are usually scheduled when a geological unit change is expected or hydrostatic pressure changes are observed. During the test, the excavation chamber pressure is gradually decreased, allowing groundwater inflow. Slurry lines remain active so that the STP can measure the volume change. According to the volume change, a new excavation chamber pressure is set, and the boring process continues. The last activity is repairing the cutterhead drive engines. Delays from this activity are considered under the “Unforeseen Delays” module. A mechanical or an electrical problem can cause a delay.

After assigning activities and delays to relevant CSM2020 modules, raw data was meticulously inspected, and any anomalies within the datasets were removed. The anomalies that were removed had low frequencies but high durations, such as slurry pump installation, which happened only once and took 6720 minutes to complete. According to the model setup mentioned earlier, the assigned frequency for this activity should be equal to the total number of data points divided by the total number of strokes, which would be 0.4%. These types of events are not necessarily stochastic instead, they are typically scheduled activities. Hence, they would create spikes during the model runs, affect utilization and downtime contribution results, and negatively impact the sensitivity analyses.

Additionally, the datasets that inherited the anomalies showed higher squared error than those that did not inherit anomalies. The square error parameter is critical for creating probability

distributions to determine the best curve fit to the relevant dataset. These distributions define the duration of the activities and delays in CSM2020. Thus, removing the anomalies was a requirement to evaluate most tunneling activities properly. The probability distributions and associated histogram charts with statistical parameters are explained in Chapter 5 and Appendix B.

Furthermore, it must be noted that this requirement brought its' own limitations. By ignoring some of the downtimes (anomalies), the model result couldn't be expected to match the actual utilization perfectly. This limitation was the reason for having a higher utilization rate than the originally observed field utilization during the creation of total and downtime contribution charts. This situation is further discussed in Chapter 5.

After removing the anomalies from the data, the project downtime composition was created to show the contribution of each activity. Also, field utilization was calculated by using the ratio between tunnel boring time and total time as a percentage. The calculated field utilization was 43.3% before removing the anomalies, and it went up to 50.64% afterward. Figures 4.2 and 4.3 show the pie charts of allocated times in TBM operation. The total time contribution chart includes "Tunnel Boring" activity, but the downtime contribution chart does not. The total time contribution can be used to observe the machine utilization directly from the data. The downtime contribution can be used to identify which tunneling activities and delays are the most impactful among downtimes.

Total Time Contribution

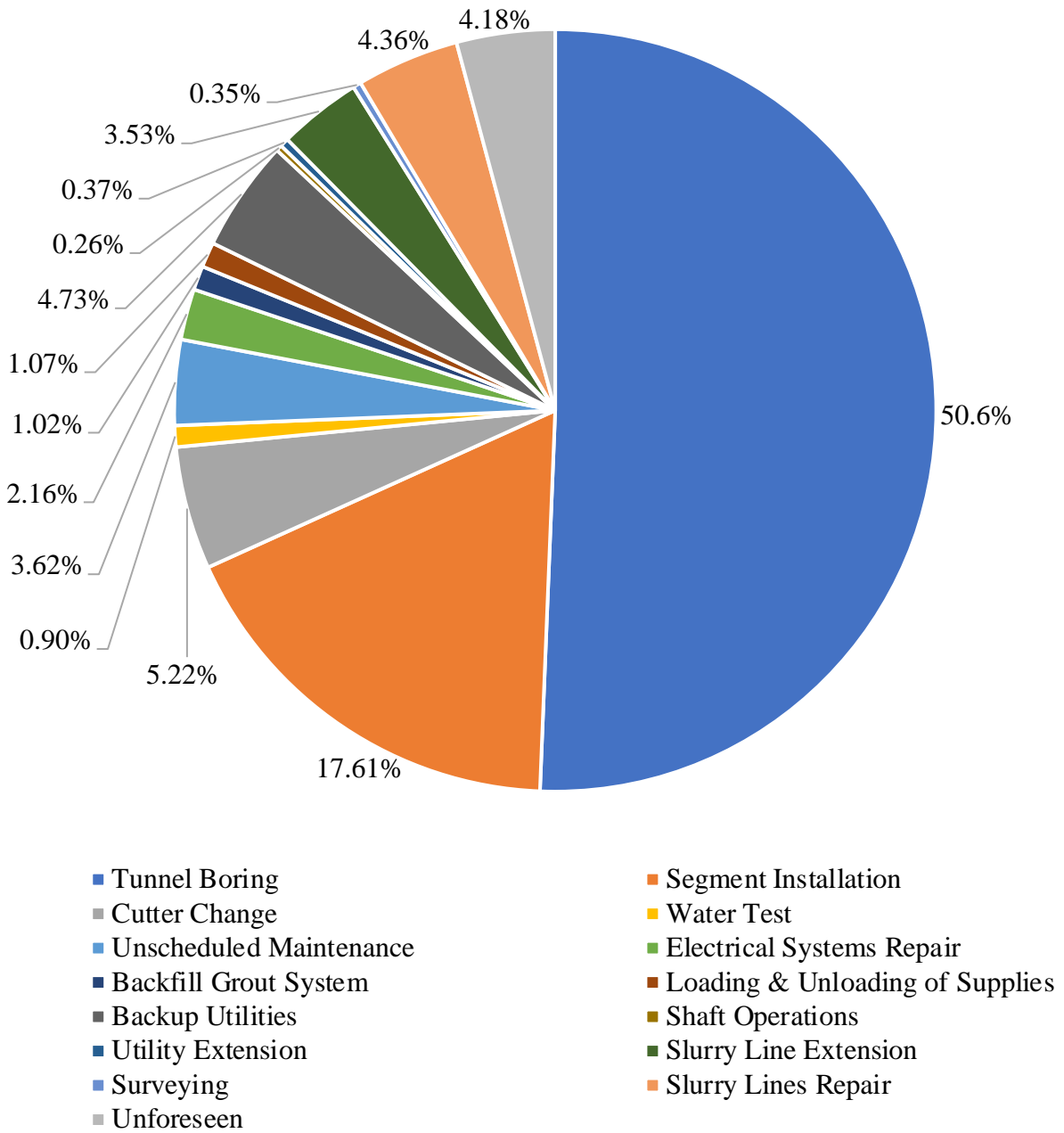


Figure 4.1: Total time contribution according to field data, after removal of the anomalies.

Downtime Contribution

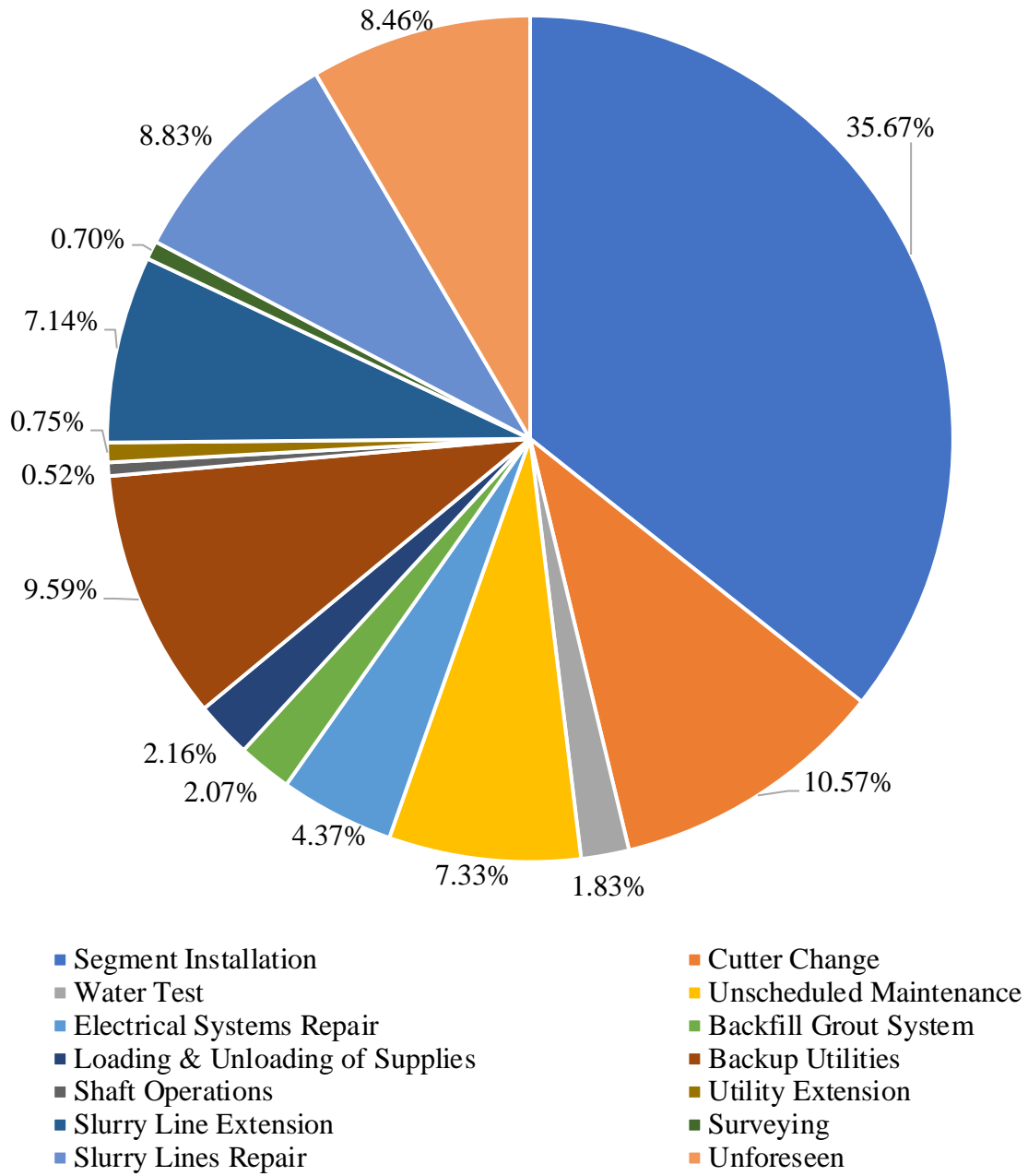


Figure 4.2: Downtime contribution according to field data.

CHAPTER 5

VALIDATION OF CSM2020 MODEL

CSM2020 was developed for open type and shielded hard rock TBMs. Since the data used in this study was collected from a slurry TBM, it was not possible to completely mimic the process that the CSM2020 simulated. However, the classification of the raw data, as was explained in the previous chapter, made it possible to use the CSM2020 model for this study. For validation, the model was used to simulate the tunneling operation and to observe the estimated machine utilization, where the result matched the field utilization within the 3%. The model simulated 349 meters of the tunnel where the data was collected. Each push was considered to be 1.5 meters as in the actual operation. Three 8-hour shifts were used in modeling. 232 pushes and 60 shifts were defined in the model to simulate the evaluated tunnel section. No California switches or muck cars were used. The Conveyor belt module was used to simulate the slurry muck transportation system.

New time distributions were created for relative modules using the Input Analyzer extension of Arena® using the data collected from the field. Input Analyzer provides histograms, descriptive statistics, the goodness of fit tests, and distribution parameters that can be used in Arena®, such as location, shape, and scale values. The extension automatically applies Chi-square and least mean square error to determine the best fitting distribution. In the goodness of fit tests, the AD (Anderson-Darling) statistic measures how well the data follows each distribution. Lower AD values represent better fits. There are two hypotheses for the AD test.

H_0 : The data follow a specific distribution.

H_1 : The data do not follow a specific distribution.

The p-value is the measure of the strength of the evidence in a particular dataset against the null hypothesis. If available, the corresponding p-value can be used to test if the data come from the desired distribution. The null hypothesis can be rejected if the p-value is less than the alpha, normally set as 0.05 or 0.1, which means that the data is coming from a specific distribution. A higher p-value indicates a better fit, while a lower value indicates that alternative hypotheses, such as another distribution, might better fit the dataset. Also, the sum of squared errors can be used to determine the best fit among the selected distributions for the datasets. In this case, the lowest square error value indicates the best fit. If squared error values are close to each other, additional criteria, such as the p-value, must be considered to determine the best fitting distribution.

According to these considerations, datasets were introduced to the Input Analyzer. Probability distributions for each activity are determined. Also, their frequencies per the ratio of the number of data points to the number of strokes were calculated. Activities evaluated under utility extension (such as ventilation extension and power cable extension) did not have a distribution, while the frequency for these modules was based on predetermined stroke intervals. Also, there were insufficient data to create a distribution for these activities, and their durations were considered constant. Activities like segment installation and tunnel boring do not have frequencies assigned to them because they happen at each stroke during modeling. However, they still have probability distributions to define their durations.

During the creation of new probability distributions, most of the datasets showed low p-values (< 0.05) and high square errors ($> 10\%$) for the goodness of fit tests. Two independent factors were affecting these results. The first one was the limited amount of data. It must be noted that Khetwal (2020) used data from eight projects and had an ample number of data points

to create distributions. This study uses data from one project within a limited period. In addition, the recording format of the data was based on shift reports that allowed the field records based on 5 minutes, meaning that recorded data points can only be 5 minutes or its positive multipliers. Also, not every 5-minute interval had data points for all activity categories. For example, datasets related to tunnel boring and segment installation have data points at each interval, such as 5-10, 10-15, 15-20, etc. However, most of the other activities do not have this consistency.

Table 5.1 provides best-fitting probability distributions that were evaluated using the Input Analyzer, their relative activities, and frequencies. Histograms and statistical parameters for these probability distributions are presented in Appendix B.

Table 5.1: Best fitting probability distributions for each activity with their squared error values per the Input Analyzer extension.

Activity	Frequency (%)	Probability Distribution (minutes)	R ² (%)
Utility Extension	N/A	CONSTANT (80)	N/A
Loading & Unloading of Supplies	3.02	4.5 + 66 * BETA (0.594, 0.683)	15.7
Segment Installation	N/A	9.5 + 21 * BETA (0.799, 1.63)	20.7
Slurry Line Extension	N/A	4.5 + 31 * BETA (0.694, 1.18)	13.2
Surveying	2.59	4.5 + 21 * BETA (0.13, 0.212)	7.4
Unforeseen Downtimes	23.71	4.5 + 56 * BETA (0.601, 2.23)	13.4
Shaft Operations	2.59	4.5 + 21 * BETA (0.321, 0.691)	16
Backup Utilities Repair	7.33	10 + WEIB (19.4, 0.338)	5
Cutter Change	0.43	CONSTANT (1125)	N/A
Backfill Grout System	8.62	4.5 + WEIB (5.88, 0.822)	16
Electrical Systems Repair	1.29	UNIF (15, 300)	13.3
Slurry Lines Repair	3.88	10 + EXPO (94.4)	3.2
Unscheduled Maintenance	3.02	TRIA (45, 94.3, 195)	6
Water Test	0.86	79.5 + 36 * BETA (0.299, 0.28)	21.6
Tunnel Boring	N/A	TRIA (29.5, 40, 65.5)	15.7

The probability distributions listed in Table 5.1 are introduced to the model. The model has run with 50 iterations for achieving reasonable results per Khetwal (2020). This process has been repeated ten times to verify the model accuracy, and an average 34.8% TBM utilization is

observed within a +/-0.2% margin for all the results. The repeatability of the results from individual model runs was satisfactory; however, the average utilization rate (34.8%) was highly different from the observed TBM utilization (50.6%) in the field. Therefore, the model was thoroughly investigated for potential errors. The analysis of the simulation process revealed that the time spent during the simulation for “Unforeseen Delays” was unusually high. According to field observations, the expected value was close to 1000 minutes; however, the model determined 25000 minutes of duration for the “Unforeseen Delays”. It was detected that at the end of each iteration, the entity was only visiting “Unforeseen Delays” and “Scheduled Maintenance” modules within the “Surveying maintenance and unforeseen events” area. A couple of attempts have been made to prevent this behavior¹, including changing module connections, but the issue could not be fixed. It was theorized that the problem originated due to the original model setup of CSM2020 because Khetwal (2020) considered two 10-hour long shifts for production and one 4-hour shift for the scheduled maintenance every day. The “Unforeseen Delays” dataset was evaluated under another module (Trailing Conveyor) within the TBM face and backup delay area to prevent the excess duration for these modules. The “Trailing Conveyor” module was chosen because no other dataset was assigned to it.

After assigning the “Unforeseen Delays” dataset to the “Trailing Conveyor” model, the model was rerun. The simulation runs provided an average of 46.6% TBM utilization. Additional simulation runs with different distribution settings were used to get closer to the TBM utilization in the field, where two trials were examined with activity time distributions other than the best fitting distributions. The first trial used triangular distributions for all activities, defining minimum, mean, and maximum values for each dataset. The model run determined 44.6% TBM

¹ This was done with the help of Dr. Anuradha Khetwal who had developed CSM2020 model

utilization. The second trial used only the mean values of each dataset and determined 49.9% TBM utilization.

Table 5.2 provides the results of these trials, comparing the time spent for each activity with the observed field results.

Table 5.2: VA Time results for the validation test runs (All units are in minutes per activity).

Activities	Field	I. Trial	II. Trial	Best fit activity time distribution
Utility Extension	80	90	90	90
Loading & Unloading of Supplies	230	265	230	249
Segment Installation	3795	4356	3804	3815
Slurry Line Extension	760	1078	940	919
Surveying	75	90	80	83
Shaft Operations	55	75	51	59
Unforeseen Downtimes	900	1545	903	899
Backup Utilities Repair	1020	1489	979	2022
Cutter Change	1125	1485	1102	1012
Backfill Grout System	220	307	223	219
Electrical Systems Repair	465	514	514	509
Slurry Lines Repair	940	1305	995	1015
Unscheduled Maintenance	780	875	846	852
Water Test	195	188	181	242
Tunnel Boring	10915	10998	10904	10441
Summary of Results				
Total time	21555	24660	21842	22426
Utilization	50.6%	44.6%	49.9%	46.6%

The closest results were observed when only the mean values were used to model the operation, followed by the best fit and triangular distributions. The best fit distributions provided a close TBM utilization during validation; however, the type of probability distribution was subjected to change when the mean of the relevant dataset was varied. This was because the mean implies a mid-point in the dataset, whereas some of the distribution functions did not follow a normal/symmetrical distribution, rather had a tendency to concentrate on one or another

end of the measured ranges for the selected variables. It must be noted that sensitivity analysis is performed by modifying each parameter by various quantities, re-running the model, and computing the changes in the model output relative to its output with the original run (Massada et al., 2008). This is done by keeping every other parameter constant and changing one parameter at a time. For this reason, it was decided to continue using mean values as constants and triangular distributions to evaluate the impact of chosen activity during the sensitivity analysis. Also, any potential computing errors or anomalies within the results could be easily determined. Table 5.3 shows the values used to represent tunneling activities in triangular distributions.

Table 5.3: Tunneling activities and their statistical values.

Activities	Minimum (min)	Mean (min)	Maximum (min)
Loading & Unloading of Supplies	5	32.9	70
Segment Installation	10	16.4	30
Slurry Line Extension	5	16.5	35
Surveying	5	12.5	25
Shaft Operations	5	9.2	25
Unforeseen Downtimes	5	16.4	60
Backup Utilities Repair	10	60	185
Cutter Change	1125	1125	1125
Backfill Grout System	5	11	30
Electrical Systems Repair	15	155	300
Slurry Lines Repair	10	104.4	330
Unscheduled Maintenance	45	111.4	195
Water Test	80	97.5	115
Tunnel Boring	30	47	65

CHAPTER 6

SENSITIVITY ANALYSIS

Sensitivity analyses evaluate how the uncertainty on the model inputs influences the model output (Morio, 2011). It is the study of how the variation in the output of a model (numerical or otherwise) can be apportioned, qualitatively or quantitatively, to different sources of variation (Saltelli et. al., 2008). There are two types of sensitivity analysis, local and global. During their study on reactor design with uncertainty, Haaker and Verheijen (2004) explain the local sensitivity analysis as the sensitivity of the model output when only one input factor is changed at a time while all other input factors are held fixed. On the other hand, Reuter and Liebscher (2008) described the global sensitivity analysis as a tool to provide information about the respective significance of structural input random parameters onto considered responses. When compared, local sensitivity techniques are more suitable to linear models (such as the CSM2020 in predicting future values from historical data), and they measure the impact of a single input parameter.

Khetwal (2020) used local sensitivity analysis to show how the model utilization reacts by varying the input parameters, such as duration of tunneling delays. During the analysis, Khetwal (2020) mentioned that CSM2020 has an overshadowing effect due to the frequencies and distributions of the modules. For the sensitivity analysis, if the change in the mean of the evaluated activity dataset is lesser than the mean of dominant activities, the utilization output of the model will be governed by the activity with the most significant contribution to the downtime.

For this study, local sensitivity analysis is used by varying the mean of each dataset on 10% intervals, ranging between +50% to -50%. Using a lesser interval has provided more precise results and contributed to analyzing the sensitivity limits of CSM2020.

Results are evaluated through the manual utilization calculation mentioned earlier in Chapter 3, using accumulated VA Time records.

$$Utilization (\%) = \frac{Accumulate\ VA\ Time\ for\ Tunnel\ Boring}{Accumulated\ VA\ Time\ for\ all\ activities} \times 100 \quad (6.1)$$

In addition to utilization, downtime contributions of tunneling activities are observed, and their change with varied relative mean values is recorded. It must be noted that according to Khetwal's (2020) explanations, the utilization output of the model alone could not be a satisfactory parameter to determine if the estimation is possible due to the overshadowing effect. One must consider the downtime contribution of each activity that is subjected to sensitivity analysis and observe a reasonable trend versus the mean variation.

For the sensitivity analyses, mean values of the previously mentioned datasets were varied, and new triangular distributions were introduced to the model while every other input parameter in the model was kept the same. This allowed the observation of the change in downtime contribution and utilization, allowing the most impactful tunneling activities to be identified. The following methodology was embraced during this process.

If a dataset is X, it has a mean of m_x , and a standard deviation of Sd_x . Varying the mean will create a new dataset, which can be named Y, with a mean of m_y , and a standard deviation of Sd_y . If a random data sample from X is X_i , it can be transformed into new data by normalizing it with the following formula.

$$Z_i = \frac{X_i - m_x}{Sd_x} \quad (6.1)$$

If the mean is selected as m_Y and the standard deviation is chosen as Sd_Y , the following formula gives Y_i .

$$Y_i = \frac{X_i - m_X}{Sd_X} Sd_Y + m_Y \quad (6.2)$$

This way, each data point can be transformed to create a new dataset with the desired new mean and standard deviation. The creation of new datasets has allowed the calculation of new triangular distributions and evaluation of new downtime contributions. These new triangular distributions were introduced to the CSM2020 model, and machine utilization and downtime contributions were observed. Activities that respond with reasonable trends to the changes identified as estimable in terms of delay times.

At this point, it must be noted that the segment installation is a unique activity that has the same activity time as delay time. Boring must stop for the single shield machines to install the segmental liner. Hence, sensitivity analysis for this activity explores the possibility of estimation of both activity time and delay time. All the other analyses can only explore the possibility of estimating delay time distributions for their relative modules.

In the following sub-sections, tunneling activities with overall downtime contribution and frequency greater than 1% were evaluated through local sensitivity analysis. Charts describing the change in utilization and downtime contribution were presented with a mean variation. Three charts are presented for each activity under relative sub-sections, such as a combined chart for utilization and downtime contribution and two individual ones to evaluate separately. Activities that show expected trends in these charts are identified as estimable in terms of delay times, and activity time only for segment installation.

6.1 Segment Installation

The following charts provide information on utilization and downtime contribution output by varying segment installation time. Figure 6.1 presents the results for both downtime contribution and utilization change by mean variation for segment installation. Figure 6.2 presents the downtime contribution change for the same activity. Lastly, Figure 6.3 shows utilization change for the variable values of segment installation time.

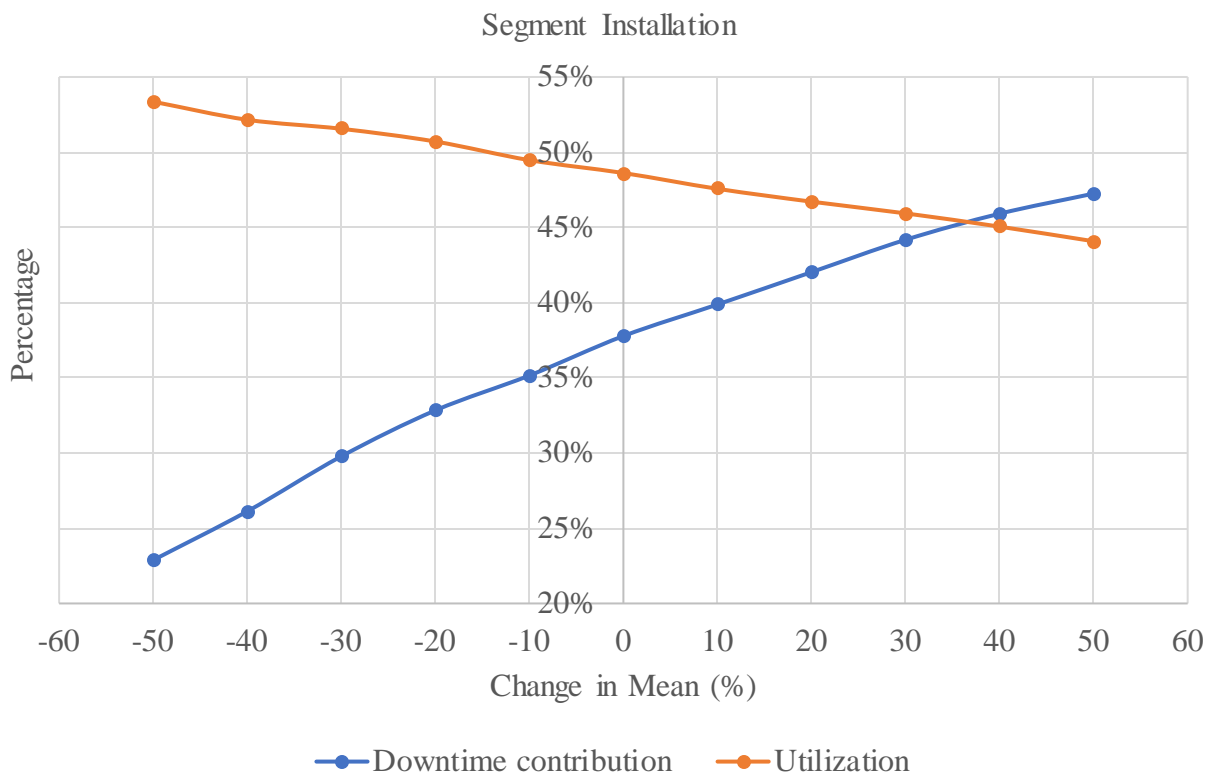


Figure 6.1: Variation in downtime contribution and utilization by changing mean values of segment installation.

Results for utilization rate are inversely proportional with the mean of the dataset. On the contrary, downtime contribution results are directly proportional to the mean as expected. These findings verify the possibility of estimation of activity time for segment installation activity.

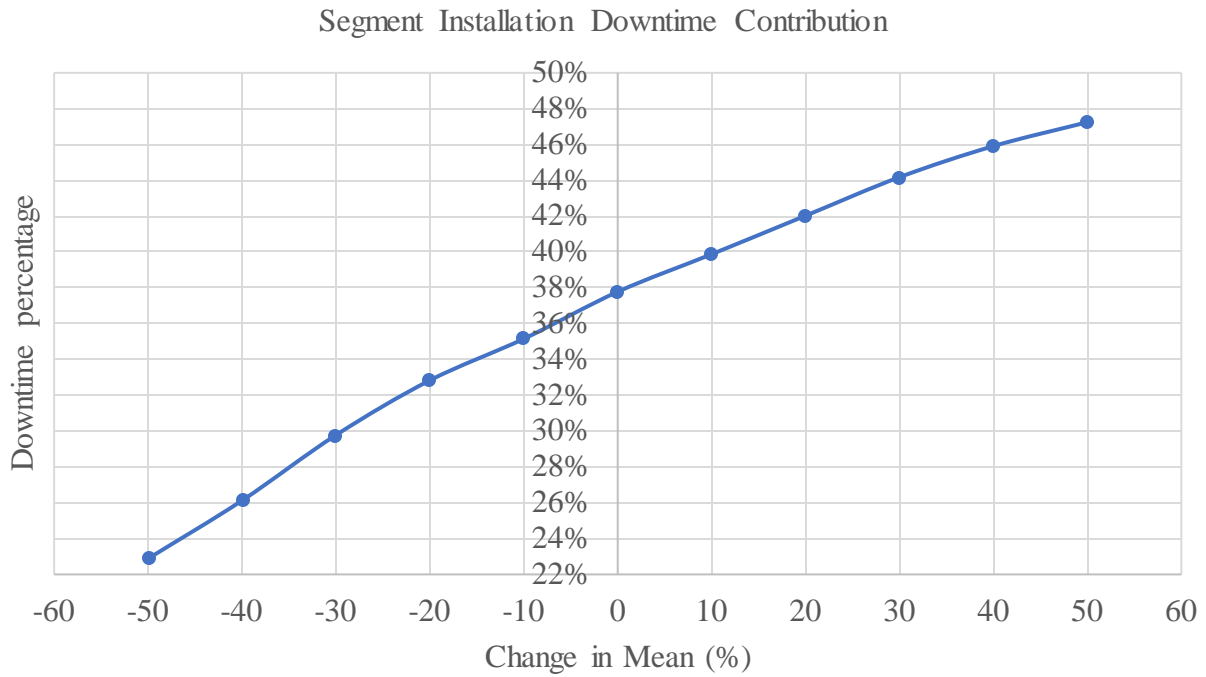


Figure 6.2: Variation in downtime contribution by variation of the mean value of segment installation.

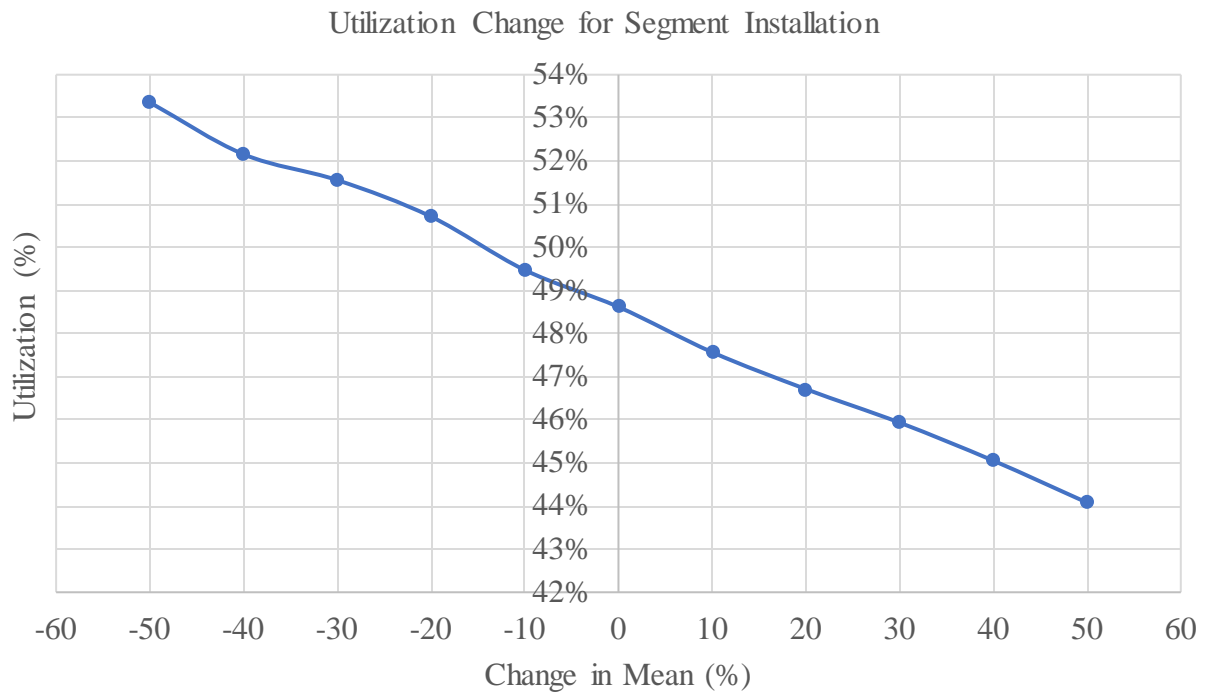


Figure 6.3: Change in TBM Utilization as a function of the mean value of segment installation.

6.2 Unscheduled Maintenance

The same approach was used to evaluate the impact of unscheduled maintenance on machine utilization and downtime contribution shown in Figures 6.4, 6.5, and 6.6.

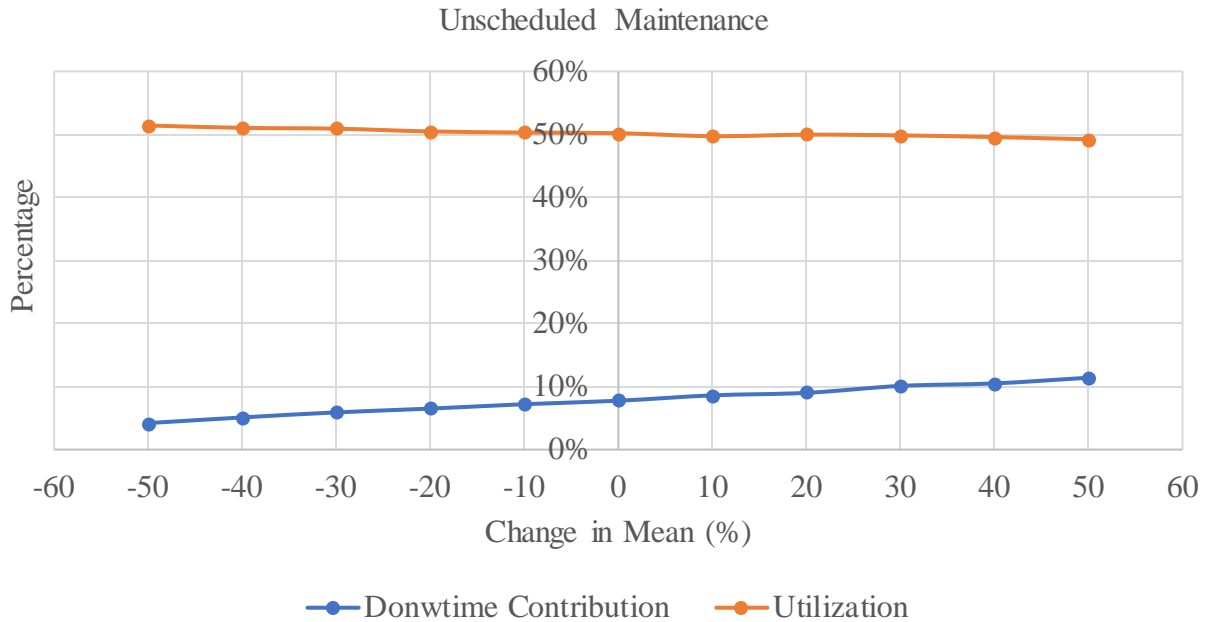


Figure 6.4: Variation in downtime contribution and utilization by changing mean values of unscheduled maintenance.

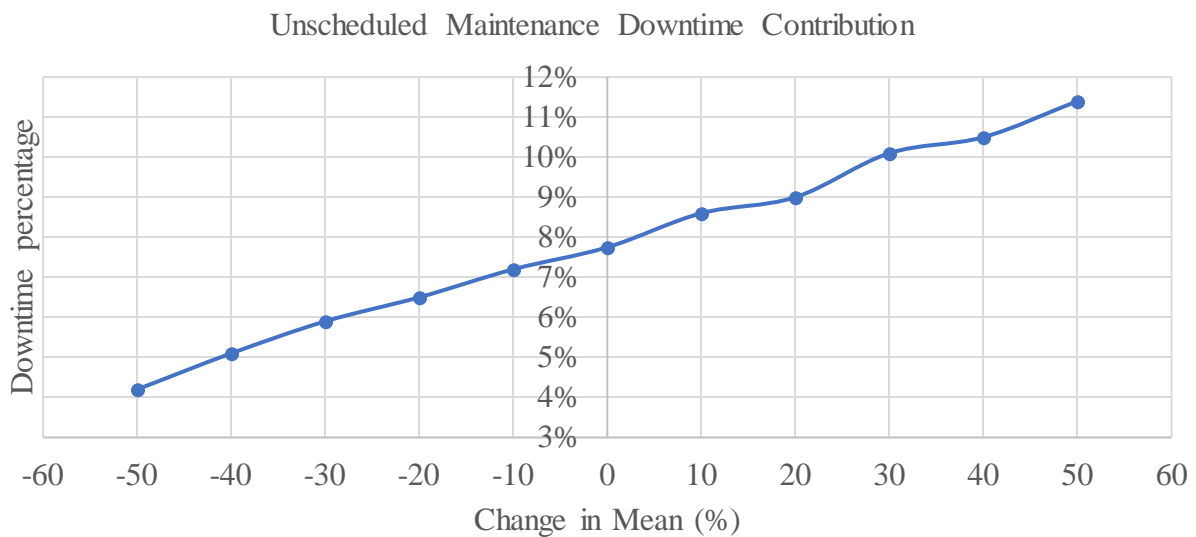


Figure 6.5: Variation in downtime contribution by variation of the mean value of unscheduled maintenance.

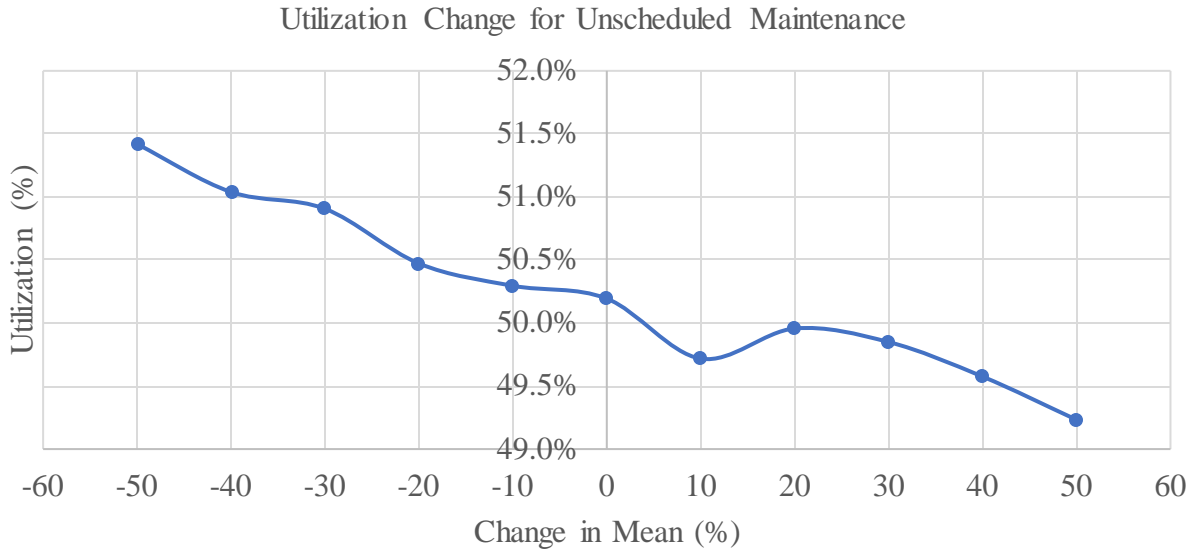


Figure 6.6: Change in TBM Utilization as a function of the mean value of unscheduled maintenance.

6.3 Electrical Systems Repair

The same approach was used to evaluate the impact of electrical systems repair on machine utilization and downtime contribution shown in Figures 6.7, 6.8, and 6.9

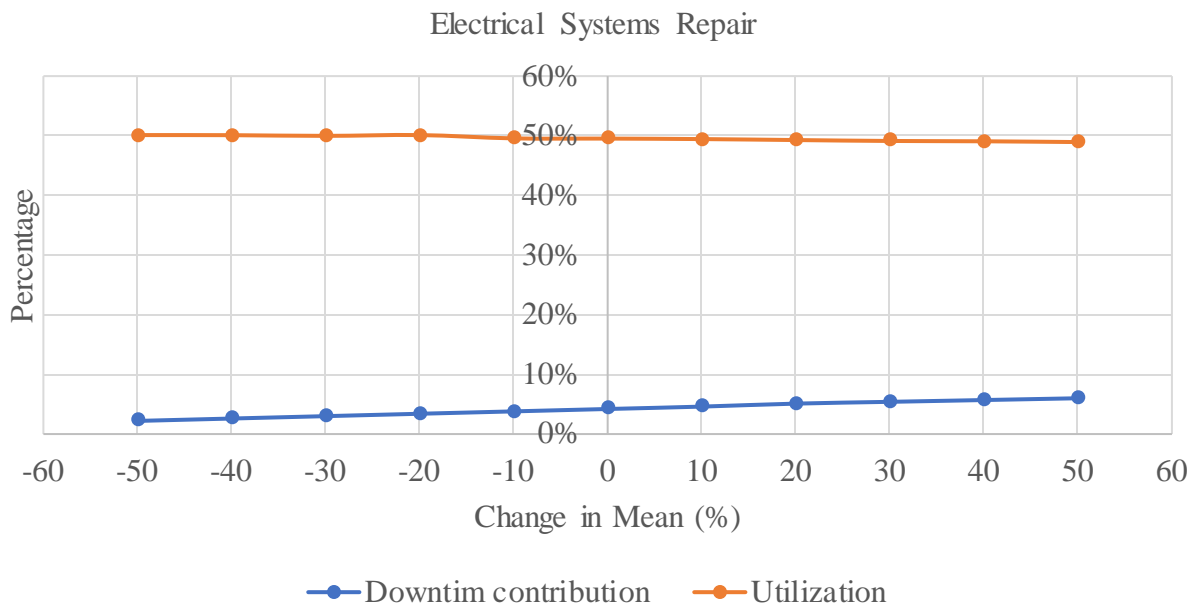


Figure 6.7: Variation in downtime contribution and utilization by changing mean values of electrical systems repair.

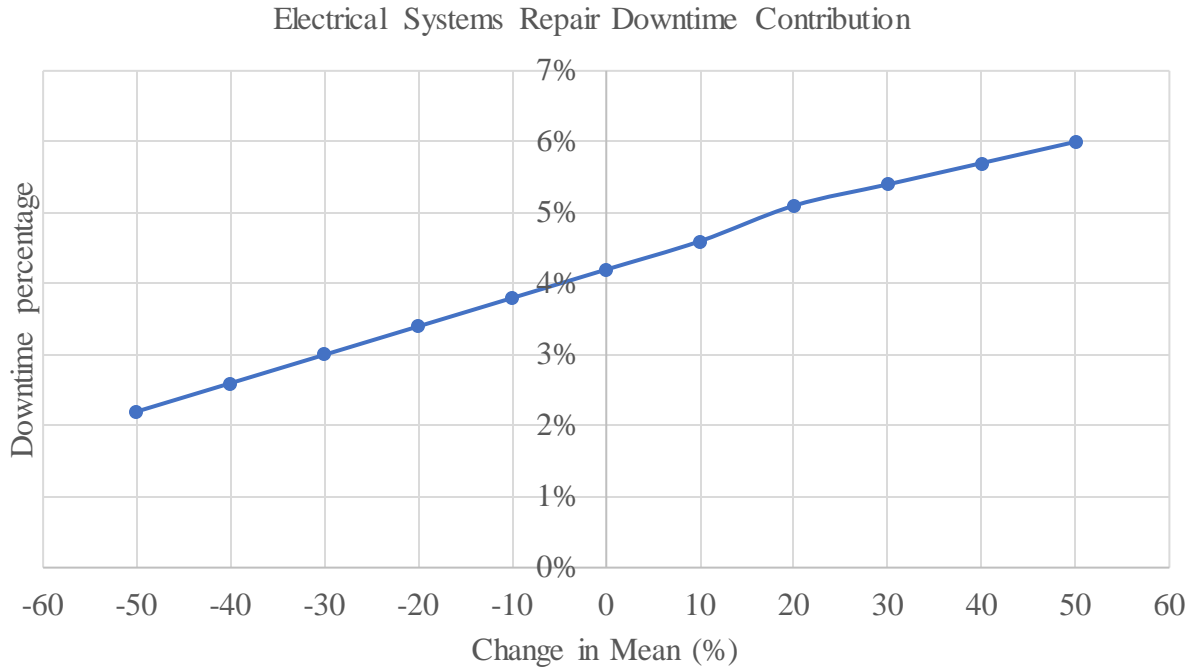


Figure 6.8: Variation in downtime contribution by variation of the mean value of electrical systems repair.

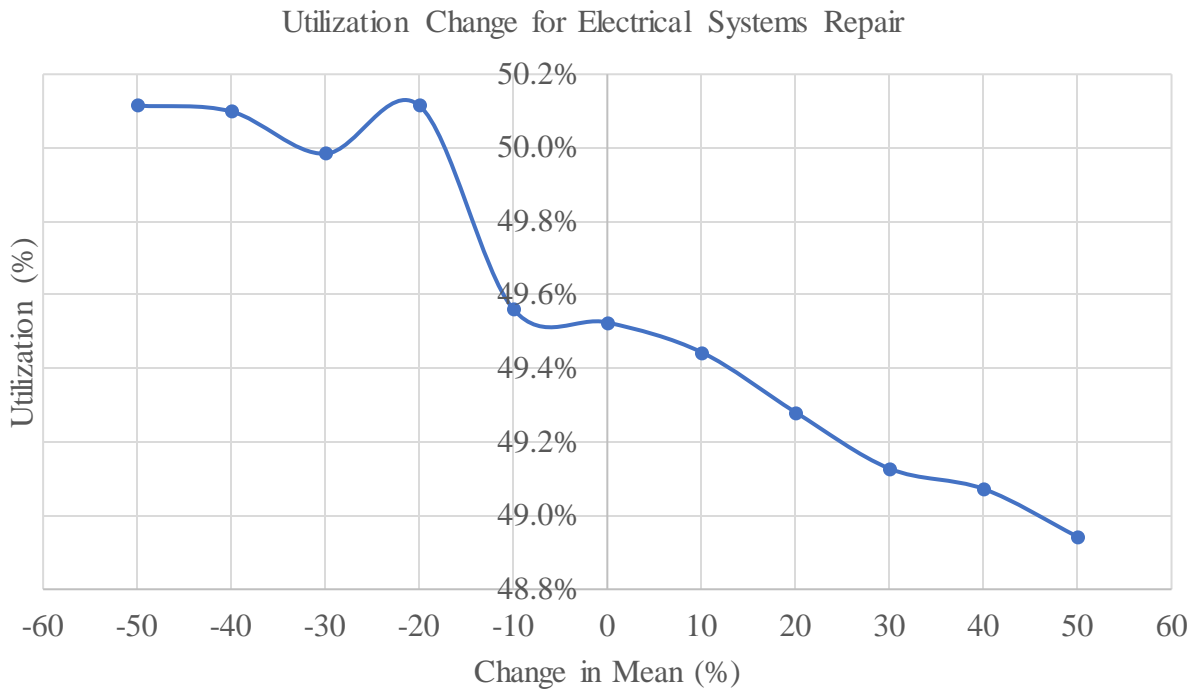


Figure 6.9: Change in TBM Utilization as a function of the mean value of electrical systems repair.

6.4 Backfill Grout System

The following charts (Figures 6.10, 6.11, and 6.12) present the impact of the backfill grout system on machine utilization and downtime contribution using the same approach as before.

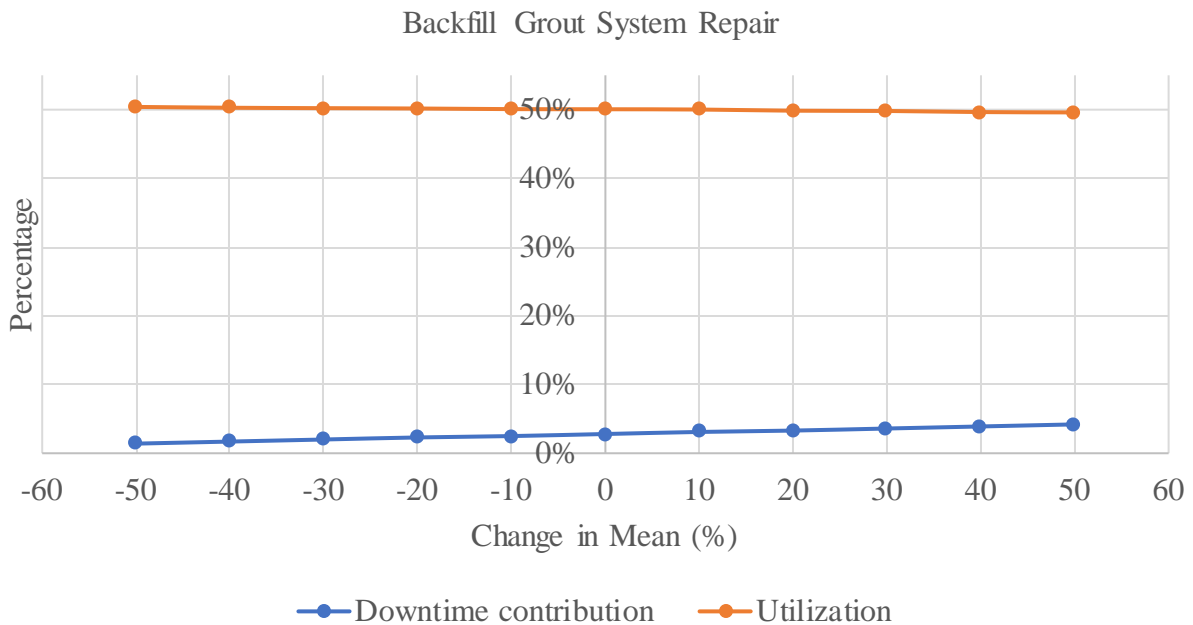


Figure 6.10: Variation in downtime contribution and utilization by changing mean values of backfill grout system.

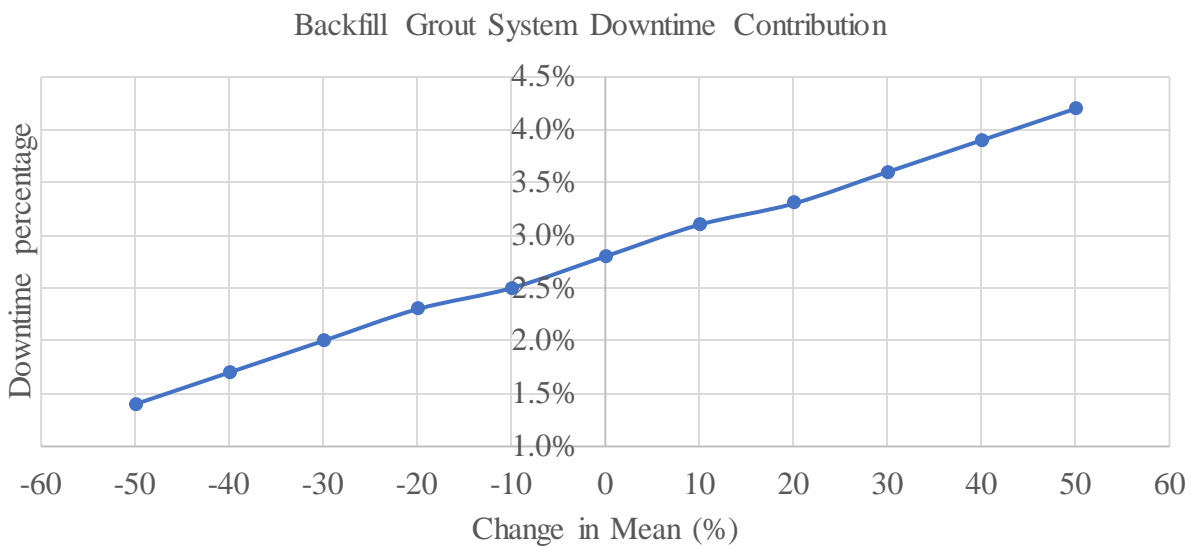


Figure 6.11: Variation in downtime contribution by variation of the mean value of backfill grout system.

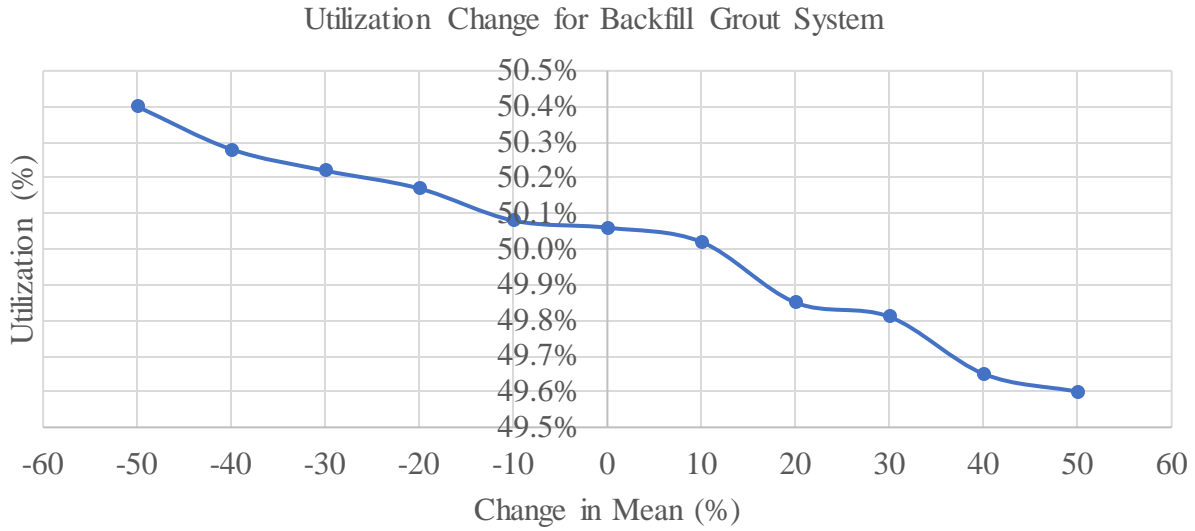


Figure 6.12: Change in TBM Utilization as a function of the mean value of backfill grout system.

6.5 Loading & Unloading of Supplies

The following charts (Figures 6.13, 6.14, and 6.15) present the impact of loading & unloading of supplies on machine utilization and downtime contribution using the same approach as before.

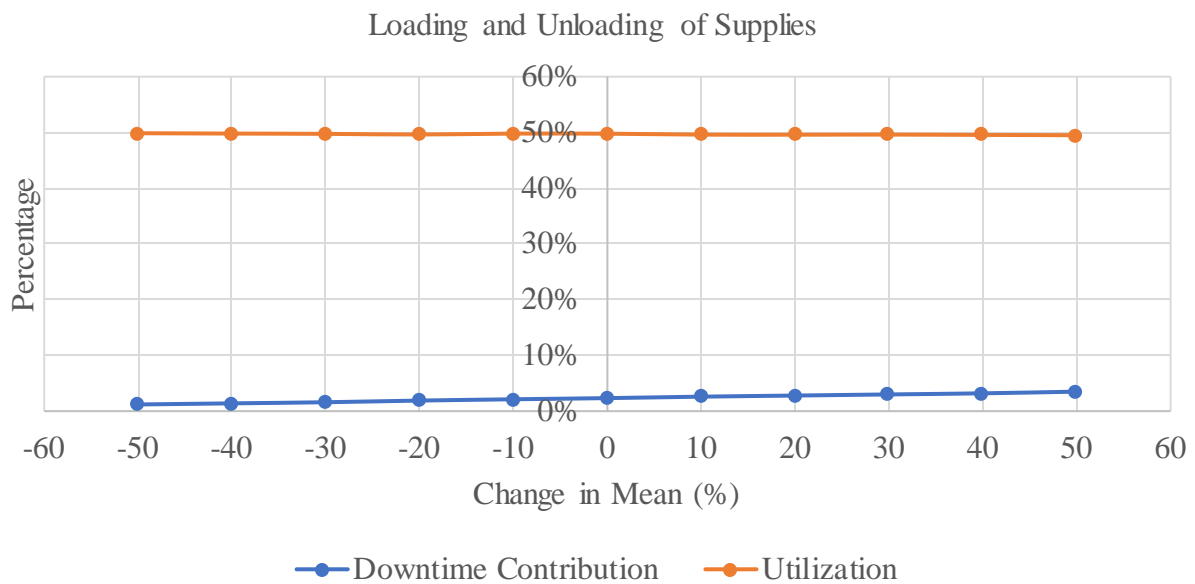


Figure 6.13: Variation in downtime contribution and utilization by changing mean values of loading & unloading of supplies.

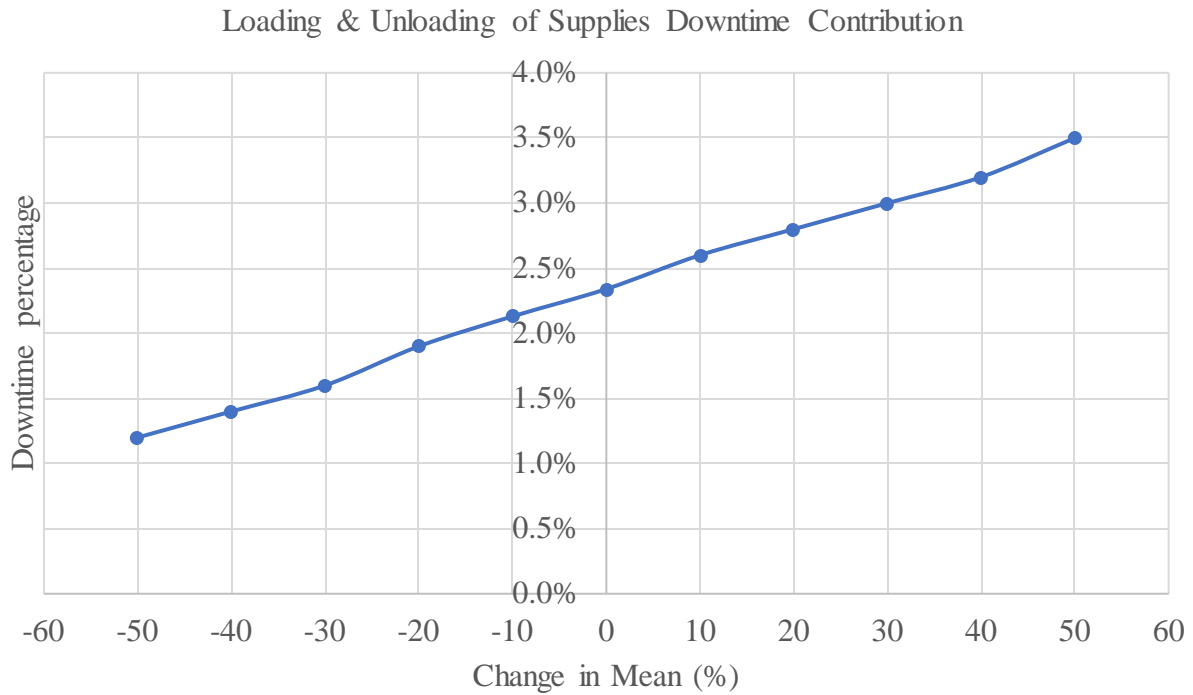


Figure 6.14: Variation in downtime contribution by variation of the mean value of loading & unloading of supplies.

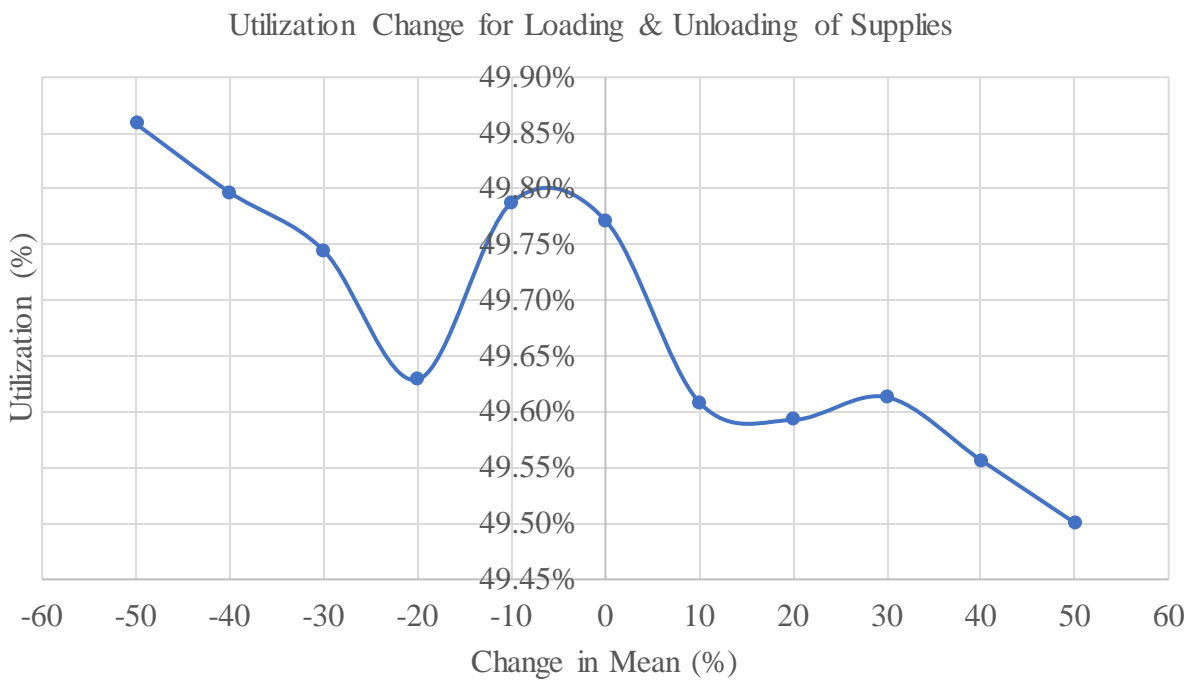


Figure 6.15: Change in TBM Utilization as a function of the mean value of loading & unloading of supplies.

6.6 Backup Utilities Repair

The following charts (Figures 6.16, 6.17, and 6.18) present the impact of backup utilities repair on machine utilization and downtime contribution using the same approach as before.

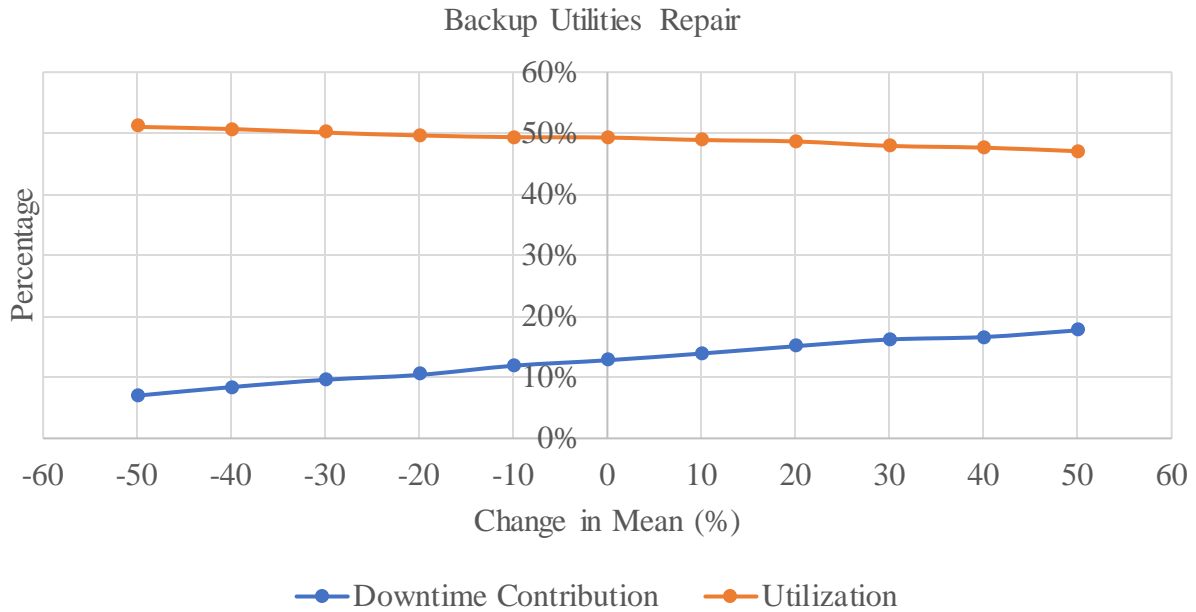


Figure 6.16: Variation in downtime contribution and utilization by changing mean values of backup utilities repair.

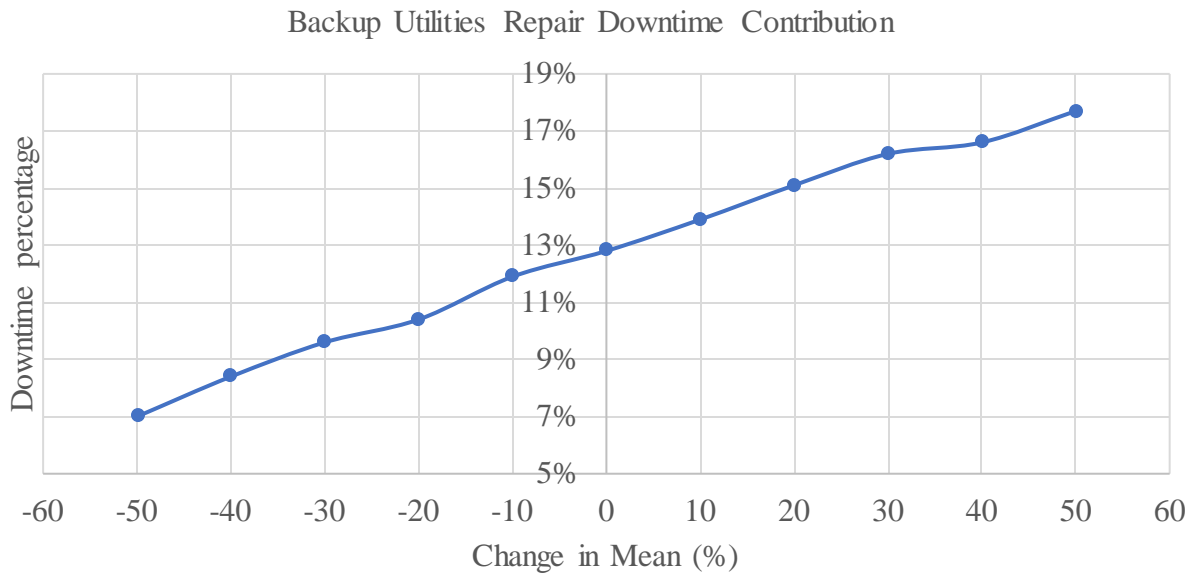


Figure 6.17: Variation in downtime contribution by variation of the mean value of backup utilities repair.

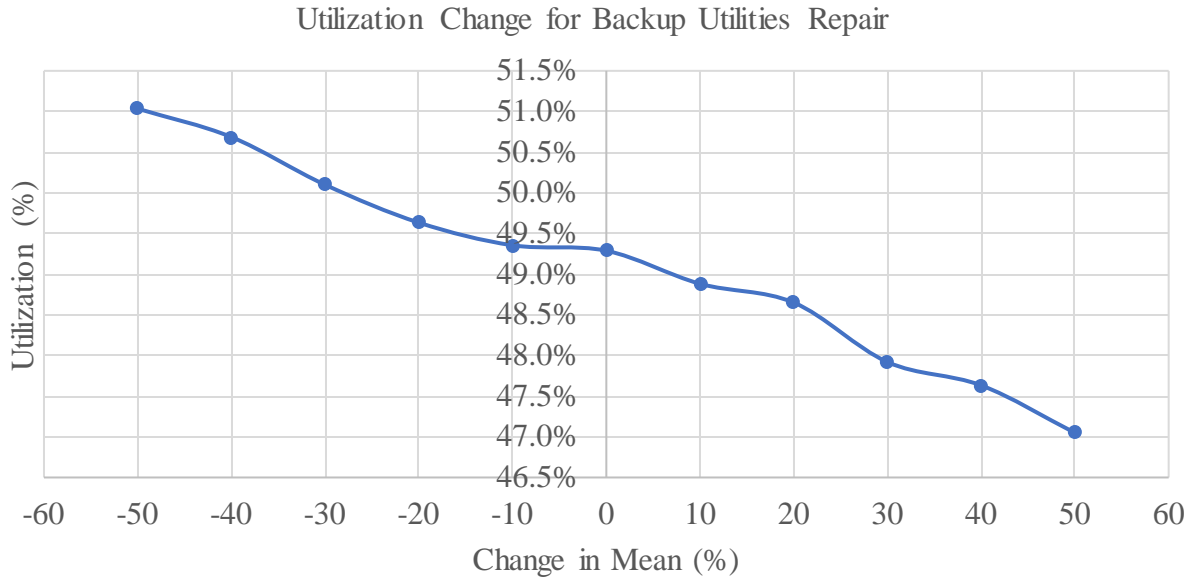


Figure 6.18: Change in TBM Utilization as a function of mean value of backup utilities repair.

6.7 Unforeseen Delays

The following charts (Figures 6.19, 6.20, and 6.21) present the impact of unforeseen delays on machine utilization and downtime contribution using the same approach as before.

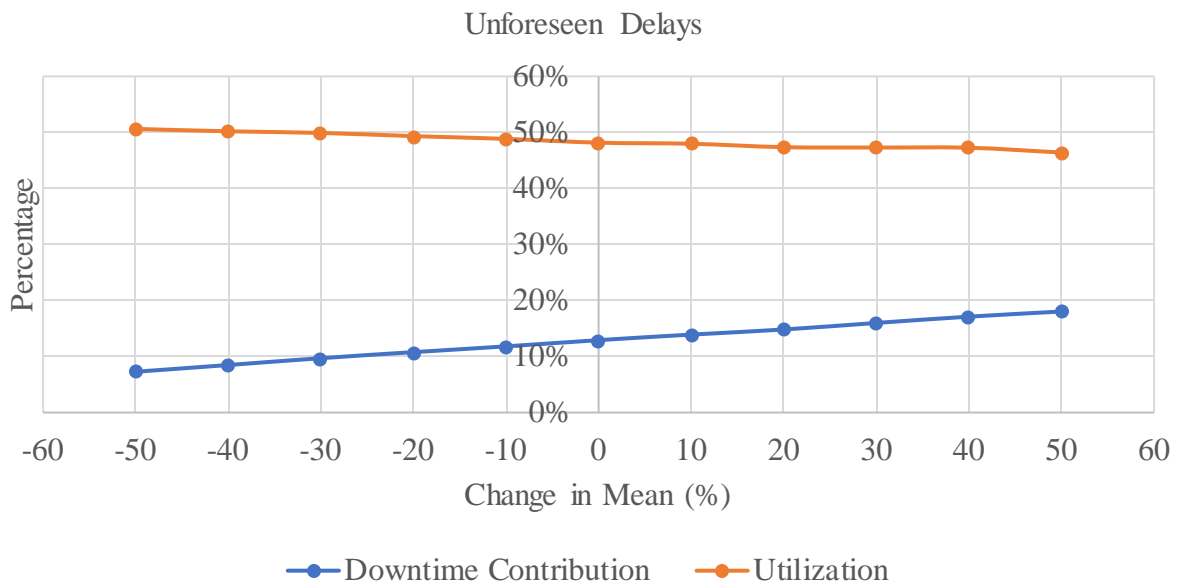


Figure 6.19: Variation in downtime contribution and utilization by changing mean values of unforeseen delays.

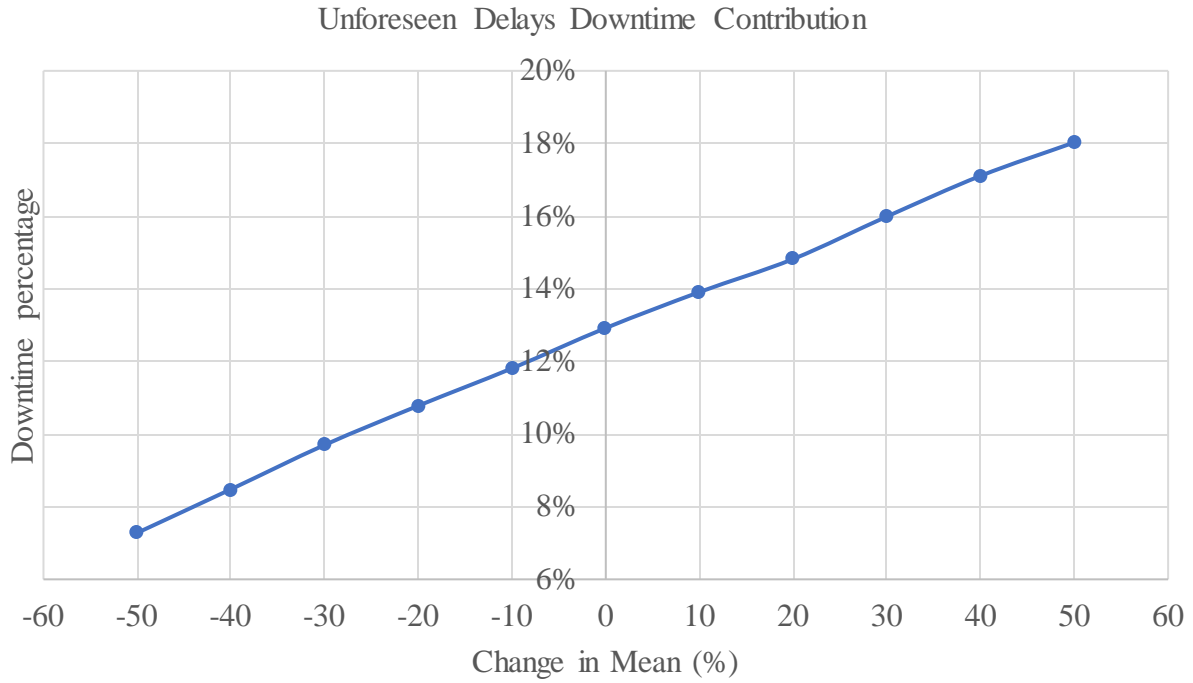


Figure 6.20: Variation in downtime contribution by variation of the mean value of unforeseen delays.

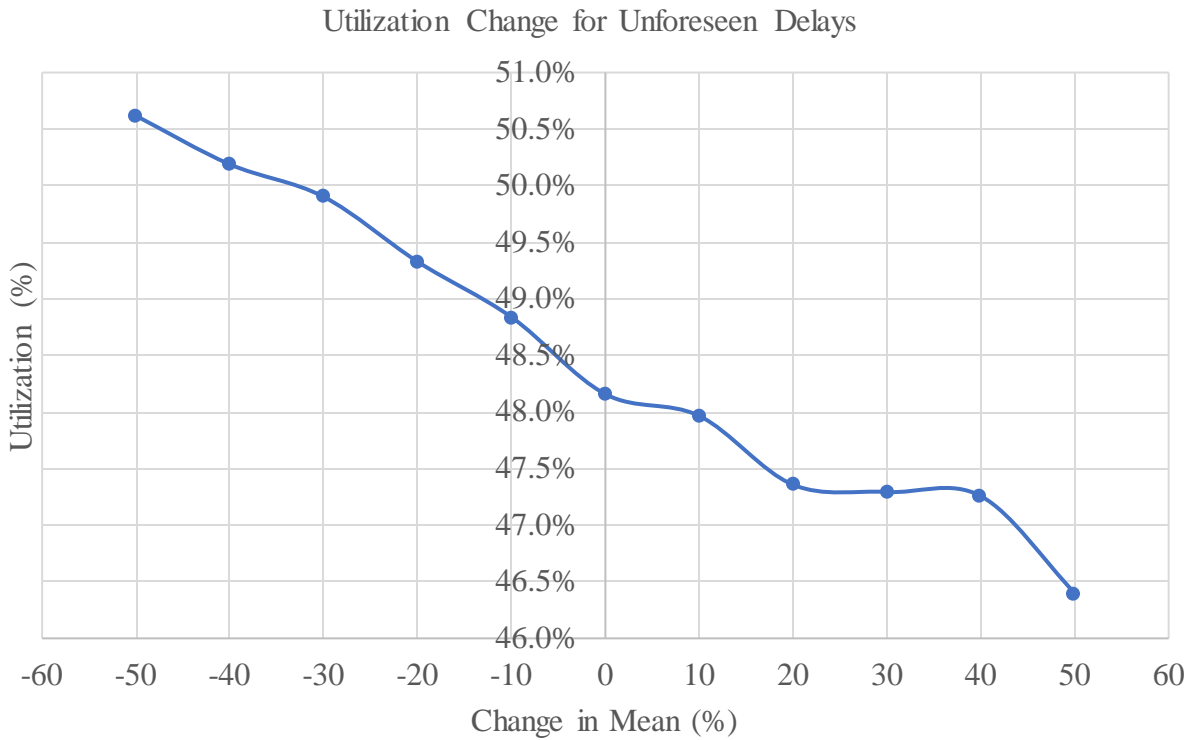


Figure 6.21: Change in TBM Utilization as a function of the mean value of unforeseen delays.

6.8 Slurry Line Extension

Following charts (Figures 6.22, 6.23, and 6.24) present the impact of slurry line extension on machine utilization and downtime contribution using the same approach as before.

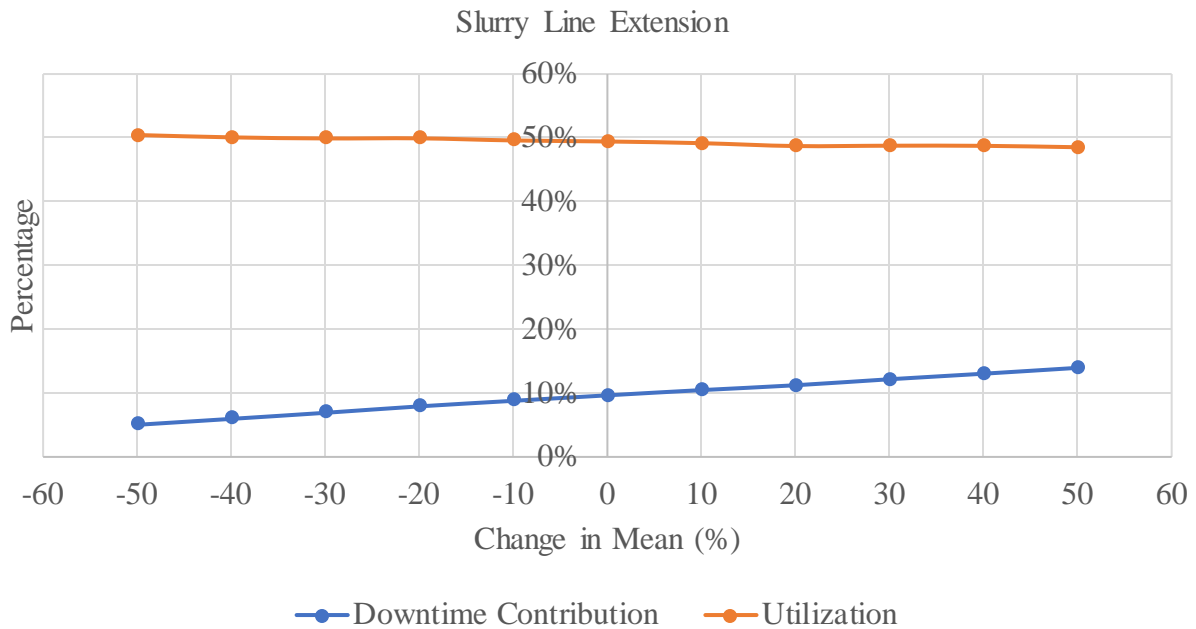


Figure 6.22: Variation in downtime contribution by variation of the mean value of slurry line extension.

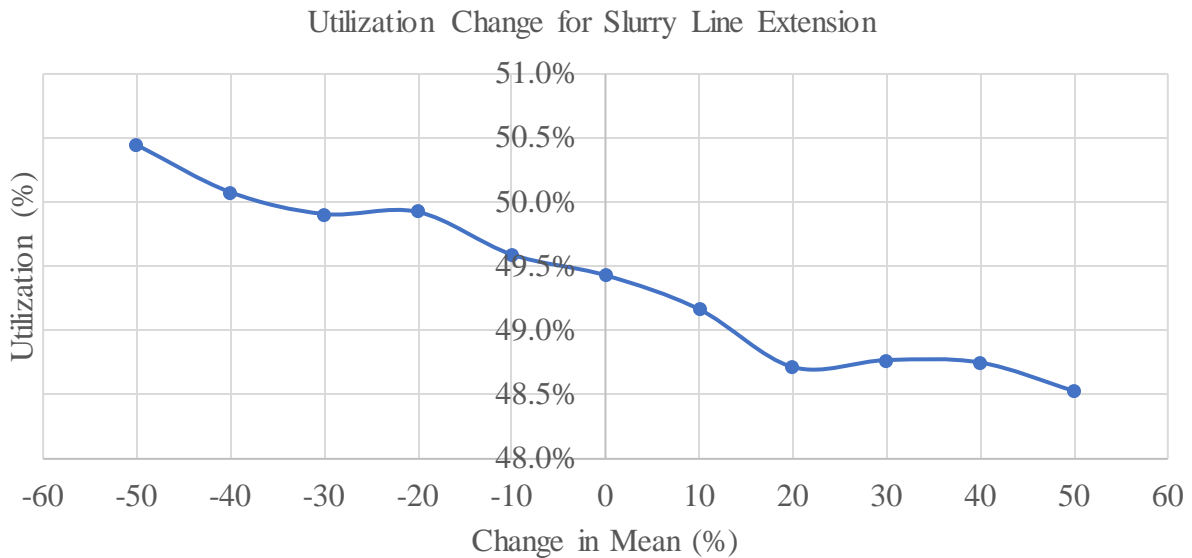


Figure 6.23: Variation in downtime contribution by variation of the mean value of slurry line extension

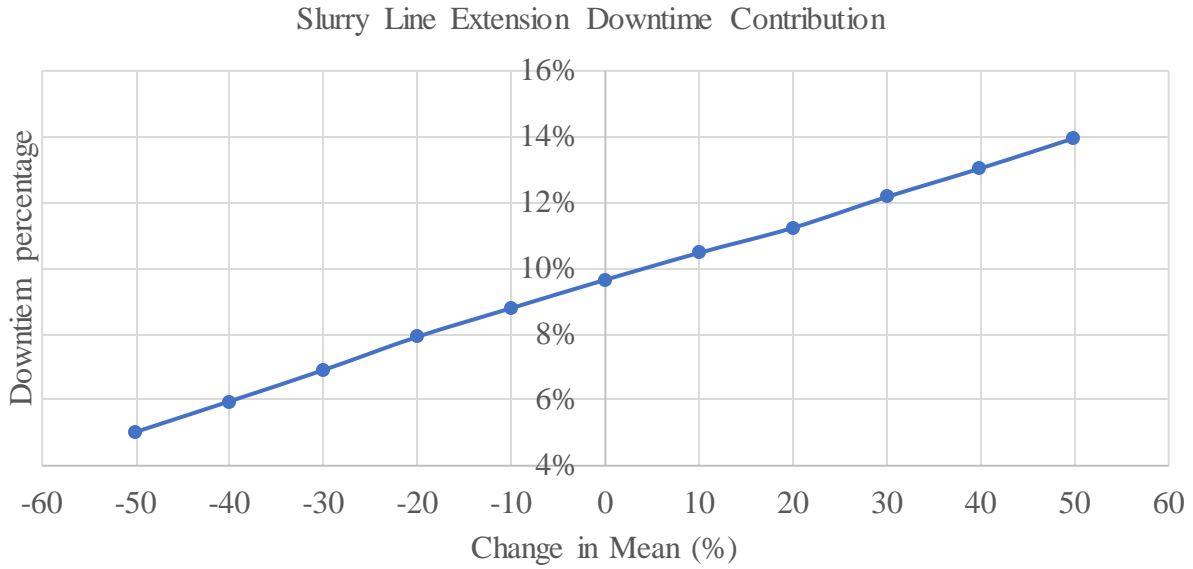


Figure 6.24: Change in TBM Utilization as a function of the mean value of slurry line extension.

6.9 Slurry Lines Repair

Following charts (Figures 6.25, 6.26, and 6.27) present the impact of slurry lines repair on machine utilization and downtime contribution using the same approach as before.

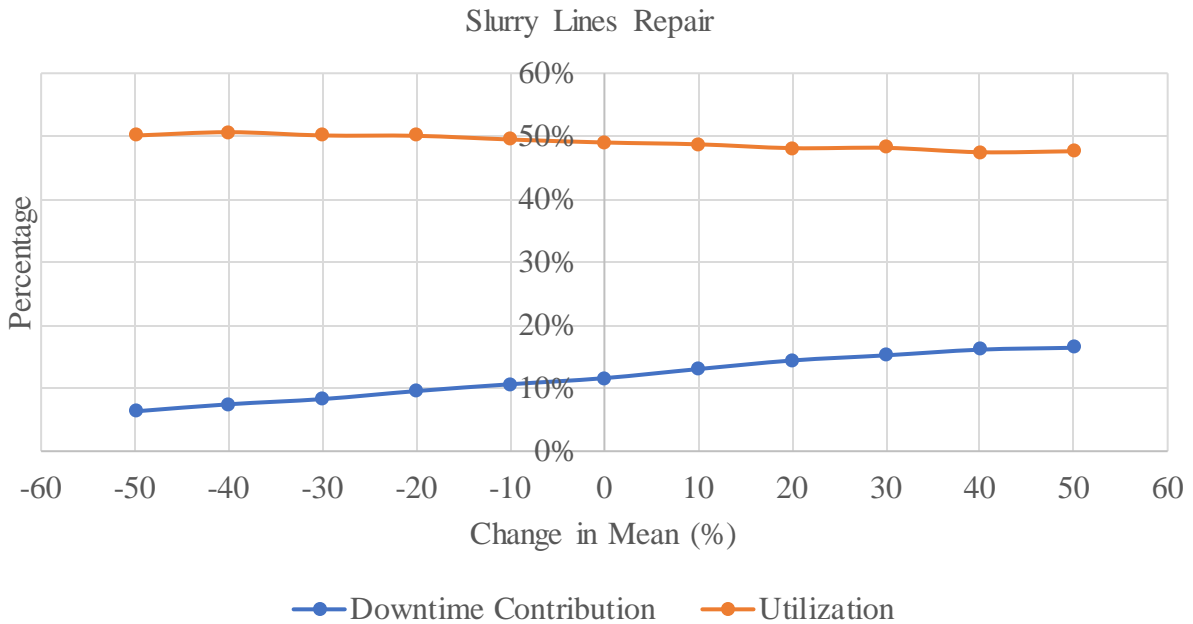


Figure 6.25: Variation in downtime contribution and utilization by changing mean values of slurry lines repair.

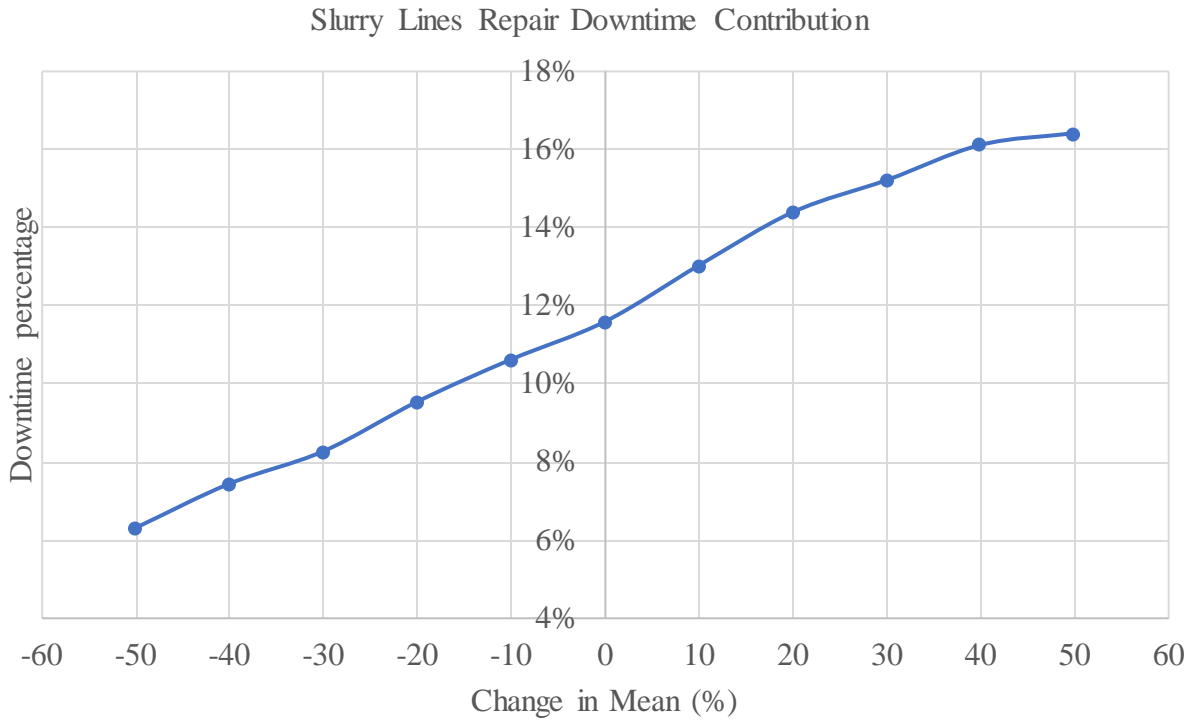


Figure 6.26: Variation in downtime contribution by variation of mean value of slurry lines repair.

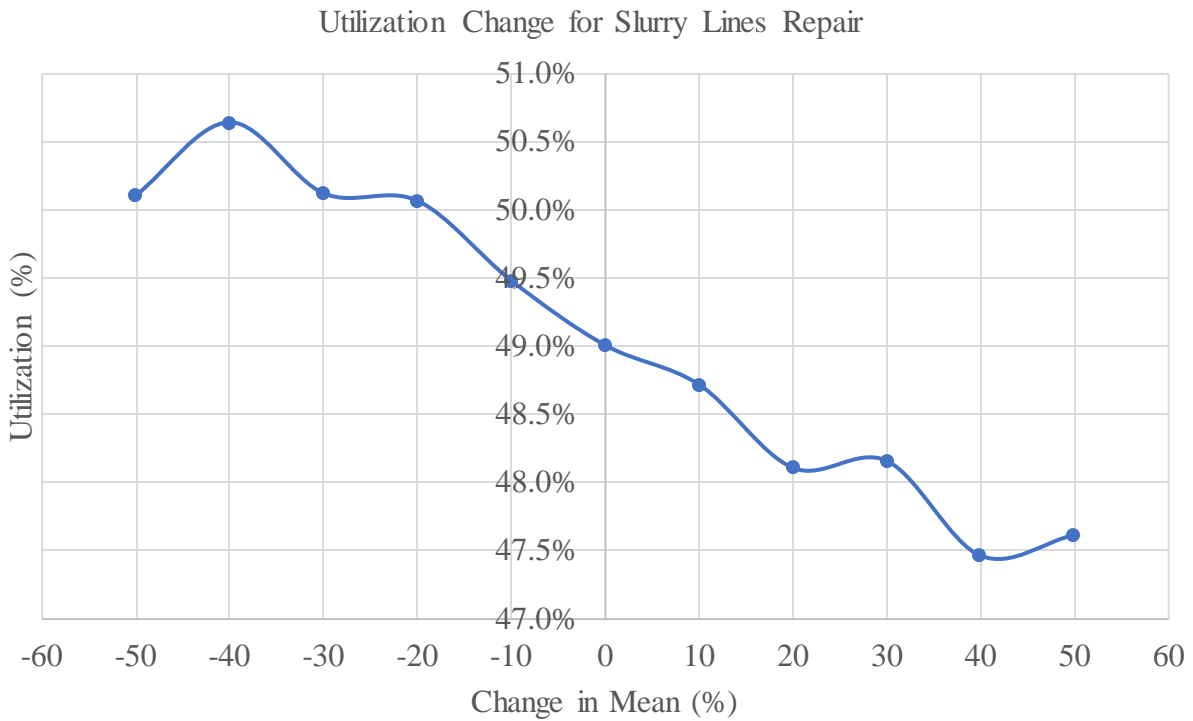


Figure 6.27: Change in TBM Utilization as a function of the mean value of slurry lines repair.

6.10 Discussion

The CSM2020 model was used to simulate a section of an ongoing tunneling project that was completed by a slurry TBM operation in this study. During the validation process, the model provided a good agreement with the downtime contribution trends by comparing the estimated utilization and downtimes with those observed in the field. The subsequent comparison of the result of modeling using different distributions, including the best fit, triangular, and fixed values, the response of simulation models to the changes in the different activity time distributions was examined. The results showed that the use of fixed mean values can generate a reasonable estimate of utilization, but this did not allow for stochastic simulation of the site activities. For sensitivity analysis, localized sensitivity analysis was conducted using different distribution functions and changing means for individual activities to see the model reaction to such changes. Based on the knowledge gained from this study, there are several points to highlight.

- It was noted that the correct implementation of Arena® concepts is vital to observe accurate results (such as number of shifts scheduled, and number of shifts marked as busy).
- Using shift numbers and delay times as inputs is counterintuitive with the predictive purpose of the model.
- The original model setup requires revisiting because it would not allow for simulating three 8-hour shift operations, especially for the modules like Unforeseen Delays.
- The activity time distribution database needs to expand to provide better results and create more accurate probability distributions to prevent over/underestimation of the value-added time for the relative activities.

- According to the sensitivity analysis, utilization rate alone did not provide satisfactory results to show the impacts of changing activity times, except for the activities directly mapping into delays and/or are a large portion of downtime.
- Lack of response of the utilization to activity times with low percentage contribution to overall operation was expected due to the overshadowing effect of dominant activities and their contributions to overall downtime. This effect was observed in the sensitivity analysis part of this study.
- In addition to the utilization rate, downtime contributions of each module should be evaluated, and their inversely proportional trends with mean variances provided reasonable trends.
- The trends, which are presented in this chapter, support the hypothesis of estimation of activity time for segment installation and delay times for other activities from recorded downtime field data, using the CSM2020 as a numerical simulation tool.

CHAPTER 7

CONCLUSIONS AND RECOMMENDATIONS FOR FUTURE STUDIES

This study examined the possibility of estimating tunneling activity time distributions for a slurry TBM project using the CSM2020 discrete event simulation program as the TBM performance prediction tool and subjecting each activity to mean changes through sensitivity analyses. According to the results of the analyses, both utilization and downtime contributions of relevant tunneling activities were evaluated. The following sections discuss conclusions based on the analysis results and recommendations for future work.

7.1 Conclusions

- Estimation of tunneling activity time distributions that directly contribute to a delay time category (such as segment installation) is possible with the current version of the CSM2020 model. Estimation of other activity time distributions is not possible with the current version. Only the estimation of delay times for these activities, which partially contribute to a delay time category, is possible.
- It is possible to simulate slurry TBM operations in hard rock conditions with CSM2020 through appropriate modifications.
- Creation and use of probability distributions in CSM2020 based on a limited database are susceptible to producing over/underestimation of activity durations measured by the model. This is because of the possibility of having some anomalies included in the recorded activity or delay times that may shift the reasonable distribution of a given activity time distribution. In such cases, the anomalies (unusually long delays) should be treated differently, perhaps included in an unforeseen delay category.

- When close to completing every iteration, the model entity only visits “Unforeseen Delays” and “Scheduled Maintenance” modules, thus creating excess value-added time records for these activities, affecting the utilization rate. This issue could not be solved for unclear reasons. According to information provided by Khetwal (2020), it was theorized that the reason for this behavior is the original model setup, which is based on two 10-hour production shifts and one 4-hour maintenance shift per day.
- The original model setup cannot capture the general workflow for three 8-hour shift projects without assigning some of the datasets, such as unforeseen delays, to unused modules outside their specified modeling area.
- CSM2020 cannot evaluate concurring delays within the same delay group, such as electrical systems repair and unscheduled maintenance under the TBM Face Delays area. The only exceptions are the ground support activities for the open-type machines and the tunnel boring/segment installation pair for the double shield machines. This is because both of these activities are directly recorded as machine delays and reflected in downtime calculations.
- Implementation of Arena® concepts in the CSM2020 requires revisiting. Some of the modules in the Arena program requires in depth knowledge of the software to function properly.
- Input and output parameters of the CSM2020 may require rethinking and reorganizing since there are some mismatches between the activity times and the recorded parameters by the program as downtime.

The analysis carried out during this study was the first attempt of exploring the possibility of estimation of tunneling activity times using the CSM2020 discrete event simulation.

Contributions of this study can be summarized as the following:

- Recording of activity times and creation of new time distributions for a slurry type TBM
- Modifying the CSM2020 to include the slurry machine operational settings for the selected section of the tunnel that was used in the simulation
- Examining and validating the modified program with field data
- Applying various activity time distributions in the DES simulation model to see their impact on machine utilization and downtime distributions
- Exploring the possibility of using delay and downtime information to develop reasonable estimates of activity time distributions where they have not been directly measured in the field

7.2 Recommendations

- Using a limited database was one of the significant limitations of this study. Additional data on tunneling activities and expansion of the database for various tunneling operations, TBM types, and site settings are strongly recommended.
- The CSMS2020 uses a combination of delay and activity time distribution data as input and produces machine utilization. The model should be further modified to focus on using activity times as the primary input instead of delays. Proper adjustments can be made (such as using more entities) for the model to produce delay times as the output in addition to utilization rate. This can allow future research to use the same methodology that is outlined in this study and estimate tunneling activity times.

- The CSM2020 requires users to determine and input the total number of shifts needed to complete the evaluated tunnel length before running the model. This requirement is counterintuitive with using CSM2020 as a prediction tool. The number of shifts should be an output of the model, and it is recommended further studies work to adjust this issue in the model.
- The CSM2020 uses a number, such as number of shifts to define scheduled parameters and repetition of Arena® simulations, with the goal of estimating machine utilization. However, this makes the model highly susceptible to producing erroneous results by the definition of these parameters. Details of this issue are explained in Chapter 3. The CSM2020 can be further developed and adjusted to work with more than one entity (i.e., number of shifts) to avoid this issue.
- The number of scheduled activities can be determined for different projects and TBM types (considering a more extensive database is established) and introduced to the model as a base to facilitate calculation of instantaneous utilization rates, scheduled utilization, and the number of busy resources.
- Relative to the points above, using more than one entity can also enable the CSM2020 to evaluate simultaneous activities, not only the ones that are only applicable to open-type TBM. For example, the model can consider more than one activity to be performed simultaneously, record the longest duration randomly selected from the relative time distributions, and apply it as the delay. This way, a more realistic simulation of tunneling operation is possible.
- The CSM2020 uses frequencies to determine if an activity is necessary. The nature of calculating these frequencies can be developed into a distribution rather than a simple

ratio between the number of data points of the relative dataset and the number of strokes required to complete the desired tunnel length. In reality, there is no way to determine these delays before they occur; hence it is not possible to calculate their frequencies because they are simply unknown. However, the frequencies of these delays can be evaluated by inspecting the data of a specific period of any project. This period can be a month or longer. Using a Monte Carlo simulation, these events can be defined to the selected period. Their occurrences can form a probability distribution specific for that event, replacing the frequencies currently used by the CSM2020 and potentially increasing the model accuracy. This way, shorter tunnel sections (such as sections representing different geological units) can be better evaluated.

- Some activities such as scheduled maintenance, shaft operations, or slurry pump or conveyor booster installations are not stochastic; instead, they are planned. Evaluating these activities using frequencies and probability distributions can be problematic. Using frequencies and probability distributions to define tunneling activities in a discrete event simulation model should be investigated in more detail by future work.
- Human input, such as delays caused by crews, can be evaluated using specific entities with assigned attributes. The number of people in a crew can be specified with the same number of entities with attributes, such as electrician, mechanic, TBM operator, engineer, etc. Each entity, or crew member, could be responsive to only those activities that concern them.
- Using a platform other than Arena® can decrease program run time when the user needs to perform a higher number of iterations but contain the time required for simulation.

Also, a code-based platform (such as MATLAB®) can better address the issues about the model and the input/output data structure.

REFERENCES

- Alber, M., 2000. Advance rates of hard rock TBM's and their effect on project Economics. *Tunneling and Underground Space Technology* 15 (1), 55–64.
- Al-Jalil, Y., 1998. Analysis of Performance of Tunnel Boring Machine-based Systems. The University of Texas at Austin.
- Barton, N. R. (2000). *TBM tunneling in jointed and faulted rock*. Crc Press.
- Benardos A G, Kaliampakos D C. Modeling TBM performance with artificial neural networks. *Tunn Undergr Space Technol*, 2004, 19(3): 597-605
- Bieniawski, Z. T., Tamames, B., Fernandez, J., & Hernandez _Alvarez, M. (2006). Rock Mass Excavability (RME) indicator: New way to select the optimum tunnel construction method. *Tunneling and Underground Space Technology*, 21, 237{237.
- Bruland, A. 1998. *Hard rock tunnel boring*, Trondheim: Norwegian Institute of Technology (NTNU), Trondheim, Norway.
- Einstein, H, Indermitte, C, Sinfield, J, Descoedres, F, Dudt, J-P. (1999). DECISION AIDS FOR TUNNELING. *Transportation Research Record*, Vol. 1656, p. 6-13.
- Farrokh, E., Rostami, J. and Laughton, C. (2012). Study of various models for estimation of penetration rate of hard rock TBMs, *Tunnel. Undergr. Space Technol.* 30: 110-123.
- Farrokh, E., 2012. Study of Utilization Factor and Advance Rate of Hard Rock TBMs. PhD Thesis Dissertation. Department of Energy and Minerals Engineering, The Pennsylvania State University
- Frank F. Roxborough, Huw R. Phillips, Rock excavation by disc cutter, *International Journal of Rock Mechanics and Mining Sciences & Geomechanics Abstracts*, Volume 12, Issue 12, 1975, Pages 361-366, ISSN 0148-9062.
- Frough, Omid & Torabi, Seyed. (2013). An application of rock engineering systems for estimating TBM downtimes. *Engineering Geology*. 157. 112–123. 10.1016/j.enggeo.2013.02.003.
- Frough O., Rostami J., 2014. Analysis of TBM Performance in Two Long Mechanized Tunnels, Case History of Karaj Water Conveyance Tunnel Project Lots 1. and 2 (Iran). *Proceedings of the World Tunnel Congress – Tunnels for a Better Life*. Foz do Iguacu, Brazil
- Frough O., Khetwal, A., Rostami, J., 2019, Predicting TBM utilization factor using discrete event simulation models.

- Gholamnejad J., Tayarani N., 2010. Application of artificial neural networks to the prediction of tunnel boring machine penetration rate, *Mining Science and Technology (China)*, Volume 20, Issue 5, Pages 727-733, ISSN 1674-5264.
- Gong, Q., Jiao, Y., & Zhao, J. (2006). Numerical modeling of the effects of joint spacing on rock fragmentation by TBM cutters. *Tunneling and Underground Space Technology*, 21 (1), 46-55.
- Gong, Q.-M., Zhao, J., & Jiao, Y.-Y. (2005). Numerical modeling of the effects of joint orientation on rock fragmentation by TBM cutters. *Tunneling and Underground Space Technology*, 20 (2), 183-191.
- Gong, Q., & Zhao, J. (2009). Development of a rock mass characteristics model for TBM penetration rate prediction. *International Journal of Rock mechanics and mining sciences*, 46 (1), 8-18.
- Grima M A, Bruines P A, Verhoef P N W. Modeling tunnel boring machine performance by neuro-fuzzy methods. *Tunnel Underground Space Technol*, 2000, 15: 259- 269.
- Haaker, M. P. R., Verheijen, P. J. T., 2004, Local and Global Sensitivity Analysis for a Reactor Design with Parameter Uncertainty, *Chemical Engineering Research and Design*, Volume 82, Issue 5, Pages 591-598,
- Hassanpour, J., Rostami, J. and Zhao, J. (2011). A new hard rock TBM performance prediction model for project planning, *Tunnel Underground. Space Technol.* 26 (5): 595-603.
- Hudson, J. (1992). *Rock engineering systems. Theory and practice*. Chichester: Ellis Horwood.
- Kelton, W. Professor Department of Operations, Business Analytics, and Information Systems University of Cincinnati, Randall P. Sadowski, Retired, Nancy B. Zupick, Manager. — *Simulation with Arena*, Sixth edition, 2015
- Khademi Hamidi, J., Shahriar, K., Rezai, B., Rostami, J., 2010. Performance prediction of hard rock TBM using rock mass rating (RMR) system. *Tunneling and Underground Space Technology*, pp 333-345
- Khademi Hamidi, J., Shahriar, K., Rezai, B. and Rostami, J. (2011). Response by the authors to S. Yagiz discussion to the paper: J. Khademi Hamidi et al. (2010). Performance prediction of hard rock TBM using Rock Mass Rating (RMR) system, *Tunnelling and Underground Space Technology*. 25: 333-345. *Tunneling and Underground Space Technology* 26 (6): 795-797.
- Khetwal, A., J. Rostami, O. Frough, 2019. Sensitivity analysis of effect of tunneling activities on TBM utilization factor using discrete event simulation approach. In proceedings of TBM DIGs international conference, Golden, Colorado, 13-15 November 2019, pp 149-156
- Khetwal, A., J. Rostami, O. Frough, 2019. Simulation of TBM operation to assess the impact of geology on the muck transportation. In *Tunnels and Underground Cities, Engineering and*

Innovation meet Archaeology, Architecture and Art, Proceedings of WTC 2019, Naples, Italy, 3-9 May 2019, Taylor & Francis Group

- Khetwal, A., Rostami, J., Nelson, P.P. (2020). Investigating the impact of TBM downtimes on utilization factor based on sensitivity analysis. *Tunneling and Underground Space Technology*, Volume 106, pp. 1-13
- Khetwal, A., Rostami, J., Nelson, P.P. (2020a). Comparison between discrete event simulation approach and various existing empirically-based models for estimation of TBM utilization. Submitted
- Kim, T. (2004). Development of a fuzzy logic-based utilization predictor model for hard rock tunnel boring machines. Ph.D. thesis, Colorado School of Mines.
- Laughton, C. (1998). Evaluation and prediction of tunnel boring machine performance in variable rock masses. Ph.D. thesis, The University of Texas at Austin
- Macias, Javier & Jakobsen, Pål & Bruland, Amund & Log, Sindre & Grørv, Eivind. (2014). The NTNU Prediction Model: A Tool for Planning and Risk Management in Hard Rock TBM Tunnelling. 10.13140/2.1.4652.7364
- Massada, A. B., Carmel, Y. (2008), Incorporating output variance in local sensitivity analysis for stochastic models, *Ecological Modelling*, Volume 213, Issues 3–4, Pages 463-467,
- Mikaeil, R., Naghadehi, M. Z., & Ghadernejad, S. (2018). An extended multifactorial fuzzy prediction of hard rock TBM penetrability. *Geotechnical and Geological Engineering*, 36 (3), 1779{1804.
- Morio, J., 2011, Global and local sensitivity analysis methods for a physical system, *Eur. J. Phys.* 32 1577
- Morshedlou, Amid, Beyranvand, Nasrin, Dehghani, Hesam (2014). Estimation of the Penetration Rate of Tunnel Boring Machine using Monte Carlo simulation method.
- Nelson, P. P., Al-Jalil, Y. A., Laughton, C. (1994): Tunnel Boring Machine Project Data and Construction Simulation. The University of Texas at Austin, Austin.
- Nelson, P.P., O'Rourke, T.D. 1983. Tunnel boring machine performance in sedimentary rocks, Report to Goldberg-Zoino Associates of New York, P.C., by School of Civil and Environmental of Civil Engineering. Cornell University, 438p, Ithaca, NY.
- O'Connell, R., 2021, Investigating the Impact of TBM Downtimes on Utilization Factor Based on Sensitivity Analyses, Rapid Excavation and Tunneling Conference 2021 Proceedings, pg. 875-885.
- Okubo S, Fukui K, Chen W. Expert system for applicability of tunnel boring machines in Japan. *Rock Mechanics and Rock Engineering*, 2003, 36(4): 305-322.

- Ozdemir, L. 1977. Development of theoretical equations for predicting tunnel borability. PhD. Thesis, T-1969, Colorado School of Mines, Golden, Co
- Reuter, U., & Liebscher, M. (2008). Global sensitivity analysis in view of nonlinear structural behavior. LSDYNA Anwenderforum, Bamberg.
- Rostami, J., Ozdemir, L. 1993. A new model for performance prediction of hard rock TBMs. In: Bowerman, L.D. et al. (eds), Proceedings of Rapid Excavation and Tunneling Conferences, chapter 50, 793–809, Boston MA USA.
- Rostami, J. 1997. Development of a force estimation model for rock fragmentation with disc cutters through theoretical modeling and physical measurement of crushed zone pressure. PhD. Thesis, 382p., Department of Mining Engineering, Colorado School of Mines. Colorado USA
- Rostami, J., Farrokh, E., Laughton, C., & Eslambolchi, S. S. (2014). Advance rate simulation for hard rock TBMs. *KSCE Journal of Civil Engineering*, 18 (3), 837{852.
- Rostami, J., 2016, Performance prediction of hard rock Tunnel Boring Machines (TBMs) in difficult ground, *Tunnelling and Underground Space Technology*, Volume 57, Pages 173-182, ISSN 0886-7798,
- Salimi, A., & Esmacili, M. (2013). Utilizing of linear and non-linear prediction tools for evaluation of penetration rate of tunnel boring machine in hard rock condition. *International Journal of Mining and Mineral Engineering*, 4 (3), 249{264
- Saltelli, A., Ratto, M., Andres, T., Campolongo, F., Cariboni, J., Gatelli, D., & Tarantola, S. (2008). *Global sensitivity analysis: the primer*. John Wiley & Sons.
- Yagiz, S. (2002). Development of rock fracture and brittleness indices to quantify the effects of rock mass features and toughness in the CSM Model basic penetration for hard rock tunneling machines. Ph.D. Thesis, Department of Mining and Earth Systems Engineering, Colorado School of Mines, Golden, Colorado, USA. 289 P.
- Yagiz, S. April 2003. A model for prediction of TBM performance in hard rock conditions. Conference Paper
- Yagiz, S. 2006b. A Model for prediction of tunnel boring machine performance. Proceedings of 10th IAEG Congress, paper no. 383, (in DVD), the Geological Society of London, Nottingham, U.K.
- Yagiz S. 2008. Utilizing rock mass properties for predicting TBM performance in hard rock conditions. *Tunneling and Underground Space Technology* 23, 326–339.
- Yagiz S. and Karahan H. 2011. Prediction of hard rock TBM penetration rate using particle swarm optimization. *International Journal of Rock Mechanics and Mining Sciences* 48, 427–433.

APPENDIX A

PERMISSION TO PUBLISH

The below image shows the e-mail conversation with the author of “Introducing Uniform Discrete Event Simulation Model Using Arena© Software” and “Investigating the Impact of TBM Downtimes on Utilization Factor Based on Sensitivity Analyses” papers regarding the copyright permission.

Re: Request for Copyright Permission for Thesis (2021)

Anuradha Khetwal <akhetwal@mines.edu>

Mon 6/28/2021 10:01 PM

To: Hazar Kumas <hazarkumas@mymail.mines.edu>

Dear Hazar,

You can use the figures with proper reference.

All the best.

Anuradha

Get [Outlook for Android](#)

From: Hazar Kumas <hazarkumas@mymail.mines.edu>

Sent: Monday, June 28, 2021 9:22:44 PM

To: Anuradha Khetwal <akhetwal@mines.edu>

Subject: Request for Copyright Permission for Thesis (2021)

Hello Anuradha,

I hope this email finds you well.

I would like to use the Table 4.2 as a figure in my thesis from your "Introducing Uniform Discrete Event Simulation Model Using Arena© Software" paper. Also, I would like to use Figure 4.1 from the same paper.

In addition to these, I would like to use Table 7.1 as two individual figures in my thesis from your "Investigating the Impact of TBM Downtimes on Utilization Factor Based on Sensitivity Analyses" paper.

There are certain copyright laws that I need to follow before using these images in my thesis. I appreciate if you give me permission to use them with proper citation. I will include the phrase "Reprinted with permission" when citing the figures. The figures are attached to this email.

Thank you,

Table 4.2. List of modeling variables considered in CSM2D3 model

Parameter	Assumes	Scale / provided value
Excavation	Excavation rate	Linear, provided
	Excavation variability	Linear, provided
	Excavation variability	Linear, provided
	Excavation variability	Linear, provided
	Excavation variability	Linear, provided
Drilled rock-holding	Drilled rock-holding	Linear, provided
	Drilled rock-holding	Linear, provided
	Drilled rock-holding	Linear, provided
	Drilled rock-holding	Linear, provided
	Drilled rock-holding	Linear, provided
Maintenance	Maintenance time	Linear, provided
	Maintenance variability	Linear, provided
	Maintenance variability	Linear, provided
	Maintenance variability	Linear, provided
	Maintenance variability	Linear, provided
Utility	Utility	Linear, provided
	Utility variability	Linear, provided
	Utility variability	Linear, provided
	Utility variability	Linear, provided
	Utility variability	Linear, provided
Transportation	Transportation time	Linear, provided
	Transportation variability	Linear, provided
	Transportation variability	Linear, provided
	Transportation variability	Linear, provided
	Transportation variability	Linear, provided
Sewer	Sewer	Linear, provided
	Sewer variability	Linear, provided
	Sewer variability	Linear, provided
	Sewer variability	Linear, provided
	Sewer variability	Linear, provided
Miscellaneous	Miscellaneous	Linear, provided
	Miscellaneous variability	Linear, provided
	Miscellaneous variability	Linear, provided
	Miscellaneous variability	Linear, provided
	Miscellaneous variability	Linear, provided
Unassigned variables	Unassigned variables	Linear, provided
	Unassigned variables	Linear, provided
	Unassigned variables	Linear, provided
	Unassigned variables	Linear, provided
	Unassigned variables	Linear, provided
Cost	Cost	Linear, provided



Figure 4.1. Flowchart showing the modeling in Arena© model for CSM2D3 model for T1 excavation

Table 7.1. Distributions used for the analysis (Gibson et al., 2003; Tanaka and Dinkov, 2000)

Distribution type	Distribution	Expression	Range	Mean	Variance	Used to represent
Normal	$f(x) = \frac{1}{\sigma\sqrt{2\pi}} e^{-\frac{(x-\mu)^2}{2\sigma^2}}$	μ, σ	$-\infty < x < \infty$	μ	σ^2	Excavation rate, Excavation variability, Drilled rock-holding, Maintenance, Utility, Transportation, Sewer, Miscellaneous
Lognormal	$f(x) = \frac{1}{x\sigma\sqrt{2\pi}} e^{-\frac{(\ln x - \mu)^2}{2\sigma^2}}$	μ, σ	$x > 0$	e^{μ}	$e^{2\sigma^2} - 1$	Excavation rate, Excavation variability, Drilled rock-holding, Maintenance, Utility, Transportation, Sewer, Miscellaneous
Gamma	$f(x) = \frac{\lambda^k}{\Gamma(k)} x^{k-1} e^{-\lambda x}$	k, λ	$x > 0$	k/λ	k/λ^2	Excavation rate, Excavation variability, Drilled rock-holding, Maintenance, Utility, Transportation, Sewer, Miscellaneous
Exponential	$f(x) = \lambda e^{-\lambda x}$	λ	$x > 0$	$1/\lambda$	$1/\lambda^2$	Excavation rate, Excavation variability, Drilled rock-holding, Maintenance, Utility, Transportation, Sewer, Miscellaneous
Uniform	$f(x) = \frac{1}{b-a}$	a, b	$a < x < b$	$(a+b)/2$	$(b-a)^2/12$	Excavation rate, Excavation variability, Drilled rock-holding, Maintenance, Utility, Transportation, Sewer, Miscellaneous

Table 7.1 (Continued)

Distribution type	Distribution	Expression	Range	Mean	Variance	Used to represent
Logistic	$f(x) = \frac{e^{-x}}{(1+e^{-x})^2}$		$-\infty < x < \infty$	0	$\pi^2/12$	Excavation rate, Excavation variability, Drilled rock-holding, Maintenance, Utility, Transportation, Sewer, Miscellaneous
Weibull	$f(x) = \frac{k}{\lambda} \left(\frac{x}{\lambda}\right)^{k-1} e^{-(x/\lambda)^k}$	k, λ	$x > 0$	$\lambda \Gamma(1/k)$	$\lambda^2 [\Gamma(2/k) - \Gamma(1/k)^2]$	Excavation rate, Excavation variability, Drilled rock-holding, Maintenance, Utility, Transportation, Sewer, Miscellaneous
Rayleigh	$f(x) = \frac{x}{\lambda^2} e^{-x^2/\lambda^2}$	λ	$x > 0$	$\lambda \sqrt{\pi}/2$	$\lambda^2 (2 - \pi/2)$	Excavation rate, Excavation variability, Drilled rock-holding, Maintenance, Utility, Transportation, Sewer, Miscellaneous
Gamma	$f(x) = \frac{\lambda^k}{\Gamma(k)} x^{k-1} e^{-\lambda x}$	k, λ	$x > 0$	k/λ	k/λ^2	Excavation rate, Excavation variability, Drilled rock-holding, Maintenance, Utility, Transportation, Sewer, Miscellaneous

APPENDIX B

HISTOGRAMS AND STATISTICAL PARAMETERS OF PROBABILITY DISTRIBUTIONS

This Appendix consists of histograms with PDF curve fits, relevant statistical parameters, and processed datasets by Input Analyzer for each activity discussed in Chapter 5.

B.1 Tunnel Boring

The following histogram illustrates the best fit probability distribution for the tunnel boring dataset. Y-axis shows the frequency of data points within their corresponding bins. The X-axis shows the bins according to activity time in minutes. Tables B.1 and B.2 show the statistical parameters that belong to this dataset.

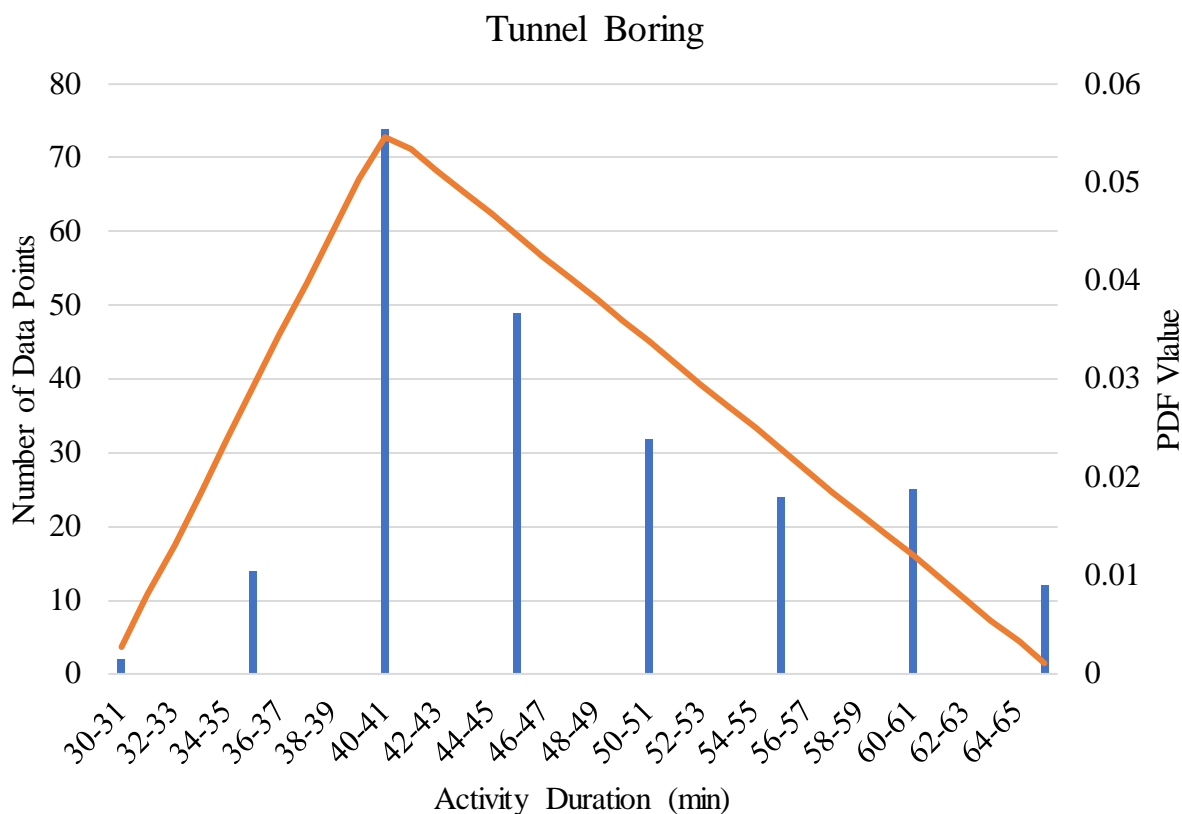


Figure B.1: Histogram chart of segment installation dataset.

Table B.1: Statistical parameters of tunnel boring dataset.

PDF Expression	Square Error	P-Value	Number of Data Points	Min	Max	Mean	Standard Deviation
TRIA (29.5, 40, 65.5)	0.15706	< 0.005	232	30	65	47	8.41

Table B.2: Processed tunnel boring dataset in Input Analyzer.

Interval No	Number of Data Points	x	PDF		CDF	
			Data	Function	Data	Function
0	2	30	0.00862	0.00265	0.00862	0.00265
1	0	31	0	0.00794	0.00862	0.0106
2	0	32	0	0.0132	0.00862	0.0238
3	0	33	0	0.0185	0.00862	0.0423
4	0	34	0	0.0238	0.00862	0.0661
5	14	35	0.0603	0.0291	0.069	0.0952
6	0	36	0	0.0344	0.069	0.13
7	0	37	0	0.0397	0.069	0.169
8	0	38	0	0.045	0.069	0.214
9	0	39	0	0.0503	0.069	0.265
10	74	40	0.319	0.0546	0.388	0.319
11	0	41	0	0.0534	0.388	0.373
12	0	42	0	0.0512	0.388	0.424
13	0	43	0	0.049	0.388	0.473
14	0	44	0	0.0468	0.388	0.52
15	49	45	0.211	0.0447	0.599	0.564
16	0	46	0	0.0425	0.599	0.607
17	0	47	0	0.0403	0.599	0.647
18	0	48	0	0.0381	0.599	0.685
19	0	49	0	0.0359	0.599	0.721
20	32	50	0.138	0.0338	0.737	0.755
21	0	51	0	0.0316	0.737	0.786
22	0	52	0	0.0294	0.737	0.816
23	0	53	0	0.0272	0.737	0.843
24	0	54	0	0.0251	0.737	0.868
25	24	55	0.103	0.0229	0.841	0.891
26	0	56	0	0.0207	0.841	0.912
27	0	57	0	0.0185	0.841	0.93
28	0	58	0	0.0163	0.841	0.947

Table B.2: Continued.

29	0	59	0	0.0142	0.841	0.961
30	25	60	0.108	0.012	0.948	0.973
31	0	61	0	0.0098	0.948	0.983
32	0	62	0	0.00763	0.948	0.99
33	0	63	0	0.00545	0.948	0.996
34	0	64	0	0.00327	0.948	0.999
35	12	65	0.0517	0.00109	1	1

B.2 Segment Installation

Figure B.2 illustrates the best fit probability distribution for the segment installation dataset. Tables B.3 and B.4 show the statistical parameters that belong to this dataset.

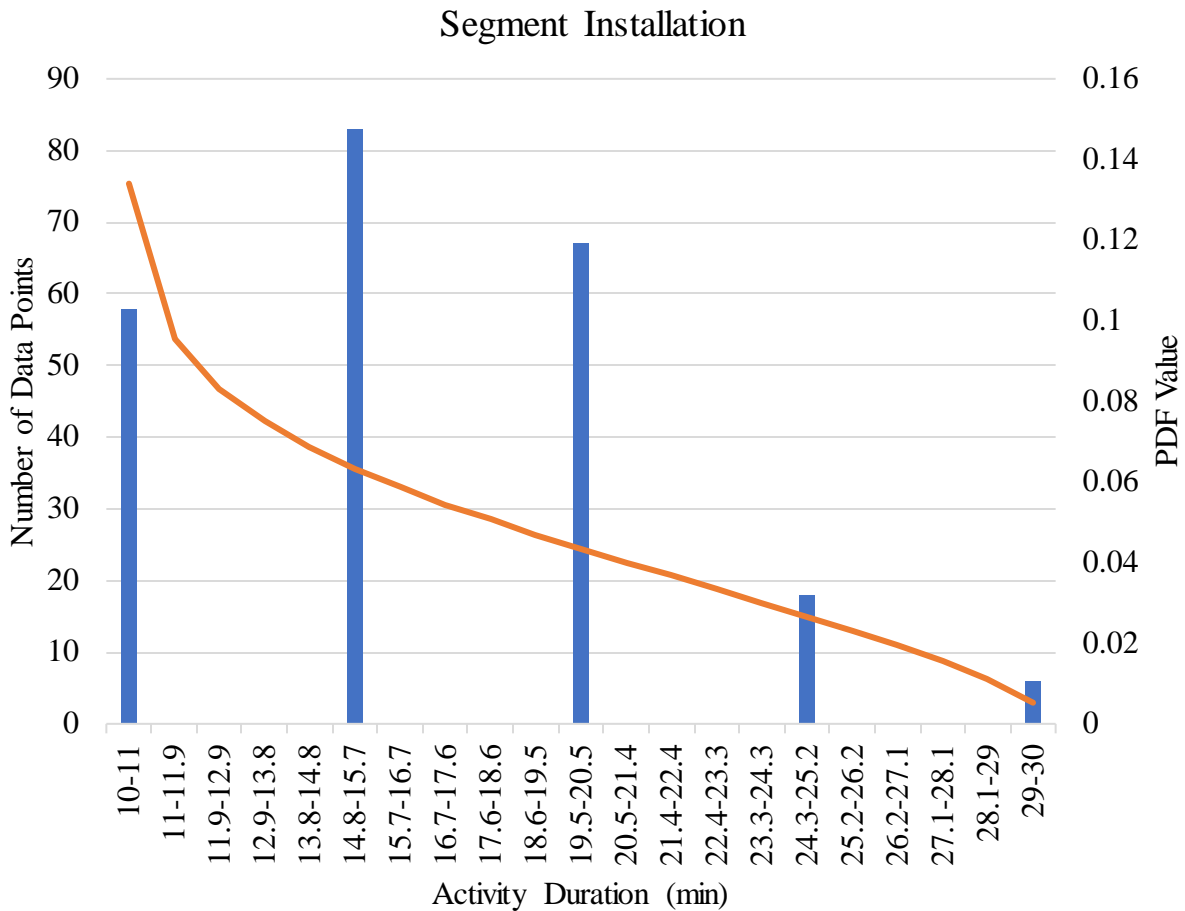


Figure B.2: Histogram chart of segment installation dataset.

Table B.3: Statistical parameters of segment installation dataset.

PDF Expression	Square Error	P-Value	Number of Data Points	Min	Max	Mean	Standard Deviation
$9.5 + 21 * \text{BETA} (0.799, 1.63)$	0.20712	< 0.005	232	10	30	16.4	5.03

Table B.4: Processed segment installation dataset in Input Analyzer.

Interval No	Number of Data Points	x	PDF		CDF	
			Data	Function	Data	Function
0	58	10	0.25	0.134	0.25	0.134
1	0	11	0	0.0955	0.25	0.23
2	0	12	0	0.0831	0.25	0.313
3	0	13	0	0.0749	0.25	0.387
4	0	14	0	0.0686	0.25	0.456
5	83	15	0.358	0.0633	0.608	0.519
6	0	16	0	0.0587	0.608	0.578
7	0	17	0	0.0545	0.608	0.632
8	0	18	0	0.0506	0.608	0.683
9	0	19	0	0.0469	0.608	0.73
10	67	20	0.289	0.0434	0.897	0.773
11	0	21	0	0.04	0.897	0.813
12	0	22	0	0.0367	0.897	0.85
13	0	23	0	0.0333	0.897	0.883
14	0	24	0	0.03	0.897	0.913
15	18	25	0.0776	0.0266	0.974	0.94
16	0	26	0	0.0232	0.974	0.963
17	0	27	0	0.0195	0.974	0.983
18	0	28	0	0.0156	0.974	0.998
19	0	29	0	0.0111	0.974	1.01
20	6	30	0.0259	0.00524	1	1.01

B.3 Unscheduled Maintenance

Figure B.3 illustrates the best fit probability distribution for the unscheduled maintenance dataset. Tables B.5 and B.6 show the statistical parameters that belong to this dataset.

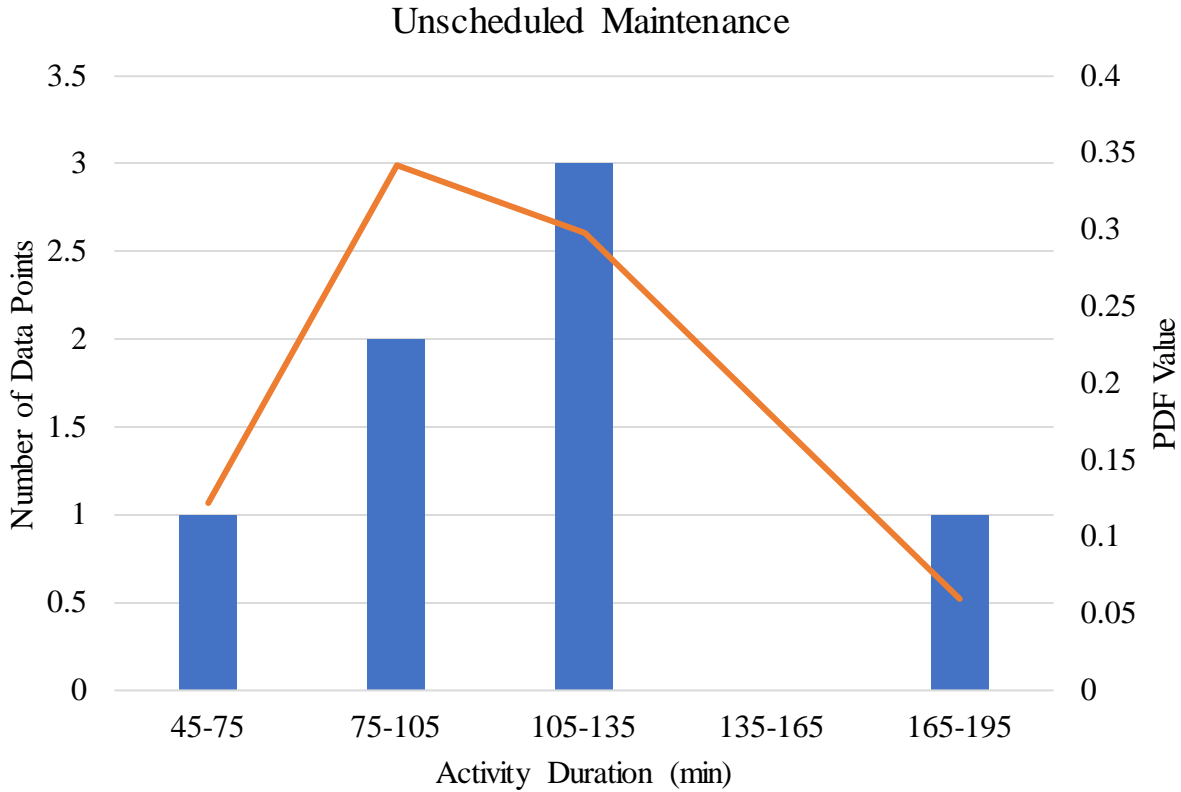


Figure B.3: Histogram chart of unscheduled maintenance dataset.

Table B.5: Statistical parameters of unscheduled maintenance dataset.

PDF Expression	Square Error	P-Value	Number of Data Points	Min	Max	Mean	Standard Deviation
TRIA (45, 94.3, 195)	0.05958	> 0.15	7	45	195	111	45.6

Table B.6: Processed unscheduled maintenance dataset in Input Analyzer.

Interval No	Number of Data Points	x	PDF		CDF	
			Data	Function	Data	Function
0	1	75	0.143	0.122	0.143	0.122
1	2	105	0.286	0.342	0.429	0.464
2	3	135	0.429	0.298	0.857	0.762
3	0	165	0	0.179	0.857	0.94
4	1	195	0.143	0.0596	1	1

B.4 Electrical Systems Repair

Figure B.4 illustrates the best fit probability distribution for the electrical systems repair dataset. Tables B.7 and B.8 show the statistical parameters that belong to this dataset

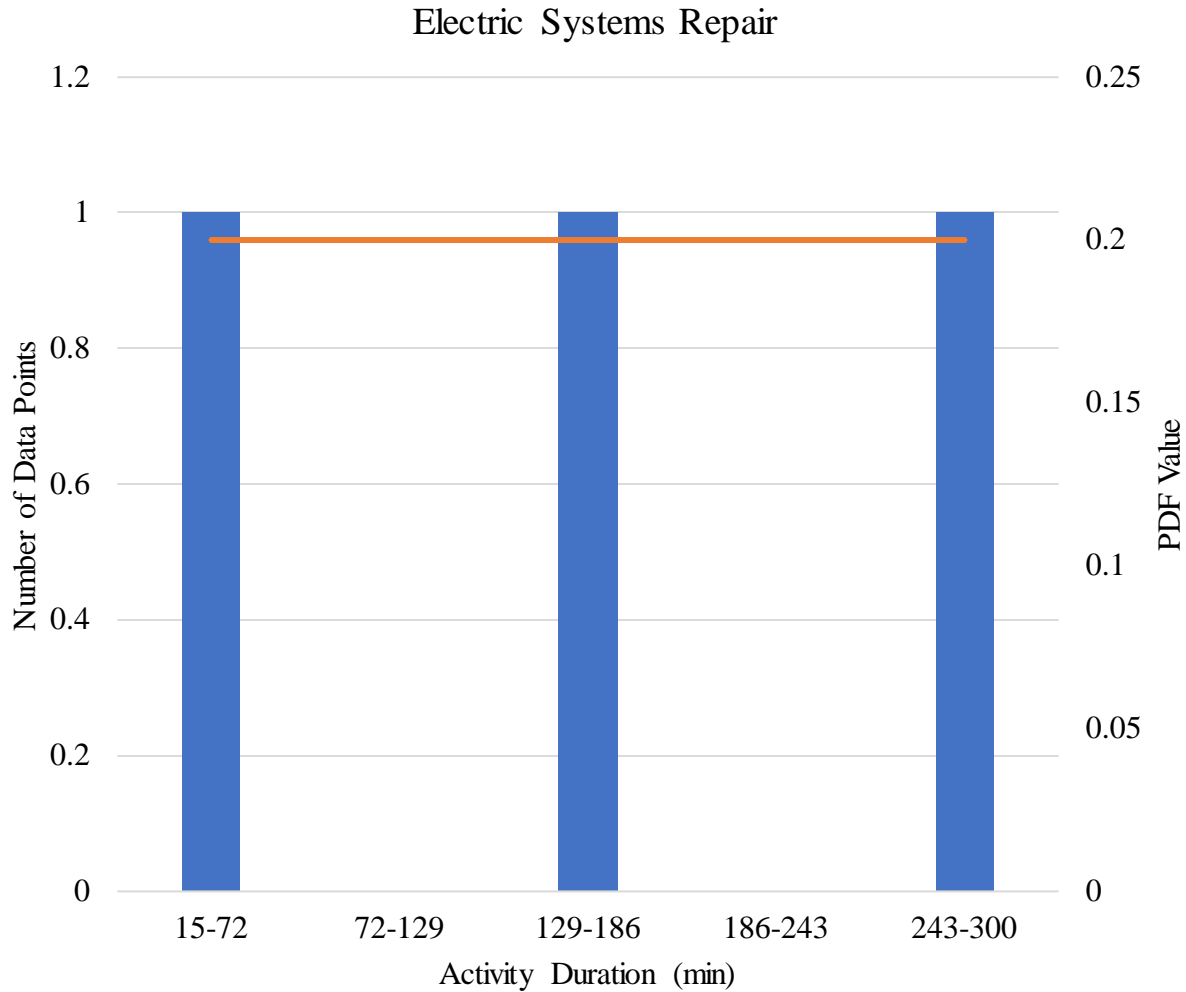


Figure B.4: Histogram chart of electrical systems repair dataset.

Table B.7: Statistical parameters of electrical systems repair dataset.

PDF Expression	Square Error	P-Value	Number of Data Points	Min	Max	Mean	Standard Deviation
UNIF (15, 300)	0.13333	> 0.15	3	15	300	155	143

Table B.8: Processed electrical systems repair dataset in Input Analyzer.

Interval No	Number of Data Points	x	PDF		CDF	
			Data	Function	Data	Function
0	1	72	0.333	0.2	0.333	0.2
1	0	129	0	0.2	0.333	0.4
2	1	186	0.333	0.2	0.667	0.6
3	0	243	0	0.2	0.667	0.8
4	1	300	0.333	0.2	1	1

B.5 Backfill Grout System

Figure B.5 illustrates the best fit probability distribution for the backfill grout system dataset. Tables B.9. and B.10 show the statistical parameters that belong to this dataset

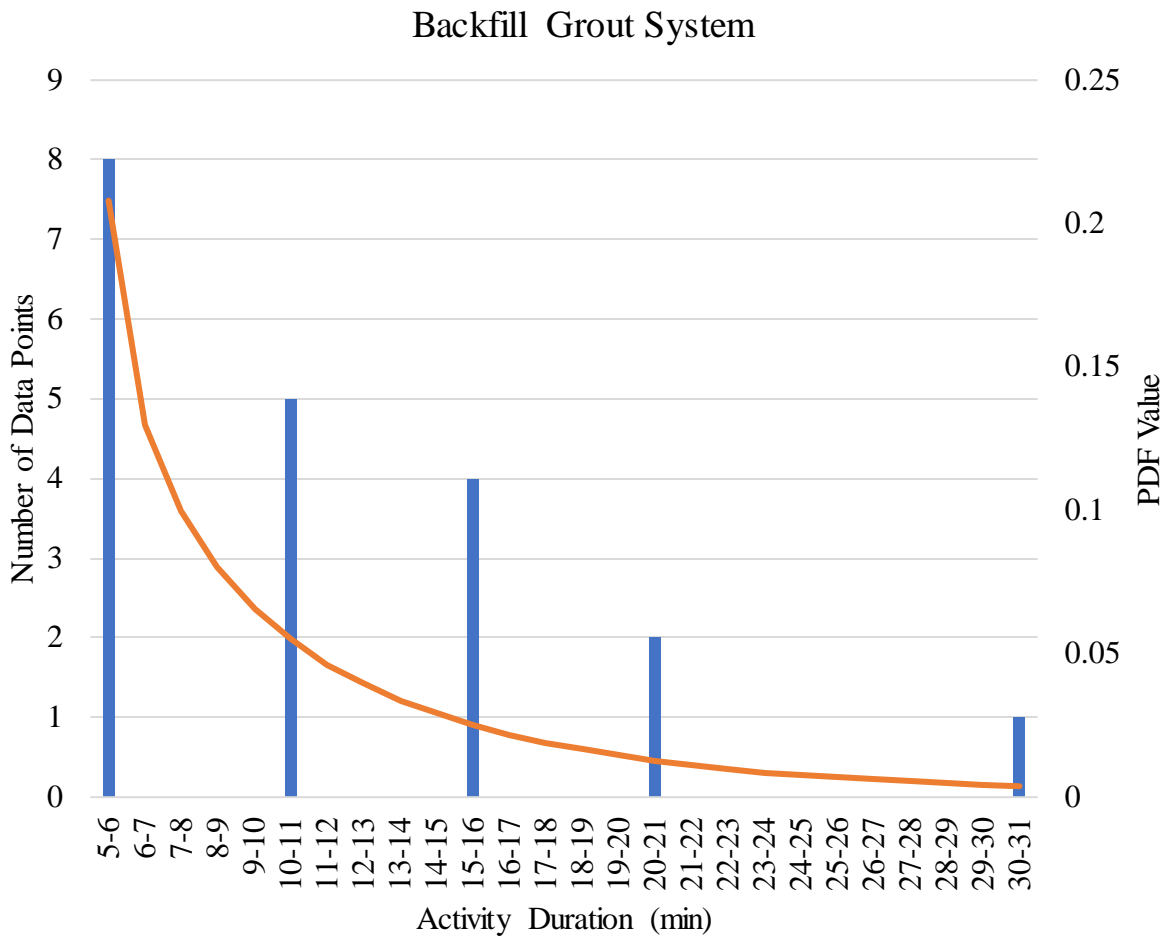


Figure B.5: Histogram chart of backfill grout system dataset.

Table B.9: Statistical parameters of backfill grout system dataset.

PDF Expression	Square Error	P-Value	Number of Data Points	Min	Max	Mean	Standard Deviation
44.5 + WEIB (5.88, 0.822)	0.1602	< 0.005	20	5	30	11	6.81

Table B.10: Processed backfill grout system dataset in Input Analyzer.

Interval No	Number of Data Points	x	PDF		CDF	
			Data	Function	Data	Function
0	8	5	0.4	0.208	0.4	0.208
1	0	6	0	0.13	0.4	0.338
2	0	7	0	0.0996	0.4	0.437
3	0	8	0	0.08	0.4	0.517
4	0	9	0	0.0658	0.4	0.583
5	5	10	0.25	0.055	0.65	0.638
6	0	11	0	0.0464	0.65	0.685
7	0	12	0	0.0395	0.65	0.724
8	0	13	0	0.0338	0.65	0.758
9	0	14	0	0.0291	0.65	0.787
10	4	15	0.2	0.0252	0.85	0.812
11	0	16	0	0.0219	0.85	0.834
12	0	17	0	0.0191	0.85	0.853
13	0	18	0	0.0167	0.85	0.87
14	0	19	0	0.0146	0.85	0.884
15	2	20	0.1	0.0128	0.95	0.897
16	0	21	0	0.0113	0.95	0.909
17	0	22	0	0.00994	0.95	0.919
18	0	23	0	0.00877	0.95	0.927
19	0	24	0	0.00776	0.95	0.935
20	0	25	0	0.00687	0.95	0.942
21	0	26	0	0.0061	0.95	0.948
22	0	27	0	0.00542	0.95	0.953
23	0	28	0	0.00482	0.95	0.958
24	0	29	0	0.00429	0.95	0.963
25	1	30	0.05	0.00382	1	0.966

B.6 Loading & Unloading of Supplies

Figure B.6 illustrates the best fit probability distribution for loading & unloading of supplies dataset. Tables B.11 and B.12 show the statistical parameters that belong to this dataset.

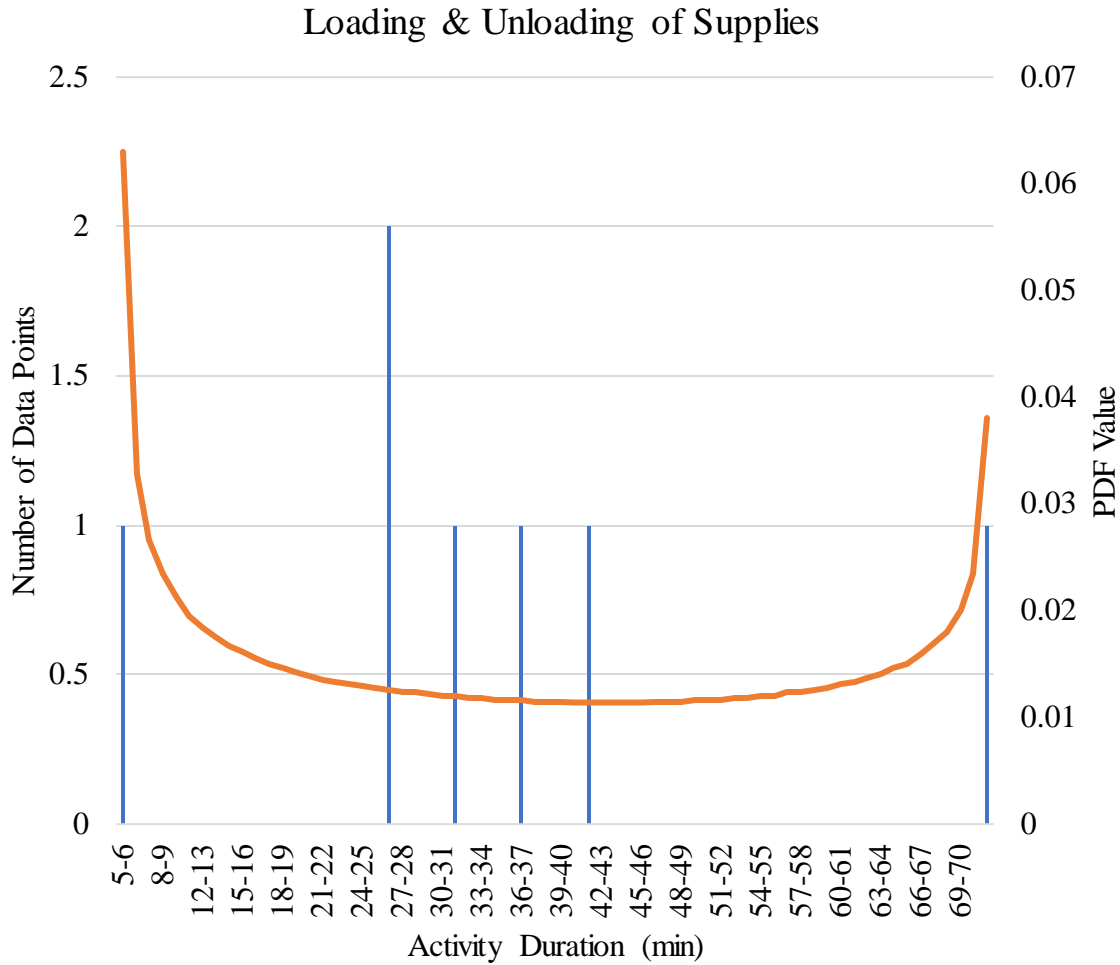


Figure B.6: Histogram chart of loading & unloading of supplies dataset.

Table B.11: Statistical parameters of loading & unloading of supplies dataset.

PDF Expression	Square Error	P-Value	Number of Data Points	Min	Max	Mean	Standard Deviation
$4.5 + 66 * \text{BETA} (0.594, 0.68)$	0.15708	< 0.005	7	5	70	32.9	19.8

Table B.12: Processed loading & unloading of supplies dataset in Input Analyzer.

Interval No	Number of Data Points	x	PDF		CDF	
			Data	Function	Data	Function
0	1	5	0.143	0.063	0.143	0.063
1	0	6	0	0.0329	0.143	0.0959
2	0	7	0	0.0267	0.143	0.123
3	0	8	0	0.0234	0.143	0.146
4	0	9	0	0.0212	0.143	0.167
5	0	10	0	0.0196	0.143	0.187
6	0	11	0	0.0184	0.143	0.205
7	0	12	0	0.0175	0.143	0.223
8	0	13	0	0.0167	0.143	0.239
9	0	14	0	0.0161	0.143	0.255
10	0	15	0	0.0155	0.143	0.271
11	0	16	0	0.015	0.143	0.286
12	0	17	0	0.0146	0.143	0.301
13	0	18	0	0.0143	0.143	0.315
14	0	19	0	0.0139	0.143	0.329
15	0	20	0	0.0136	0.143	0.342
16	0	21	0	0.0134	0.143	0.356
17	0	22	0	0.0132	0.143	0.369
18	0	23	0	0.0129	0.143	0.382
19	0	24	0	0.0128	0.143	0.395
20	2	25	0.286	0.0126	0.429	0.407
21	0	26	0	0.0124	0.429	0.42
22	0	27	0	0.0123	0.429	0.432
23	0	28	0	0.0122	0.429	0.444
24	0	29	0	0.0121	0.429	0.456
25	1	30	0.143	0.012	0.571	0.468
26	0	31	0	0.0119	0.571	0.48
27	0	32	0	0.0118	0.571	0.492
28	0	33	0	0.0117	0.571	0.504
29	0	34	0	0.0116	0.571	0.515
30	1	35	0.143	0.0116	0.714	0.527
31	0	36	0	0.0115	0.714	0.538
32	0	37	0	0.0115	0.714	0.55
33	0	38	0	0.0115	0.714	0.561
34	0	39	0	0.0114	0.714	0.573
35	1	40	0.143	0.0114	0.857	0.584

Table B.12: Continued.

36	0	41	0	0.0114	0.857	0.596
37	0	42	0	0.0114	0.857	0.607
38	0	43	0	0.0114	0.857	0.618
39	0	44	0	0.0114	0.857	0.63
40	0	45	0	0.0115	0.857	0.641
41	0	46	0	0.0115	0.857	0.653
42	0	47	0	0.0115	0.857	0.664
43	0	48	0	0.0116	0.857	0.676
44	0	49	0	0.0117	0.857	0.688
45	0	50	0	0.0117	0.857	0.699
46	0	51	0	0.0118	0.857	0.711
47	0	52	0	0.0119	0.857	0.723
48	0	53	0	0.012	0.857	0.735
49	0	54	0	0.0121	0.857	0.747
50	0	55	0	0.0123	0.857	0.76
51	0	56	0	0.0124	0.857	0.772
52	0	57	0	0.0126	0.857	0.785
53	0	58	0	0.0128	0.857	0.797
54	0	59	0	0.0131	0.857	0.811
55	0	60	0	0.0134	0.857	0.824
56	0	61	0	0.0137	0.857	0.838
57	0	62	0	0.0141	0.857	0.852
58	0	63	0	0.0146	0.857	0.866
59	0	64	0	0.0151	0.857	0.881
60	0	65	0	0.0159	0.857	0.897
61	0	66	0	0.0168	0.857	0.914
62	0	67	0	0.0181	0.857	0.932
63	0	68	0	0.02	0.857	0.952
64	0	69	0	0.0235	0.857	0.976
65	1	70	0.143	0.0381	1	1.01

B.7 Backup Utilities Repair

Figure B.7 illustrates the best fit probability distribution for backup utilities repair dataset. Tables B.13 and B.14 show the statistical parameters that belong to this dataset.

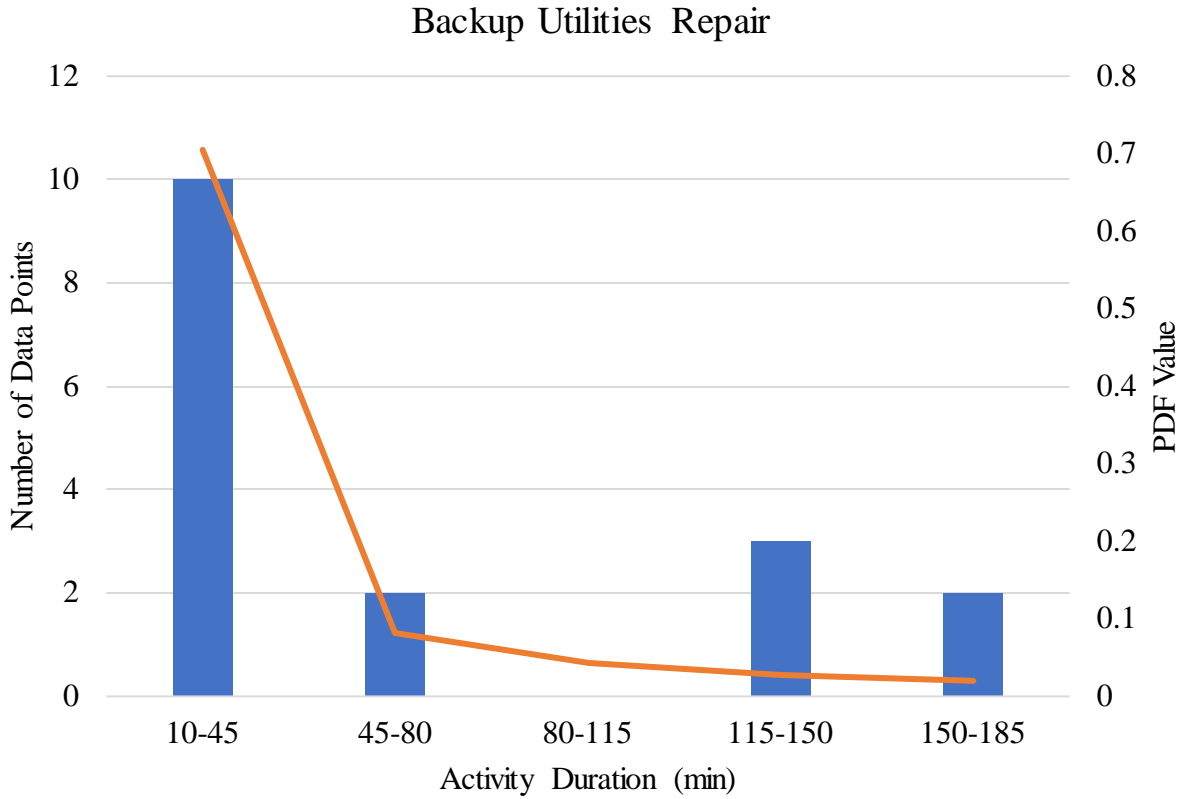


Figure B.7: Histogram chart of backup utilities repair dataset.

Table B.13: Statistical parameters of backup utilities repair dataset.

PDF Expression	Square Error	P-Value	Number of Data Points	Min	Max	Mean	Standard Deviation
10 + WEIB (19.4, 0.338)	0.04841	> 0.15	17	10	185	60	63

Table B.14: Processed backup utilities repair dataset in Input Analyzer.

Interval No	Number of Data Points	x	PDF		CDF	
			Data	Function	Data	Function
0	10	45	0.588	0.705	0.588	0.705
1	2	80	0.118	0.0813	0.706	0.787
2	0	115	0	0.0434	0.706	0.83
3	3	150	0.176	0.0282	0.882	0.858
4	2	185	0.118	0.0201	1	0.878

B.8 Unforeseen Delays

Figure B.8 the best fit probability distribution for unforeseen delays dataset. Tables B.15 and B.16 show the statistical parameters that belong to this dataset.

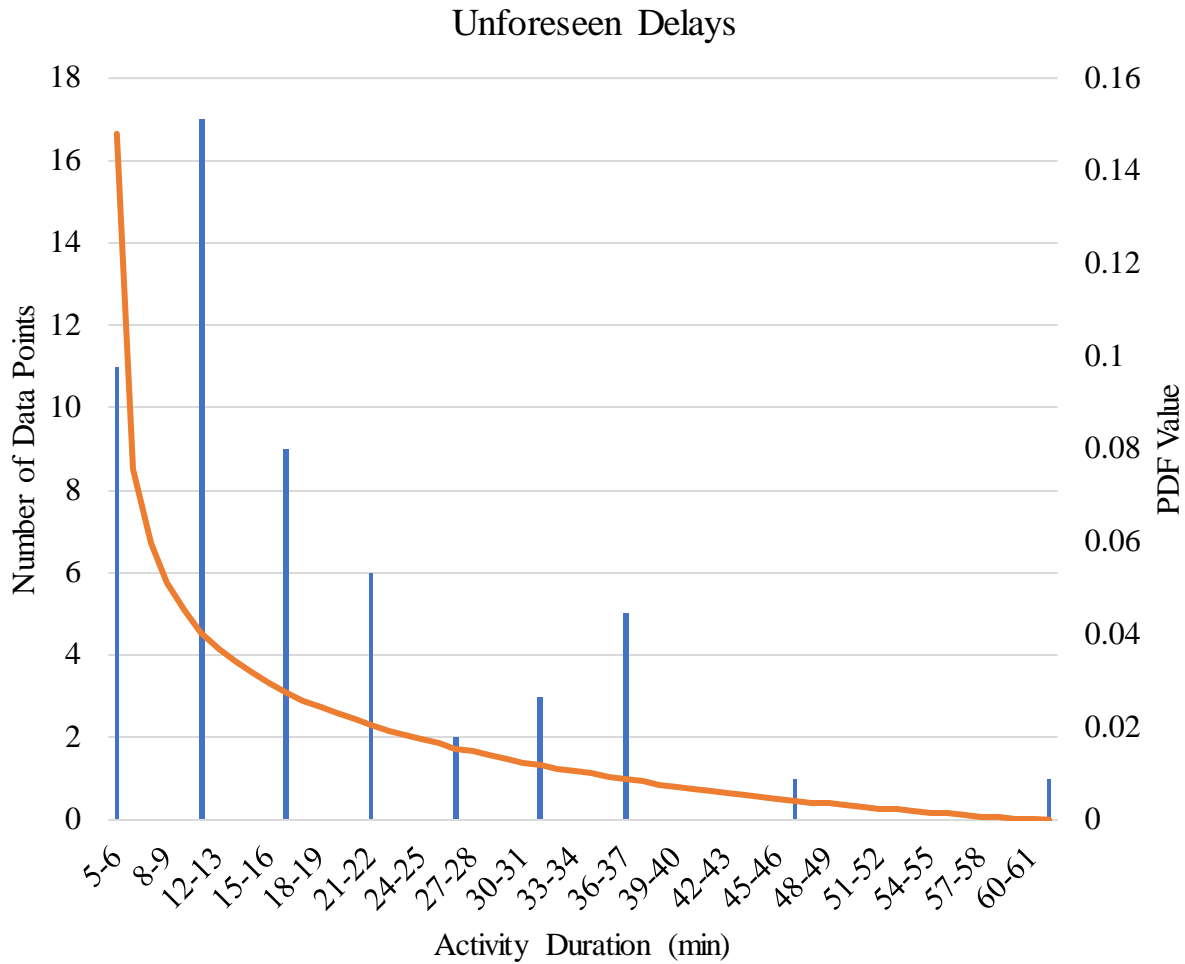


Figure B.8: Histogram chart of unforeseen delays dataset.

Table B.15: Statistical parameters of unforeseen delays dataset.

PDF Expression	Square Error	P-Value	Number of Data Points	Min	Max	Mean	Standard Deviation
$4.5 + 56 * \text{BETA} (0.601, 2.23)$	0.1341	< 0.005	55	5	60	16.4	11.7

Table B.16: Processed unforeseen delays dataset in Input Analyzer.

Interval No	Number of Data Points	x	PDF		CDF	
			Data	Function	Data	Function
0	11	5	0.2	0.148	0.2	0.148
1	0	6	0	0.0756	0.2	0.224
2	0	7	0	0.0598	0.2	0.284
3	0	8	0	0.051	0.2	0.335
4	0	9	0	0.045	0.2	0.38
5	17	10	0.309	0.0405	0.509	0.42
6	0	11	0	0.037	0.509	0.457
7	0	12	0	0.0341	0.509	0.491
8	0	13	0	0.0316	0.509	0.523
9	0	14	0	0.0294	0.509	0.552
10	9	15	0.164	0.0275	0.673	0.58
11	0	16	0	0.0258	0.673	0.606
12	0	17	0	0.0243	0.673	0.63
13	0	18	0	0.0229	0.673	0.653
14	0	19	0	0.0216	0.673	0.674
15	6	20	0.109	0.0204	0.782	0.695
16	0	21	0	0.0193	0.782	0.714
17	0	22	0	0.0183	0.782	0.732
18	0	23	0	0.0173	0.782	0.75
19	0	24	0	0.0164	0.782	0.766
20	2	25	0.0364	0.0155	0.818	0.781
21	0	26	0	0.0147	0.818	0.796
22	0	27	0	0.0139	0.818	0.81
23	0	28	0	0.0132	0.818	0.823
24	0	29	0	0.0125	0.818	0.836
25	3	30	0.0545	0.0118	0.873	0.847
26	0	31	0	0.0111	0.873	0.859
27	0	32	0	0.0105	0.873	0.869
28	0	33	0	0.00992	0.873	0.879
29	0	34	0	0.00934	0.873	0.888
30	5	35	0.0909	0.00879	0.964	0.897
31	0	36	0	0.00826	0.964	0.905
32	0	37	0	0.00775	0.964	0.913
33	0	38	0	0.00726	0.964	0.92
34	0	39	0	0.00678	0.964	0.927
35	0	40	0	0.00632	0.964	0.933

Table B.16: Continued.

36	0	41	0	0.00588	0.964	0.939
37	0	42	0	0.00545	0.964	0.945
38	0	43	0	0.00503	0.964	0.95
39	0	44	0	0.00463	0.964	0.954
40	1	45	0.0182	0.00425	0.982	0.959
41	0	46	0	0.00387	0.982	0.963
42	0	47	0	0.00351	0.982	0.966
43	0	48	0	0.00316	0.982	0.969
44	0	49	0	0.00283	0.982	0.972
45	0	50	0	0.00251	0.982	0.975
46	0	51	0	0.0022	0.982	0.977
47	0	52	0	0.0019	0.982	0.979
48	0	53	0	0.00161	0.982	0.98
49	0	54	0	0.00134	0.982	0.982
50	0	55	0	0.00108	0.982	0.983
51	0	56	0	0.00084	0.982	0.984
52	0	57	0	0.00061	0.982	0.984
53	0	58	0	0.0004	0.982	0.985
54	0	59	0	0.00021	0.982	0.985
55	1	60	0.0182	5.69E-05	1	0.985

B.9 Slurry Line Extension

Figure B.9 illustrates the best fit probability distribution for the slurry line extension dataset. Tables B.17 and B.18 show the statistical parameters that belong to this dataset.

Table B.17: Statistical parameters of slurry line extension dataset.

PDF Expression	Square Error	P-Value	Number of Data Points	Min	Max	Mean	Standard Deviation
$4.5 + 31 * \text{BETA} (0.694, 1.18)$	0.1327	< 0.005	46	5	35	16.5	8.56

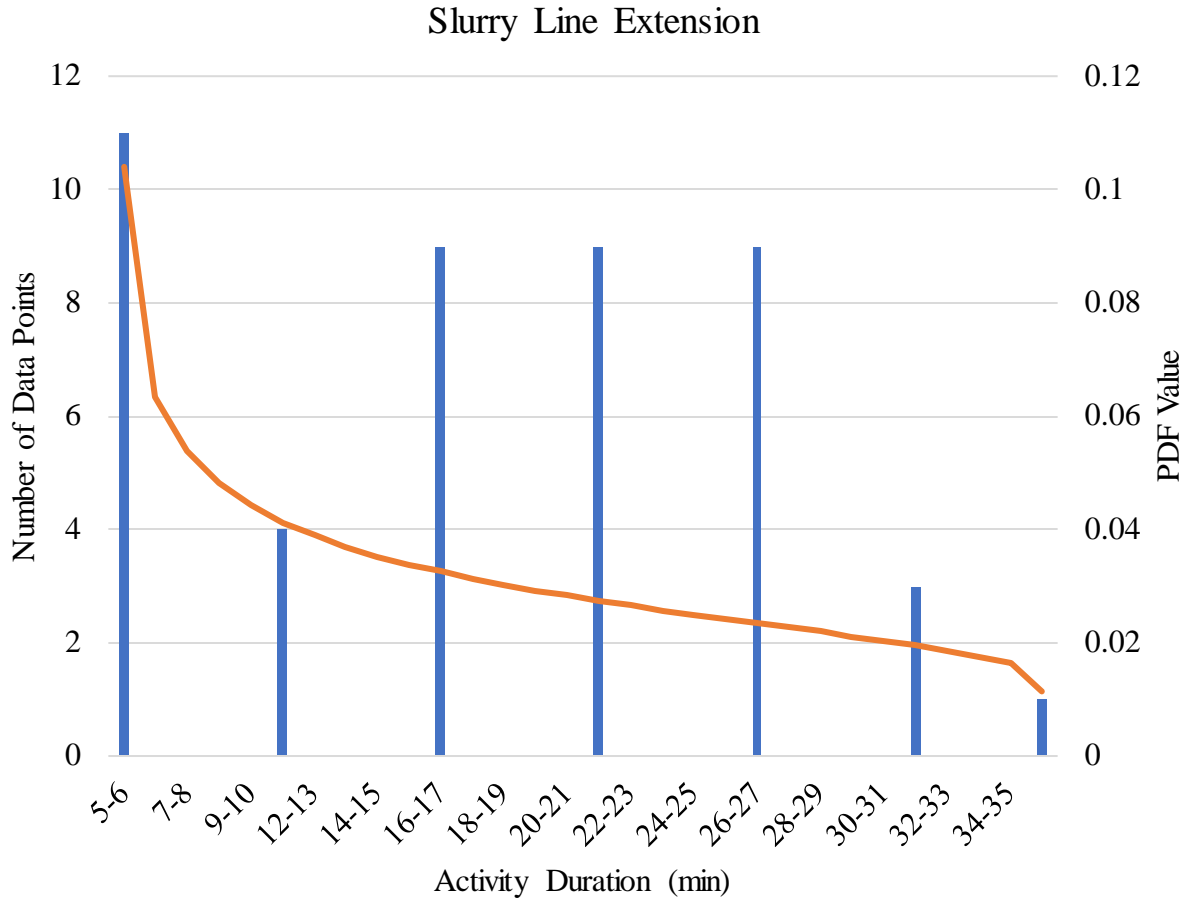


Figure B.9: Histogram chart of slurry line extension dataset.

Table B.18: Processed slurry line extension dataset in Input Analyzer.

Interval No	Number of Data Points	x	PDF		CDF	
			Data	Function	Data	Function
0	11	5	0.239	0.104	0.239	0.104
1	0	6	0	0.0635	0.239	0.167
2	0	7	0	0.0537	0.239	0.221
3	0	8	0	0.0481	0.239	0.269
4	0	9	0	0.0442	0.239	0.313
5	4	10	0.087	0.0412	0.326	0.355
6	0	11	0	0.0389	0.326	0.393
7	0	12	0	0.0369	0.326	0.43
8	0	13	0	0.0353	0.326	0.466
9	0	14	0	0.0338	0.326	0.499

Table B.18: Continued.

10	9	15	0.196	0.0325	0.522	0.532
11	0	16	0	0.0313	0.522	0.563
12	0	17	0	0.0302	0.522	0.593
13	0	18	0	0.0292	0.522	0.623
14	0	19	0	0.0283	0.522	0.651
15	9	20	0.196	0.0274	0.717	0.678
16	0	21	0	0.0266	0.717	0.705
17	0	22	0	0.0257	0.717	0.731
18	0	23	0	0.025	0.717	0.756
19	0	24	0	0.0242	0.717	0.78
20	9	25	0.196	0.0234	0.913	0.803
21	0	26	0	0.0227	0.913	0.826
22	0	27	0	0.0219	0.913	0.848
23	0	28	0	0.0211	0.913	0.869
24	0	29	0	0.0203	0.913	0.889
25	3	30	0.0652	0.0195	0.978	0.909
26	0	31	0	0.0185	0.978	0.927
27	0	32	0	0.0175	0.978	0.945
28	0	33	0	0.0163	0.978	0.961
29	0	34	0	0.0146	0.978	0.976
30	1	35	0.0217	0.0114	1	0.987

B.10 Slurry Lines Repair

Figure B.10 illustrates the best fit probability distribution for the slurry lines repair dataset. Tables B.19 and B.20 show the statistical parameters that belong to this dataset.

Table B.19: Statistical parameters of slurry lines repair dataset.

PDF Expression	Square Error	P-Value	Number of Data Points	Min	Max	Mean	Standard Deviation
10 + EXPO (94.4)	0.03185	> 0.15	9	10	330	101	114

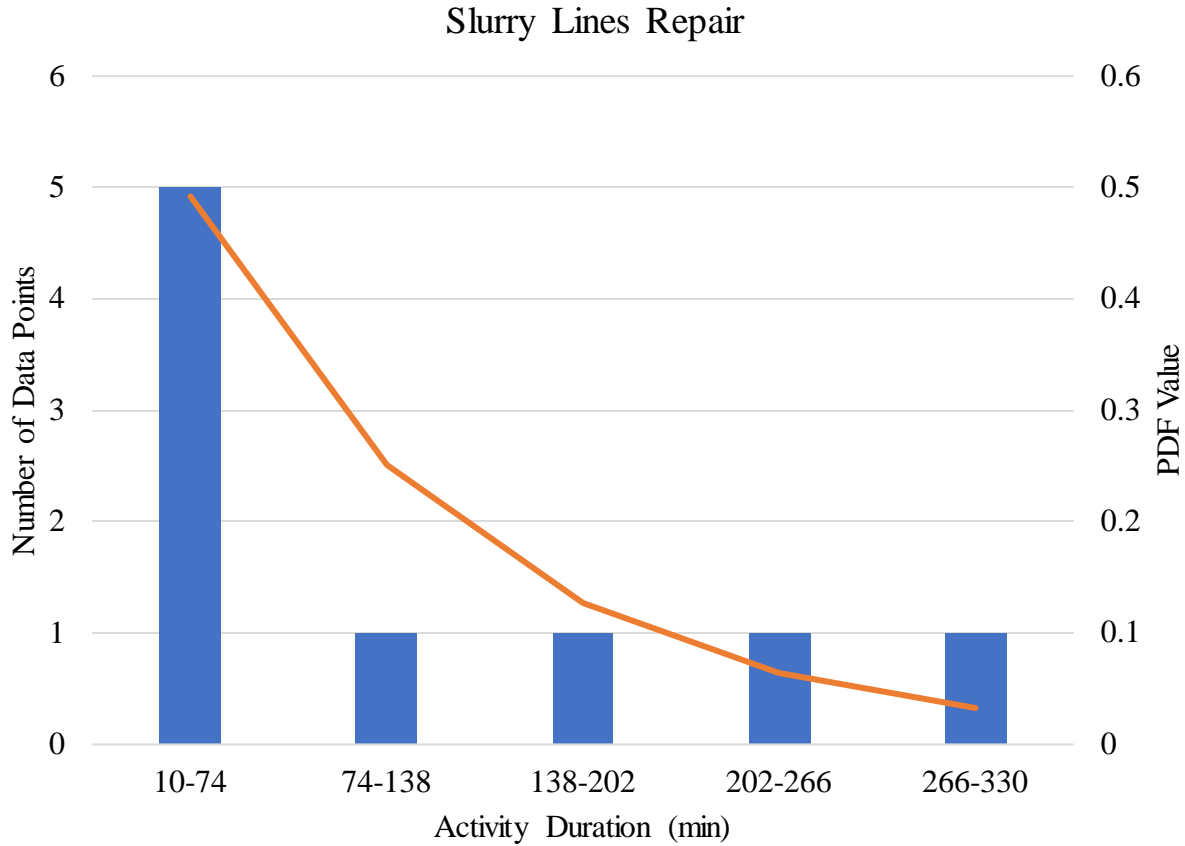


Figure B.10: Histogram chart of slurry lines repair dataset.

Table B.20: Processed slurry lines repair dataset in Input Analyzer.

Interval No	Number of Data Points	x	PDF		CDF	
			Data	Function	Data	Function
0	5	74	0.556	0.492	0.556	0.492
1	1	138	0.111	0.25	0.667	0.742
2	1	202	0.111	0.127	0.778	0.869
3	1	266	0.111	0.0645	0.889	0.934
4	1	330	0.111	0.0327	1	0.966

B.11 Water Test

Figure B.11 illustrates the best fit probability distribution for the water test dataset.

Tables B.21 and B.22 show the statistical parameters that belong to this dataset.

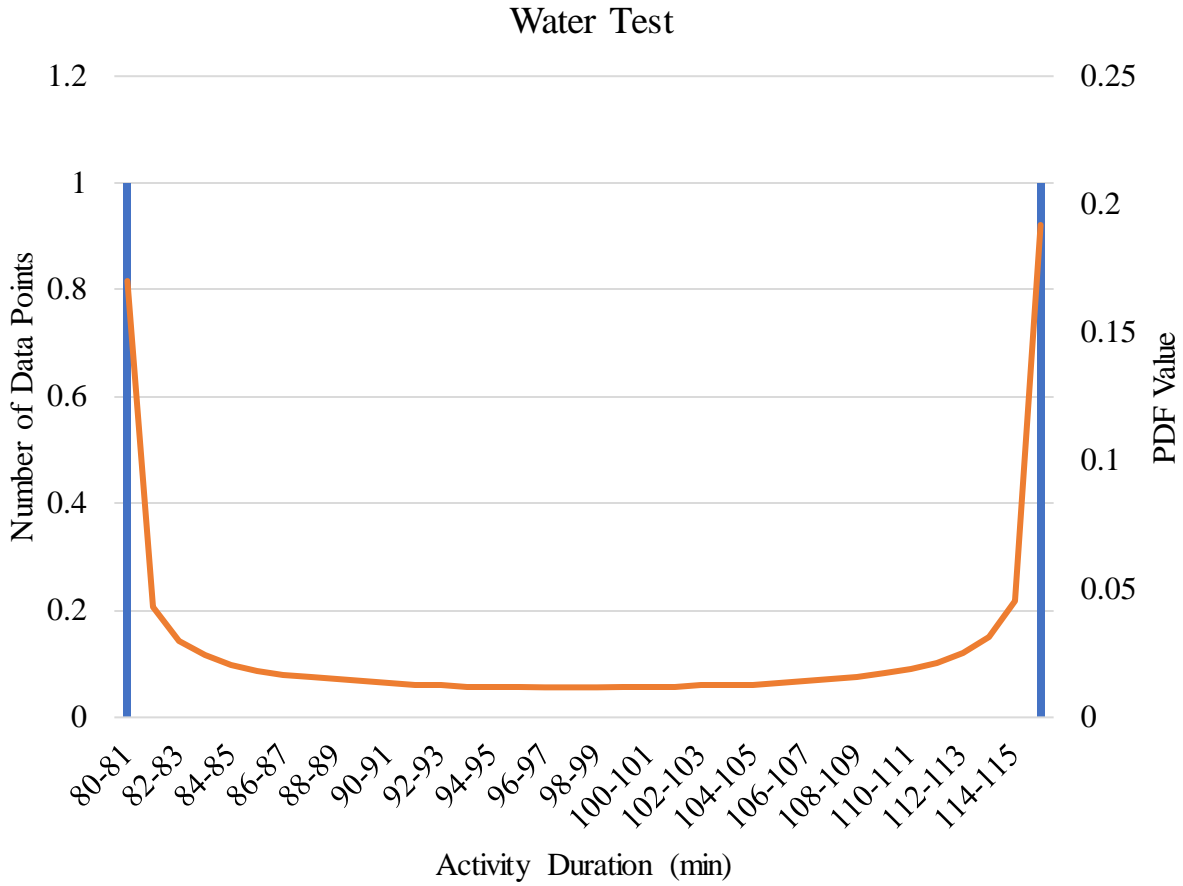


Figure B.11: Histogram chart of water test dataset.

Table B.21: Statistical parameters of the water test dataset.

PDF Expression	Square Error	P-Value	Number of Data Points	Min	Max	Mean	Standard Deviation
$79.5 + 36 * \text{BETA} (0.299, 0.28)$	0.216	< 0.005	2	80	115	97.5	24.7

Table B.22: Processed water test dataset in Input Analyzer.

Interval No	Number of Data Points	x	PDF		CDF	
			Data	Function	Data	Function
0	1	80	0.5	0.17	0.5	0.17
1	0	81	0	0.0427	0.5	0.213
2	0	82	0	0.03	0.5	0.243

Table B.22: Continued.

3	0	83	0	0.0242	0.5	0.267
4	0	84	0	0.0207	0.5	0.288
5	0	85	0	0.0184	0.5	0.306
6	0	86	0	0.0167	0.5	0.323
7	0	87	0	0.0155	0.5	0.339
8	0	88	0	0.0146	0.5	0.353
9	0	89	0	0.0139	0.5	0.367
10	0	90	0	0.0133	0.5	0.38
11	0	91	0	0.0128	0.5	0.393
12	0	92	0	0.0125	0.5	0.406
13	0	93	0	0.0122	0.5	0.418
14	0	94	0	0.012	0.5	0.43
15	0	95	0	0.0118	0.5	0.442
16	0	96	0	0.0117	0.5	0.453
17	0	97	0	0.0117	0.5	0.465
18	0	98	0	0.0117	0.5	0.477
19	0	99	0	0.0118	0.5	0.488
20	0	100	0	0.0119	0.5	0.5
21	0	101	0	0.0121	0.5	0.512
22	0	102	0	0.0123	0.5	0.525
23	0	103	0	0.0126	0.5	0.537
24	0	104	0	0.013	0.5	0.55
25	0	105	0	0.0135	0.5	0.564
26	0	106	0	0.0141	0.5	0.578
27	0	107	0	0.0149	0.5	0.593
28	0	108	0	0.0159	0.5	0.609
29	0	109	0	0.0172	0.5	0.626
30	0	110	0	0.019	0.5	0.645
31	0	111	0	0.0215	0.5	0.667
32	0	112	0	0.0252	0.5	0.692
33	0	113	0	0.0316	0.5	0.723
34	0	114	0	0.0454	0.5	0.769
35	1	115	0.5	0.192	1	0.961

B.12 Surveying

Figure B.12 illustrates the best fit probability distribution for surveying dataset. Tables B.23 and B.24 show the statistical parameters that belong to this dataset.

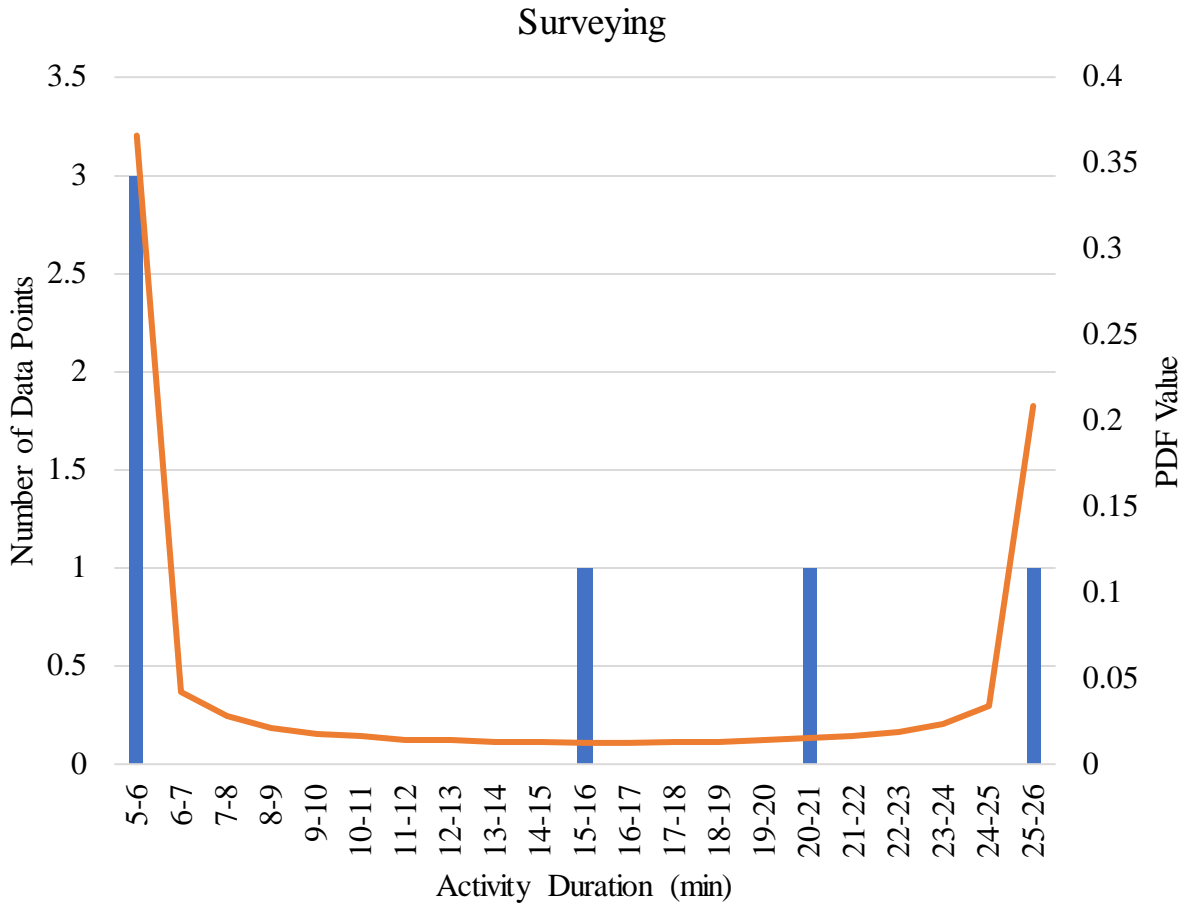


Figure B.12: Histogram chart of surveying dataset.

Table B.23: Statistical parameters of surveying dataset.

PDF Expression	Square Error	P-Value	Number of Data Points	Min	Max	Mean	Standard Deviation
$4.5 + 21 * \text{BETA}(0.13, 0.212)$	0.0740	< 0.005	6	5	25	12.5	8.8

Table B.24: Processed surveying dataset in Input Analyzer.

Interval No	Number of Data Points	x	PDF		CDF	
			Data	Function	Data	Function
0	3	5	0.5	0.366	0.5	0.366
1	0	6	0	0.0425	0.5	0.408
2	0	7	0	0.0278	0.5	0.436
3	0	8	0	0.0216	0.5	0.457
4	0	9	0	0.0181	0.5	0.476
5	0	10	0	0.016	0.5	0.492
6	0	11	0	0.0146	0.5	0.506
7	0	12	0	0.0136	0.5	0.52
8	0	13	0	0.013	0.5	0.533
9	0	14	0	0.0126	0.5	0.545
10	1	15	0.167	0.0124	0.667	0.558
11	0	16	0	0.0124	0.667	0.57
12	0	17	0	0.0126	0.667	0.583
13	0	18	0	0.013	0.667	0.596
14	0	19	0	0.0136	0.667	0.609
15	1	20	0.167	0.0147	0.833	0.624
16	0	21	0	0.0163	0.833	0.64
17	0	22	0	0.0189	0.833	0.659
18	0	23	0	0.0236	0.833	0.683
19	0	24	0	0.0343	0.833	0.717
20	1	25	0.167	0.208	1	0.925

B.13 Shaft Operations

Figure B.13 illustrates the best fit probability distribution for shaft operations dataset.

Tables B.25 and B.26 show the statistical parameters that belong to this dataset.

Table B.25: Statistical parameters of shaft operations dataset.

PDF Expression	Square Error	P-Value	Number of Data Points	Min	Max	Mean	Standard Deviation
4.5 + 21* BETA (0.321, 0.691)	0.1580	< 0.005	6	5	25	9.17	8.01

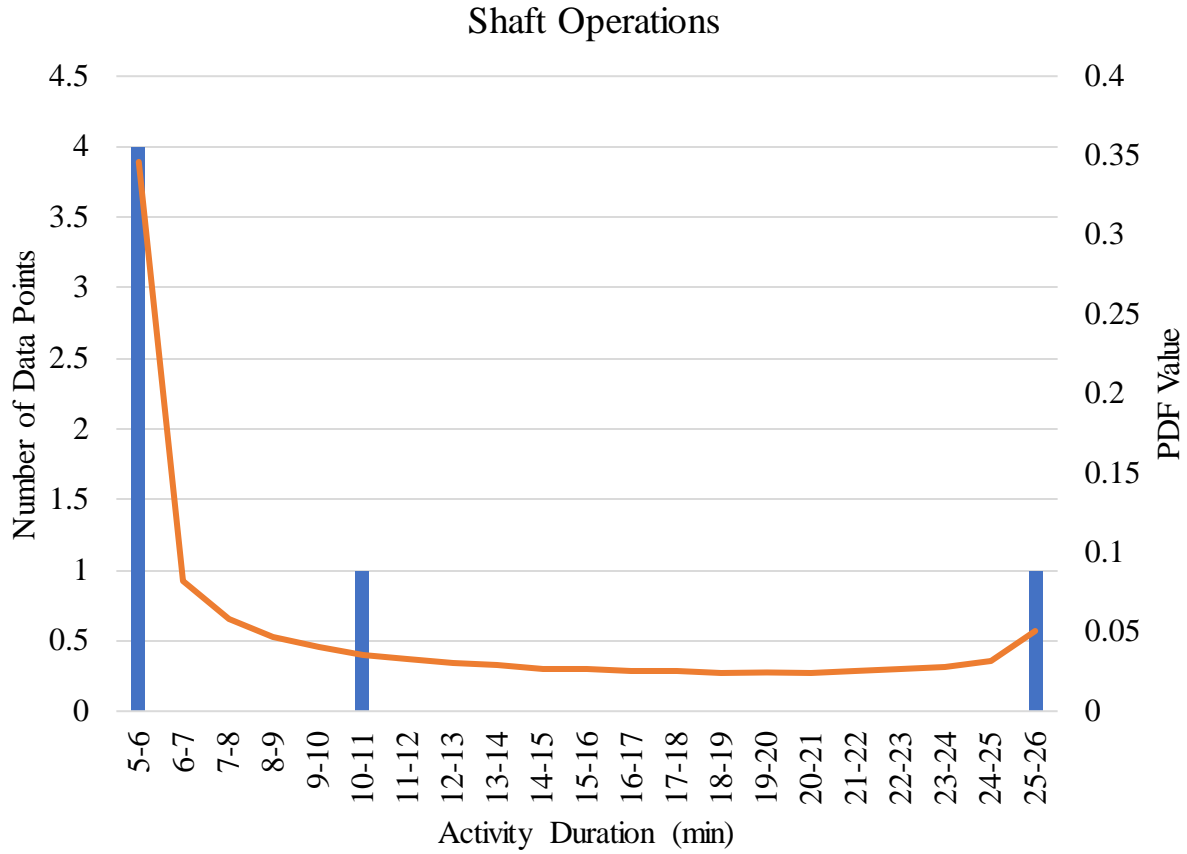


Figure B.13: Histogram chart of shaft operations dataset.

Table B.26: Processed shaft operations dataset in Input Analyzer.

Interval No	Number of Data Points	x	PDF		CDF	
			Data	Function	Data	Function
0	4	5	0.667	0.346	0.667	0.346
1	0	6	0	0.0826	0.667	0.428
2	0	7	0	0.0585	0.667	0.487
3	0	8	0	0.0472	0.667	0.534
4	0	9	0	0.0405	0.667	0.575
5	1	10	0.167	0.036	0.833	0.611
6	0	11	0	0.0328	0.833	0.644
7	0	12	0	0.0304	0.833	0.674
8	0	13	0	0.0286	0.833	0.703
9	0	14	0	0.0272	0.833	0.73
10	0	15	0	0.0261	0.833	0.756

Table B.26: Continued.

11	0	16	0	0.0254	0.833	0.781
12	0	17	0	0.0248	0.833	0.806
13	0	18	0	0.0245	0.833	0.831
14	0	19	0	0.0244	0.833	0.855
15	0	20	0	0.0245	0.833	0.879
16	0	21	0	0.025	0.833	0.904
17	0	22	0	0.026	0.833	0.93
18	0	23	0	0.0278	0.833	0.958
19	0	24	0	0.0315	0.833	0.99
20	1	25	0.167	0.0501	1	1.04

B.14 Example Activity Distribution with Anomalies

Figure B.14 illustrates the probability distribution for slurry lines repair with anomalies dataset. Tables B.27 and B.28 show the statistical parameters that belong to this dataset.

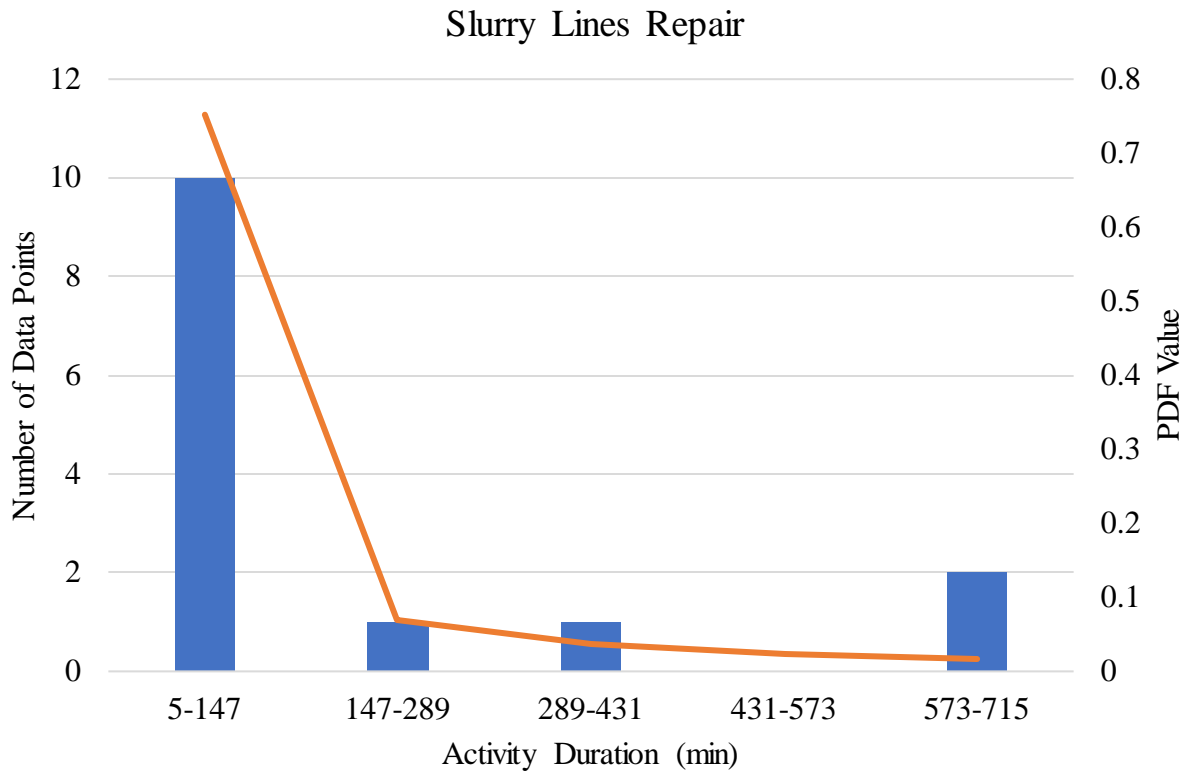


Figure B.13: Histogram chart of slurry lines repair dataset with anomalies.

Table B.27: Statistical parameters of slurry lines repair dataset with anomalies.

PDF Expression	Square Error	P-Value	Number of Data Points	Min	Max	Mean	Standard Deviation
5 + WEIB (48.8, 0.311)	0.1910	< 0.005	14	5	715	166	242

Table B.28: Processed slurry lines repair dataset with anomalies in Input Analyzer.

Interval No	Number of Data Points	x	PDF		CDF	
			Data	Function	Data	Function
0	10	147	0.714	0.752	0.714	0.752
1	1	289	0.0714	0.0707	0.786	0.823
2	1	431	0.0714	0.0368	0.857	0.86
3	0	573	0	0.0236	0.857	0.883
4	2	715	0.143	0.0167	1	0.9